U.S. Coast Guard Research and Development Center

1082 Shennecossett Road, Groton, CT 06340-6096

Report No. CG-D-10-00

Exploratory Testing Of A Sea Water Instrumented Manikin (SWIM) And Computer Simulation Software For Evaluating Personal Floatation Devices

FINAL REPORT
October 1999

Prepared for:

U.S. Department of Transportation
United States Coast Guard
Marine Safety and Environmental Protection (G-M)
Washington, DC 20593-0001

N O T I C E

This document is disseminated under the sponsorship of the Department of Transportation in the interest of information exchange. The United States Government assumes no liability for its contents or use thereof.

The United States Government does not endorse products or manufacturers. Trade or manufacturers' names appear herein solely because they are considered essential to the object of this report.

This report does not constitute a standard, specification, or regulation.

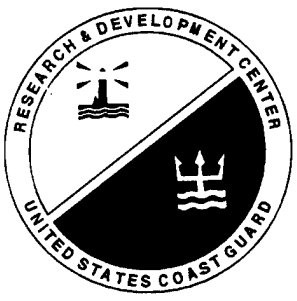

Marc B. Mandler, Ph.D.
Technical Director
United States Coast Guard
Research & Development Center
1082 Shennecossett Road
Groton, CT 06340-6096

Technical Report Documentation Page

1. Report No.	2. Government Accession Number	3. Recipient's Catalog No.
CG-D-10-00		

4. Title and Subtitle	5. Report Date
Exploratory Testing Of A Sea Water Instrumented Manikin (SWIM) And Computer Simulation Software For Evaluating Personal Floatation Devices	October 1999
	6. Performing Organization Code Project No. 3301.04.08

7. Author(s)	8. Performing Organization Report No.
Robert C. Desruisseau, Tariq Shams, Bert Macesker	R&DC-35-99

9. Performing Organization Name and Address		10. Work Unit No. (TRAIS)
U.S. Coast Guard Research and Development Center 1082 Shennecossett Road Groton, CT 06340-6096	Transport Canada Tower "C" Place de Ville 330 Sparks Street Ottawa, ON K1A ON8 Canada	11. Contract or Grant No.

12. Sponsoring Organization Name and Address	13. Type of Report & Period Covered
U.S. Department of Transportation United States Coast Guard Marine Safety and Environmental Protection (G-M) Washington, DC 20593-0001	Final Report
	14. Sponsoring Agency Code Commandant (G-MSE) U.S. Coast Guard Headquarters Washington, DC 20593-0001

15. Supplementary Notes

The R&D Center's technical point of contact is Robert C. Desruisseau, (860)441-2660, email: rdesruisseau@rdc.uscg.mil.

16. Abstract (MAXIMUM 200 WORDS)

This report presents an overview of the joint U.S. Coast Guard and Transport Canada-sponsored project to develop new research tools for evaluating personal floatation devices (PFDs). The U.S. Coast Guard and Transport Canada entered into a Joint Research Project Agreement (JARPA) in 1992 to develop new research tools to improve the understanding of the complicated effects of rough water on the performance of PFDs. Two tools were developed: 1) a computer simulation program called the Water Forces Analysis Capability (WAFAC) which simulates human body movement in a water environment, and 2) a sophisticated Sea Water Instrumented Manikin (SWIM) which can be used in the water to gather information on how the body reacts to the water environment. Preliminary testing of these two tools took place at the Institute for Marine Dynamics in St. Johns, Newfoundland, Canada, in February and March of 1999. Testing of the SWIM was completed for a variety of simple cases in still water and in simple wave fronts. The same tests were simulated using the WAFAC computer model and some test data from SWIM. The results of the comparison of these tests, real and simulated, will help to establish continuity between the two tools. The testing identified some problems with the sensors having inadequate ranges for these tests. General agreement for rise times to the surface for bottom release tests was established. There was approximate agreement in heave amplitude and frequency, while other tests required the adjustment of coefficients. It was determined that better measurements of the center of gravity and buoyancy are needed for baseline inputs for the WAFAC program.

17. Key Words	18. Distribution Statement
SWIM, manikin, PFD, WAFAC, DYNAMAN, JRPA, U.S. Coast Guard, Transport Canada, IMD	This document is available to the U.S. public through the National Technical Information Service, Springfield, VA 22161

19. Security Class (This Report)	20. Security Class (This Page)	21. No of Pages	22. Price
UNCLASSIFIED	UNCLASSIFIED	158	

Form DOT F 1700.7 (8/72) Reproduction of form and completed page is authorized.

ACKNOWLEDGEMENTS

Appreciation is expressed to André Taschereau and Gilles Gareau of Transport Canada, and to António Simões Ré, Spence Butt, Howard Mesh, Chris Meadus, Scott Newbury, Mike Walsh, Kent Brett and the staff of the Institute for Marine Dynamics, St. John's Newfoundland, Canada, for their help, insight, and problem solving during the testing of SWIM.

EXECUTIVE SUMMARY

This report presents an overview of a jointly sponsored project by the U.S. Coast Guard and Transport Canada to develop new research tools for evaluating personal floatation devices (PFDs). The U.S. and Canadian governments require approval for PFDs used in the boating community and promote research to develop safer PFDs.

At present, PFDs are only evaluated for U.S. Coast Guard approval using calm water testing in which a person wearing a PFD enters the water and simulates an unconscious state. The PFD is then evaluated for floatation and righting ability. This calm water testing cannot accurately address the effects of that same PFD in the rough water environment. A more robust testing method could safely test and better evaluate the PFD in a wider range of water situations. To this end, two research tools have been constructed and are reported on. The first tool is a full-size waterproof manikin, which represents an average male in stature, weight, and buoyancy. This manikin was constructed to collect data on how an average male floats and responds to water forces. The second tool, a computer simulation program, simulates an average male's movement in the water environment. The manikin was used to gather input data for the computer simulation model. This report describes tests using the manikin in the water environment and compares the results of the computer simulation model of those same tests.

The U.S. Coast Guard and Transport Canada entered into a Joint Research Project Agreement (JRPA) in 1992 to develop new R&D tools to improve our understanding of the effects of rough water performance of PFDs. There is little information about the performance of life jackets in rough water, and methods are not available to extrapolate the rough water performance of a PFD from calm water testing. A computer model simulation was developed at Wright-Patterson Air Force Base based on the existing Articulated Total Body Manikin (ATB) program written. The ATB program is used to evaluate the three-dimension dynamic response of a system of rigid bodies when subjected to a dynamic environment. The ATB program has been used for many years to study subject response to aircraft

ejection and automobile crashes. The new program, developed jointly by the U.S. and Canada, is referred to as Water Forces Analysis Capability (WAFAC) and has adapted the ATB model to the in-water environment. To complete the WFAC program, we had to verify the program using test data from the sophisticated Sea Water Instrumented Manikin (SWIM).

In conjunction with the development of the WAFAC program, a sophisticated SWIM was constructed and evaluated as a standard for testing PFDs. This manikin was used to gather data to validate the WAFAC model. SWIM is an anthropomorphically correct mechanical representation of a 50th percentile male with the appropriate dimensional, inertial, center of gravity, center of buoyancy and joint properties. The SWIM physical properties were taken from several proven manikins, including the Hybrid II, Hybrid III, and Advanced Dynamic Anthropomorphic Manikin (ADAM). SWIM has a self-contained data acquisition system (DAS) with 32-channel capability which translates the SWIM movement from 21 joint sensors, 4 pressure transducers, linear and angular accelerations into engineering units. Collectively, these data describe the Swim's movement in the water environment.

Validation of the SWIM and the WAFAC program was the first important step in the process of developing each as a tool. Preliminary testing was completed at the Institute for Marine Dynamics (IMD) in St. Johns, Newfoundland, Canada, in February and March of 1999. IMD has testing tanks with wave-making capability and is part of the Canadian National Research Council, the primary science and technology agency for Canada. Testing included center of buoyancy (CB) measurements, center of gravity (CG) measurements, drag measurements, simple bottom release tests from 7, 5, 4 and 3 meters of depth and wave testing in simple waves. This preliminary testing, exploratory in nature, was to help point out successes and problems with the SWIM and WAFAC model. Some mechanical and sensor problems were identified with the SWIM. There was good correlation between the actual and simulated bottom release tests when using the normal outfit weight for SWIM. Verification of SWIM and WAFAC tools will provide substantial insight into the rough water testing of PFDs. These tools will aid the Coast Guard in developing better testing methods and provide data for the PFD life-saving index. In 2000,

additional testing of SWIM will be coordinated through the USCG Office of Boating of Safety, USCG Office of Design Engineering Standards, and Transport Canada. SWIM and the WAFAC model may become tools for industry to design, build, and test new life-saving devices. In addition, these tools may be used for USCG/CCG-type approval testing and evaluation. Using the WAFAC program, manufacturers may be able to simulate a PFD prototype for use in calm and/or rough water environments eliminating actual in-water testing. SWIM could be used for actual in-water testing of new life-saving devices without subjecting a human to the hazards of those tests.

[Blank Page]

TABLE OF CONTENTS

TABLE OF CONTENTS (continued)

TABLE OF CONTENTS (continued)

LIST OF FIGURES

LIST OF FIGURES (continued)

LIST OF FIGURES (continued)

LIST OF FIGURES (continued)

LIST OF TABLES

[Blank Page]

1.0 INTRODUCTION

1.1 Research Goals

The primary goal of this research was development of a validated computer simulation capability to predict the dynamic behavior of persons wearing PFDs in rough water conditions. A computer simulation would provide a safe and cost-effective approach to testing new survival system products on various cross sections of the boating population without actual water testing. The end product is envisioned as being a public domain design tool that survival equipment manufacturers can use to optimize concepts and new products.

The secondary goal is to utilize both the program and instrumented manikin to design experiments to study the factors which are most important to survival in a man-overboard scenario. This will improve the Coast Guard's understanding of the effects of waves on the person wearing a PFD and will lead to the development of the best possible standards for PFD testing and approval, i.e., improved life saving index (LSI) data or new rough water indices.

The U.S. Coast Guard and Transport Canada jointly sponsored the development of an instrumented floatation manikin designated as the Sea Water Instrumented Manikin (SWIM) (Veridian, 1998), and the development of a computer program called the Water Forces Analysis Capability (WAFAC) (Weerappuli, 1992). Both the new manikin and the software were designed to evaluate the performance of personal floatation devices (PFDs). The U.S. Coast Guard and Transport Canada have jointly planned and executed a set of tests with SWIM to check the performance of the model for the case of the complete manikin for a number of different initial conditions. These tests, described in this report, were exploratory in nature and were intended to check out the SWIM hardware in simple water states. In addition, these tests served to examine how well the WAFAC model can simulate the motion of the actual manikin under the same initial conditions.

1.2 The U.S. Coast Guard's Life Jacket Responsibilities

The U.S. Coast Guard and Transport Canada have approval authority for new life jacket designs in North America. The Coast Guard strives to establish the best possible life jacket performance requirements for the recreational boating community. Recreational boating fatalities, as reported in the annual U.S. Department of Transportation Boating Statistics, have decreased over the past couple of decades. This

is a result of improved boater education, enhanced standards for boats, and more comfortably designed Personal Floatation Devices (PFDs). However, there continues to be a fairly steady percentage of fatalities in which drowned persons are recovered with their PFDs attached. Some of these deaths may be attributed to inadequate PFD design for rough water conditions. PFD designs will continue to evolve, as will the need for better performance standards. For example, the recent boom in personal water-craft usage will increase consumer demand for more wearable PFDs.

Testing practices are well established for evaluating the performance of PFDs in calm water, but up until now there have not been adequate tools to bridge the gap in understanding how calm water performance predictions equate to a rough water environment. PFD testing has been performed using human subjects including children; however, evaluating PFD performance on humans in anything but the calmest of conditions has drawbacks because subjects do not remain passive. Test repeatability has been difficult, and testing persons in rough water increases risk considerably.

1.3 Life Jacket Testing Practices

PFDs encompass several types (Type I to Type V's). A Type I is an offshore life jacket, has the greatest buoyancy, and is the most effective in rough water. Type II is a near-shore buoyant vest, and its buoyant turning action is slower than the Type I but is more comfortable to the wearer. The Type III is a floatation aid and is not designed to turn the wearer face up but is usually the most comfortable. The Type IV are throwable devices that are designed to be grasped and held by the user or thrown to a person who has fallen overboard. A Type V PFD is conditionally approved for restricted uses such as board sailing and may not be suitable for other recreational boating activities. The term PFD will for the purposes of this report refer to those PFDs that can be donned as a wearable life jacket.

The U.S. Coast Guard approval process requires a human subject to enter calm water wearing the candidate PFD. The subject simulates unconsciousness and the PFD is evaluated for floatation and face-up righting ability. The U.S. Coast Guard has both structural and performance standards and procedures for approval of PFDs. As an example, an excerpt from the U.S. Code of Federal Regulations (Title 46) stipulates the following approval test requirements for the approval of inflatable PFDs.

§160.176-13 Approval Tests

"(3) Some tests in this section require a lifejacket to be tested while being worn. In each of these tests the test subjects must represent a range of small, medium, and large heights and weights. Unless otherwise specified, a minimum of 18 test subjects, including both males and females, must be used. The test subjects must not be practiced in the use of the lifejacket being tested. However, they must be familiar with the use of other Coast Guard approved lifejackets. Unless specified otherwise, test subjects must wear only swim suits. Each test subject must be able to swim and relax in the water.

NOTE: Some tests have inherent hazards for which adequate safeguards must be taken to protect personnel and property in conducting the tests."

"(4) Average requirements. The test results for all subjects must be averaged for the following static measurements and must comply with the following:

(i) The average freeboard prior to positioning the head for maximum freeboard must be at least 120 mm (4.75 inches).

(ii) The average torso angle must be between 30° and 50° (back of vertical); and

(iii) The average face-plane angle must be between 20° and 50° (back of vertical).

(5) "HELP" Position. Starting in a relaxed, face-up position of static balance, each subject brings the legs and arms in towards the body so as to attain the "HELP" position, (a fetal position, but holding the head back). The life jacket must not turn the subject face down in the water."

1.4 U.S. Coast Guard Research

The U.S. Coast Guard has been sponsoring PFD research since the early 1970s. This research has mostly been limited to static calm water floatation evaluations. The underlying reason for the universal acceptance of calm water approval testing of new products and calm water research studies is that it is a safe and somewhat repeatable method for determining the gross in-water characteristics of a PFD. The lack of an available rough water standard has limited approval and research to mostly calm water.

1.4.1 1970's to 1980's

As recently as the 1980's, PFDs had only been tested in calm water. Rough water testing was conducted, (Girton, Wehr, 1984), at the David Taylor Research Center (DTRC) with human subjects in a wave making tank. These tests provided qualitative information on the effects of different PFDs on persons in rough water. Recommendations were made to evaluate the repeatability of testing PFD designs in rough water by using instrumentation to measure such items as head angle and the number of mouth and nose immersions. There are questions that calm water methods cannot address such as:

- effects of wave action on the turning moment of PFDs
- the position that should be taken by the person wearing a PFD relative to a wave front, i.e., the optimum angle of repose for his body and head angle.
- the number of mouth immersions that can be expected
- how much buoyancy is adequate in rough water

In 1988, DTRC collected quantitative data on factors influencing the performance of PFDs, (Hart, 1988). Experiments were performed on a simplistic flotation dummy referred to as "Sierra Sam" and human subjects to evaluate the natural periods of oscillation in calm water. DTRC indicated the need for new research tools and recommended the acquisition of a set of anthropometric manikins for standardization of testing and the application of the Air Force's human body dynamics simulation program.

Although a survivor's primary concern in rough water will be his or her maintenance of airway freeboard, a secondary yet important additional concern is hypothermia. The physical activity required to maintain freeboard, distance from the mouth to the water's surface, in rough water will increase heat loss. A study was conducted by the Coast Guard to evaluate the cooling rates of human volunteers wearing Coast Guard operational protective garments in cold sea-water under calm versus rough sea conditions (Steinman, 1985). The results of this experiment showed significantly faster body cooling rates in rough seas than in calm seas for the subjects wearing a thermal float coat, aviation anti-exposure coveralls, and boat crew coveralls. Significantly higher heart rates were measured in the rough water for all garments tested. The loose fitting protective garments, i.e., coveralls, performed the worse because of the wave-induced cold water flushing through the garment.

1.4.2 Life Saving Index

The U.S. Coast Guard has the responsibility to ensure that all PFDs it approves have a high probability of saving the life of boaters. Therefore, the U.S. Coast Guard is exploring the use of the Life Saving Index (LSI) as an alternative compliance path for PFDs. The LSI is a risk-based approach that could allow for improved comfort or effectiveness in a PFD design to compensate for a slight reduction in operational reliability, e.g., inflatables versus inherently buoyant PFDs. Essentially, the LSI is summarized as a number between zero and one that represents the overall lifesaving potential of a PFD design. It is based on a probability model with components of in-water effectiveness (E), reliability (R), and wearability (W):

$$LSI=ExRxW$$

Experiments with an instrumented floatation manikin and computer model sensitivity studies could provide invaluable insight and more meaningful indices for the in-water effectiveness of new designs, especially in areas of quantifying freeboard and self-righting performance in both calm and rough waters.

1.5 U.S. and Canadian Joint Research Project Agreement

An international joint project was arranged between Transport Canada and the U.S. Coast Guard because both agencies had embarked along a similar research path in 1992 and because research dollars were and continue to be scarce for this type of long-term research.

The methods of cooperation outlined in Section 5 of the agreement are as follows:

5.1a Both parties will exchange reports embodying significant research results from their activities subject to restrictions on distribution of proprietary or other sensitive data.

5.1b Researchers from both countries will participate in workshops and conferences organized by the Department of Transportation or Transport Canada to address specific PFD research issues or to provide a mechanism for the formal or informal exchange of information.

5.1c Both parties will exchange operational and assessment data and participate in the definitional phase of experimental facility planning.

5.1d Both parties will cooperate in studies to evaluate the benefits and cost of potential applications for PFD research.

5.1e Researchers from both countries will be invited to inspect experimental test facilities and to witness and/or participate in tests related to PFD research.

5.1f Both parties will exchange any developed software packages for studying the performance of personal floatation devices.

The participating program representatives are the Ship Safety Branch for Transport Canada and Lifesaving & Fire Safety Standards Division (G-MSE-4) for the U.S. Coast Guard. The joint project goals are to jointly award a contract for the development of an instrumented anthropometric floatation manikin and to develop a validated computer simulation capability for modeling persons wearing PFDs in waves.

2.0 BACKGROUND

2.1 Testing Goals

The testing goals for these preliminary tests were straightforward: using two weight states for SWIM, (one heavy and one light), and three manikin attitudes, (one straight vertical, one straight horizontal, and one configured at a right angle), collect enough data to start verification of the SWIM and the WAFAC computer model as tools. The intent behind these preliminary tests was to gather enough data to distinguish where the two tools (SWIM and WAFAC) support each other's outputs, identifying where the hardware and software emulate each other, and where they do not. This testing also addressed the shortcomings of the SWIM and WAFAC model. Validation of both the SWIM and WAFAC model is required before any practical applications for each can take place. This exploratory testing was the first step.

2.2 SWIM Overview

The SWIM is an instrumented flotation manikin tool for testing the response of PFDs and other survival equipment in still and rough water. Test data will be used to validate a computer model, which in turn will become a tool to test designs and modifications of survival equipment. The SWIM is a mechanical representation of a mid-sized male human in every respect. The performance requirements for SWIM were developed in 1992 by the U.S. Coast Guard and Transport Canada in accordance with the United States Department of Transportation/Transport Canada Joint Research Project Agreement Number 6, for the Performance Research of Floatation Devices.

The anthropomorphic performance requirements developed by the U.S. Air Force (Wright Patterson AFB, 1990), were for a 50th percentile mid-sized male, and includes 17 principal segments. They are: 1- Head., 2- Neck, 3-Thorax, 4-Abdomen, 5-Pelvis, 6-Right Upper Arm, 7-Left Upper Arm, 8-Right Forearm, 9-Left Forearm, 10-Right Hand, 11- Left Hand, 12- Right Thigh, 13- Left Thigh, 14- Right Calf, 15- Left Calf, 16- Right Foot, 17- Left Foot. Inertial properties were specified for each segment and included the mass, center of mass, magnitudes of the principal moments of inertia and the orientation of the principal axes. It was required that the manikin and segment surface shapes conform to the mid-size male. Buoyancy adjustments would have to be evenly distributed within each segment space about the long bone. Joint resistance requirements were to reflect an unconscious PFD user and adjustable joint resistance was required to simulate an appropriate muscular joint resistance for each articulated joint. The manikin was also required to have built in variable ballast to fine-tune the final buoyancy and to account for future weight growth for instrumentation.

2.2.1 SWIM Mechanical System.

The SWIM's mechanical skeletal structure is made of stainless steel, aluminum, high molecular weight polyethylene, and delrin. Each of the 17 segments is molded of vinyl with closed cell foam beneath the skin. The floatation vest is made of 5/16-inch neoprene and the chest floatation inserts are made from DOW® HI 100, high density Hygrofoam type 4.

Figure 1. Joint sensor.

The SWIM houses a suite of sensors used to measure and record the whole body and individual segment movement. Each major joint contains a sensor (for a total of 21), figure 1, which documents that segment's movement (arc distance and direction of rotation) relative to the adjacent segment. The chest houses the data acquisition system (DAS), the rechargeable battery pack and a six degree of freedom sensor package, which measure the whole body movement in roll, pitch, and yaw. It also contains a triaxiel accelerometer to record accelerations in the X, Y and Z axes. The body also includes four pressure sensors to record the immersion depth of the SWIM. All sensors are oriented and calibrated to the chest cavity, which serves as the baseline reference point for the measured joint articulations. The convention for these measurements is shown in figure 2, which displays the standard for body movement and rotation. The SWIM's 17 Segments are the minimum necessary to characterize a floating person. Each of these segment junctions include a joint sensor with range of motion similar to the human counterpart.

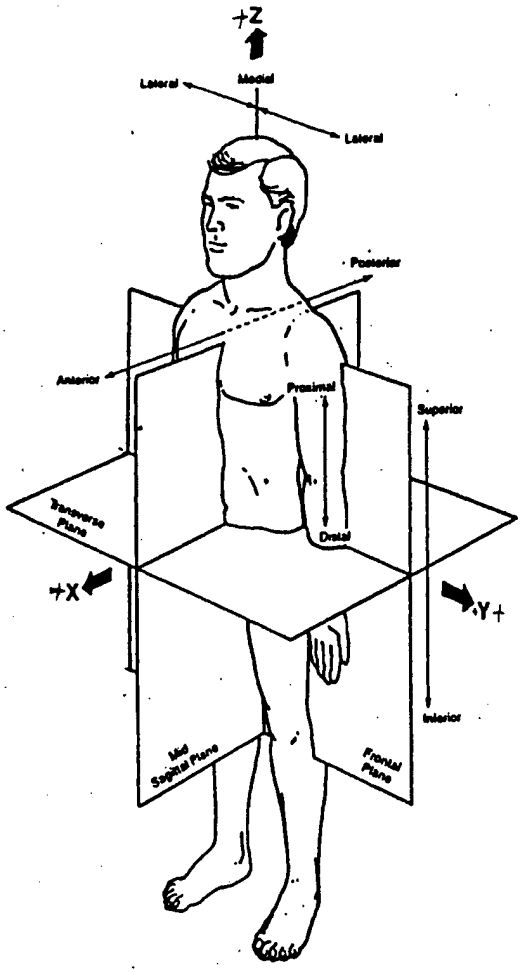

Figure 2. Standard X, Y, Z plane for anatomical measurements.

2.2.2 SWIM Design Changes

The original SWIM, (Macesker, Gareau, 1997), has undergone a few modifications to improve the design and flexibility for testing. The following modifications were made:

1. The emergency inflatable buoyancy device was moved from the mid-abdomen to the head.
2. The material for the chest and head were changed from machined aluminum to polyethylene.
3. The method of adjusting the overall buoyancy of the SWIM was changed from inflatable body segments to a buoyancy vest and a series of buoyancy pockets and ballast system.
4. The water ingestion system to estimate the frequency of head travel or dunkings underwater was removed.
5. The idea of having springs attached to the segment joints to return them to a normal attitude emulating an unconscious person in the water was eliminated for this testing.

These modifications are described as follows: Figures 3 through 9 illustrate the differences between the original SWIM design and the final SWIM as tested at the Institute of Marine Dynamics (IMD). The SWIM skull originally machined from aluminum and coated with chrome is now constructed with high molecular weight polyethylene. This change was made to lighten the overall weight of the SWIM and to provide better placement for the emergency floatation system figure 3. The emergency inflatable floatation bag originally housed in the lower abdomen is now housed in the skull along with the pressure release mechanism and CO^2 cartridge. The system is triggered by a depth sensor, and the bag inflates through flexible skin flaps in the forehead.

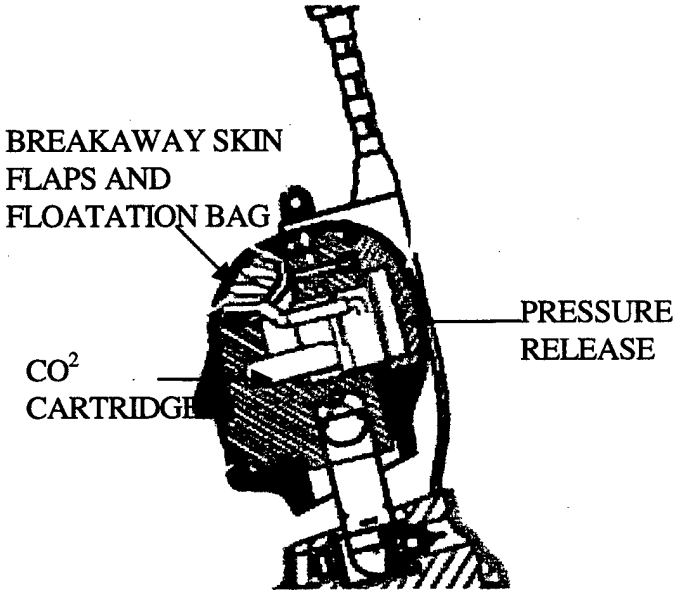

Figure 3. SWIM Emergency Floatation Assembly.

Figure 4 is a front view of the SWIM as tested without the floatation vest. Figure 5 illustrates the old SWIM design. The indentations shown on the mid thigh and similarly incorporated into each major segment are air valves which were used to partially inflate the manikin segments to adjust buoyancy.

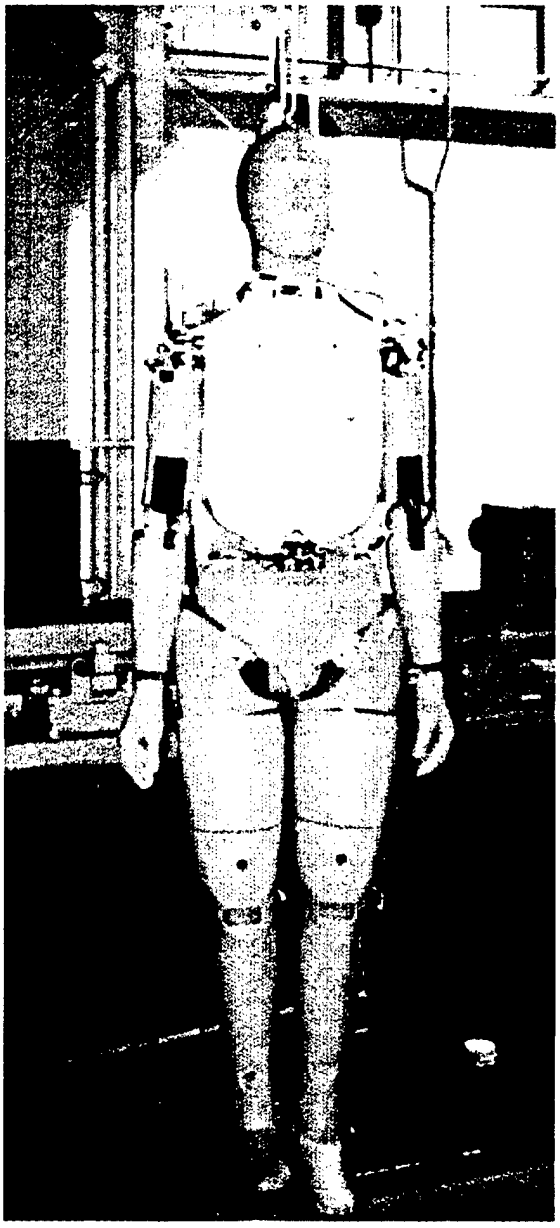

Figure 4. SWIM as tested without floatation vest.

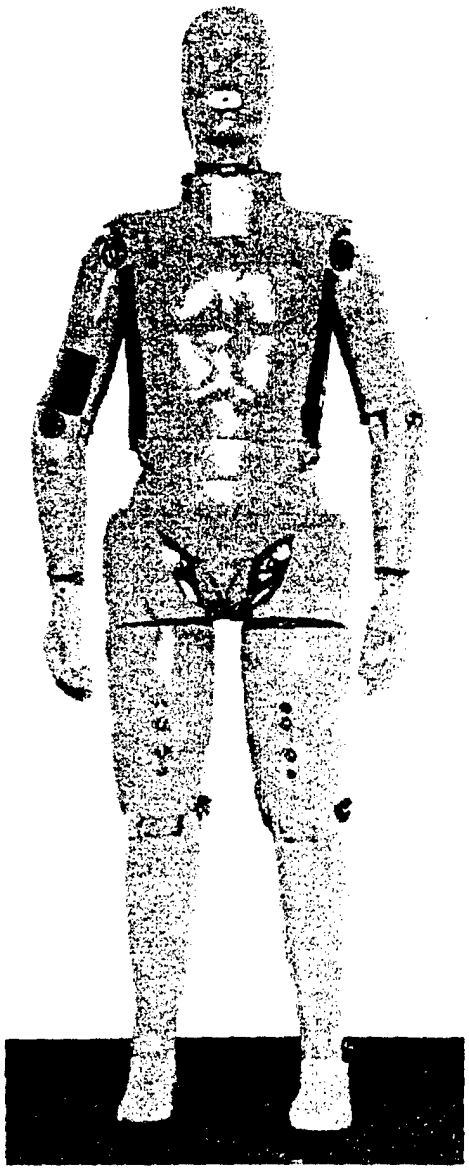

Figure 5. Old SWIM Design.

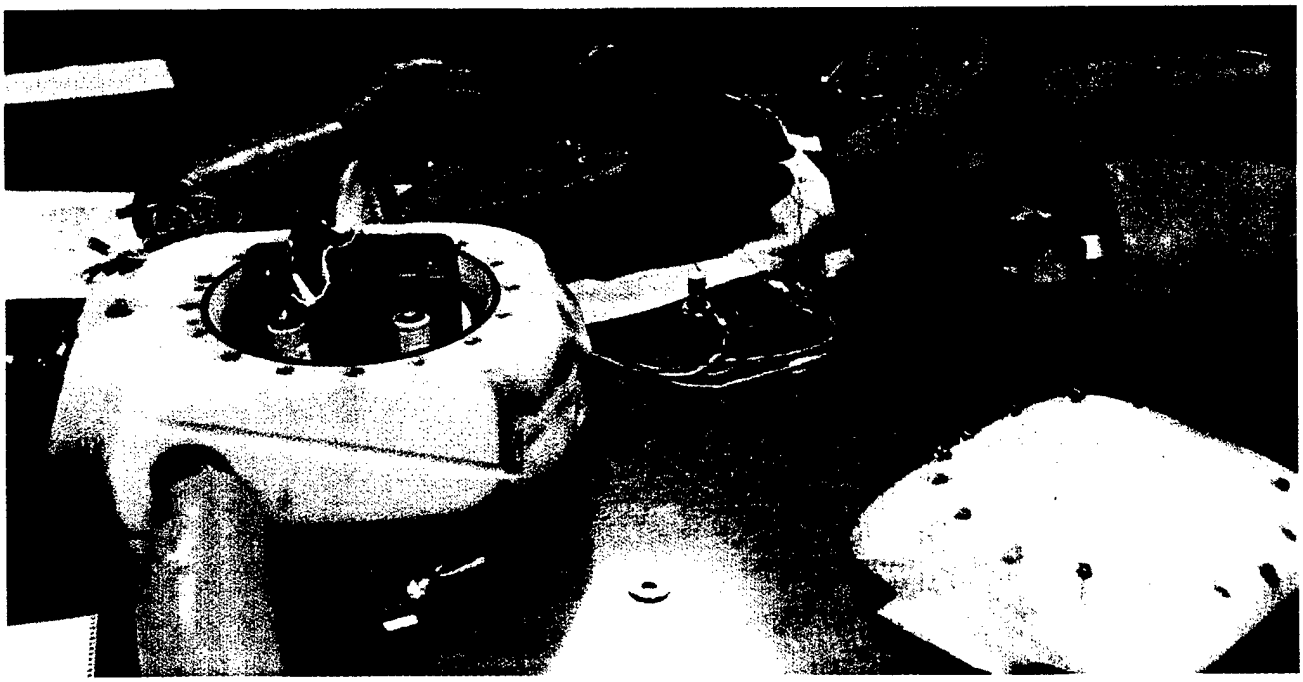

Figure 6. SWIM open-chest cavity with DAS and batteries.

This inflation technique tended to delaminate the core foam from the skin and was dropped in favor of a weighting system using buoyancy pockets which are discussed later in this report. Figure 6 shows the SWIM in a disassembled state revealing the open chest housing the DAS and sensor container, batteries and also shows the O-ring seals and bolt pattern which provide the chest with water tight integrity. Figure 7 is shown to illustrate the changes between the two. This figure shows the aluminum and delrin chest assembly of the old SWIM design. As shown the DAS, internal sensors and battery pack is housed in the chest and the chest was covered with a vinyl skin. The original SWIM design was to have two fixed sizes of chest skins, to allow the SWIM to duplicate a variety of people who tend to float or sink in the water. In figure 5 the opening in the mouth insert can be viewed. This opening was the inlet for the water ingestion system. This system was to allow water to collect through this opening into a collection bag in order to correlate how much water an unconscious person may ingest. This idea was not instituted for this testing. Springs were to be installed on each primary joint. These springs, when the SWIM was floating in the water with the joints unlocked and the segments subjected to water forces of waves, would slowly move the segments back to a preset position much like that of an unconscious person. The springs were an idea developed after the manikin was completed and proved too complex for integration into the design for these tests, however, incorporation into the design at a later time may be possible.

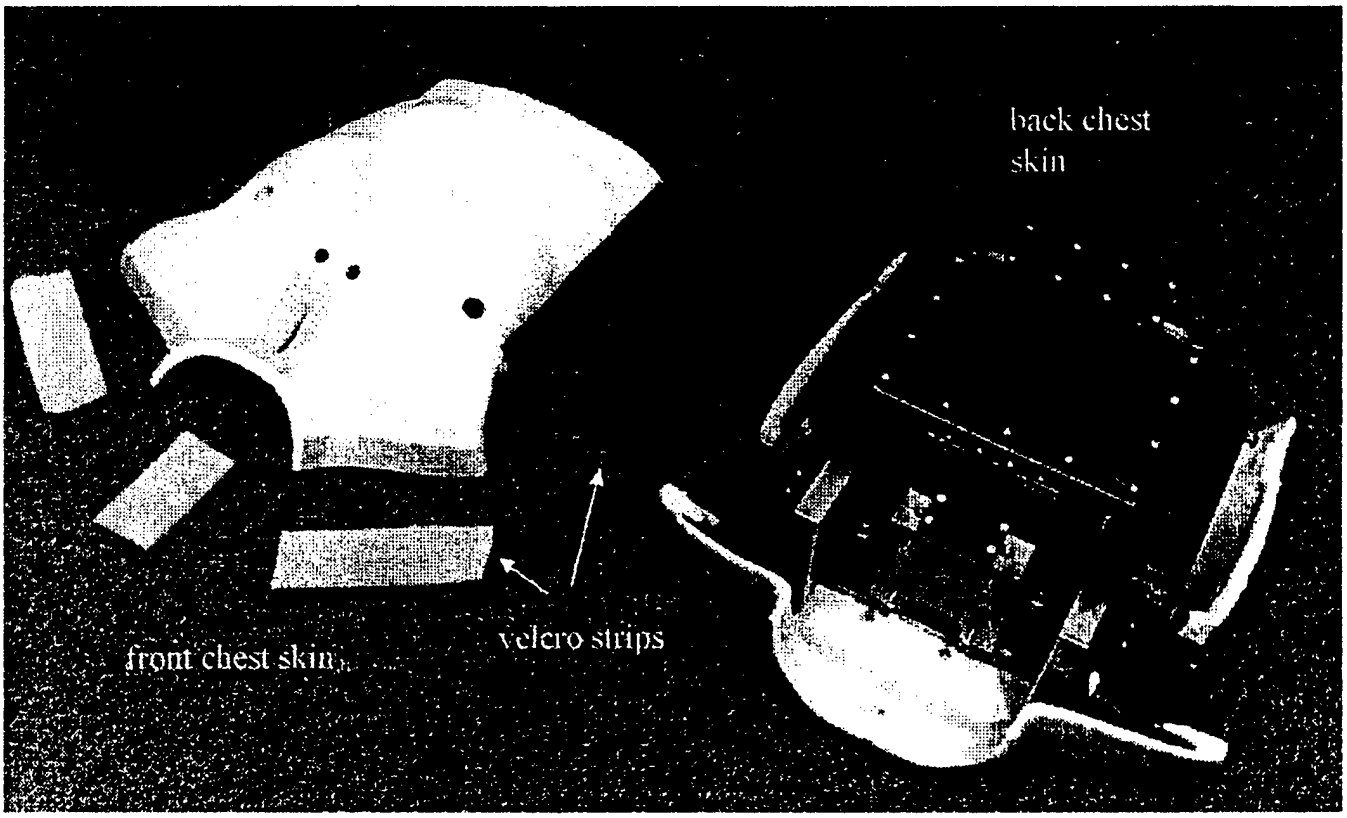

Figure 7. Old SWIM aluminum and Delrin chest cavity with skins.

The front and rear view of SWIM in figures 8 and 9 show the SWIM as tested with the neoprene floatation vest attached and the rigid foam floatation inserts inside.

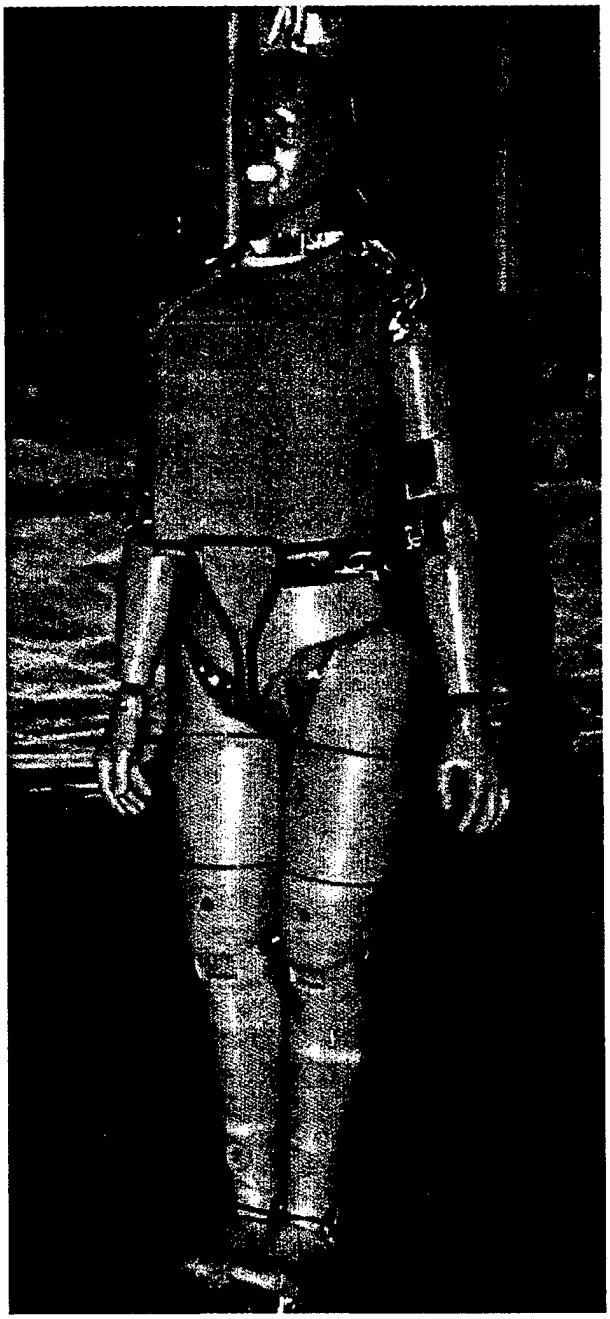

Figure 8. SWIM front view as tested at IMD.

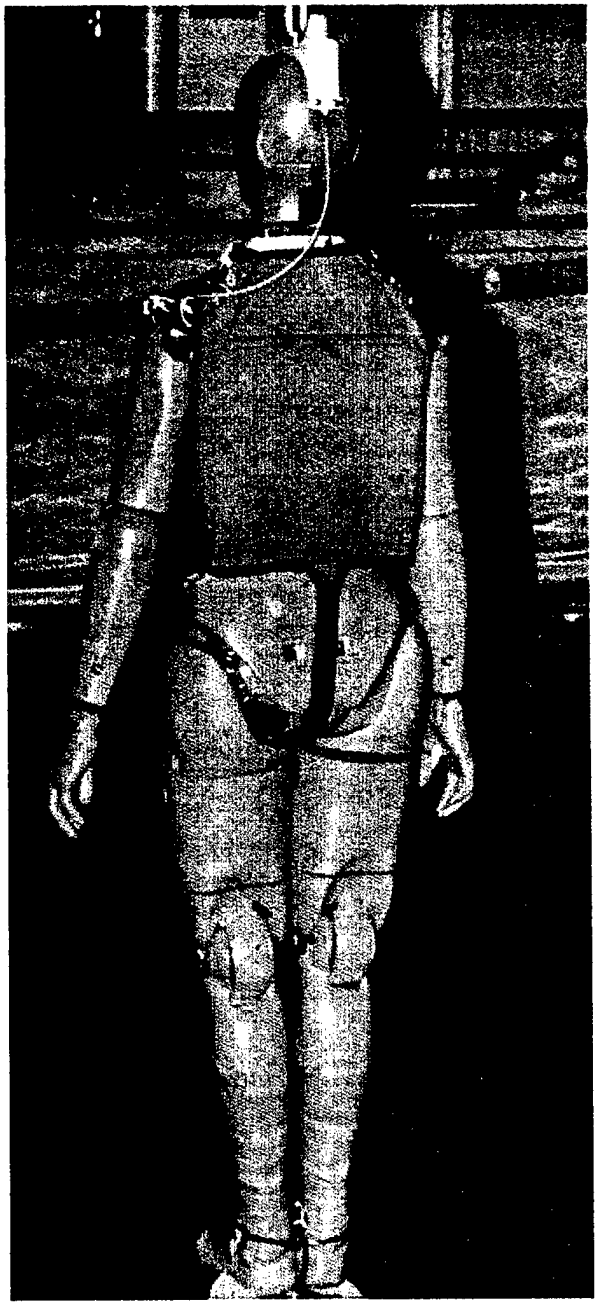

Figure 9. SWIM rear view as tested at IMD.

2.3 WAFAC Overview

The Water Forces Analysis Capability (WAFAC) model (Shams, 1996) was developed by GESAC INC. under contract to the U.S. Air Force. The WAFAC model predicts human body response to still water or to wave conditions. This model can be used to evaluate the effects of body motion in water with and without a PFD attached. The model employs linear wave theory to determine the forces on a submerged body. The forces include buoyancy, wave excitation effects, added-mass, damping, drag, and lift. Incident waves are defined by the wavelength, wave amplitude, and phase angle. The model predicts gross body motion and individual segment accelerations, velocities, and displacements. Buoyancy, added-mass, drag, lift, and wave forces are calculated in user-defined reference frames.

The items of information required to describe the motion of a person wearing a PFD floating in waves for the WAFAC model are: 1) a description of the water surface and water forces acting on the subject; 2) a complete description of the subject in the water, including characterization of individual-linked segments with their segment contour geometry, segment locations, mass-moment-of-inertia, center of mass, buoyancy, and joint torque definitions; and 3) a similar description of the PFD attached to the subject.

The solution of freely floating bodies in surface waves is difficult. The WAFAC model approach uses potential flow theory and employs a viscous treatment in the form of drag and lift effects. Developing a useful model for this application is an iterative process. WAFAC is based on an empirical approach where coefficient values for damping, added mass, and lift will be assumed from simple shape experiments and computer sensitivity studies. Experimental data on linked segments followed by whole body tests will need to be collected. A full size instrumented floatation manikin is also basic to conducting correlation experiments to fine tune and define the range of practical usefulness of the analytical model, i.e., SWIM. The data collected through testing of the SWIM will aid the iterative process of coefficient development for the WAFAC program. In time, SWIM and the WAFAC program will result in a validated computer simulation capability to predict the dynamic behavior of a person wearing a PFD in rough water conditions. In addition, they could be used by manufacturers as a tool to model and optimize survival equipment (PFDs) for boaters and seafarers, as well as set standards for approval.

The WAFAC simulation model predicts the effect of various hydrodynamic forces on the overall motion of a model of a human with or without a PFD. The computer model has been integrated to work with the general-purpose occupant simulation programs DYNAMAN and ATB. These programs are usually used in predicting the kinematics of occupants in high acceleration environments as seen in vehicle crashes or aircraft ejection.

The human being (or its surrogate, a dummy) is modeled using a set of linked segments, where the segments represent the various parts of the human or dummy, such as the head, neck, arms, legs, etc. The inertial properties of each segment are represented by a mass and by the three principal moments of inertia. The link between adjacent segments are modeled using joints with various joint properties that describe the torque versus angle response as one segment is rotated relative to its neighboring segment. The shape of each segment is represented using ellipsoids. The ellipsoids are normally treated as rigid, though for interactions with vehicle panels, some degree of deformation can be modeled.

The WAFAC model computes buoyancy, wave-excitation, added-mass, and drag forces acting on a human or dummy model immersed in water. Capability was also added to the simulation program to calculate a wave-making component of the force, when the ellipsoid is near the surface of the water. The contribution due to this force was based on the work done by (Reynolds, 1993). Sea states can be approximated by the superposition of up to ten regular waves of different wavelengths and amplitudes or by a single regular wave of amplitude and frequency derived from statistical models of sea states encountered in real ocean environments. A more complete description of this development effort has been given in (Weerapulli, 1992). The WAFAC model treats the ellipsoids associated with a system of linked segments as a set of discrete ellipsoids when computing water forces acting on the whole system; i.e., the water force acting on each ellipsoid is evaluated separately without allowing for either the blocking effects of closely located ellipsoids or the effects of overlapping ellipsoids. The model also disregards the effects of neighboring ellipsoids on the local flow pattern around a given ellipsoid.

The postprocessor used for examining the output from the simulations is a modified version of the DYNAMAN postprocessor, which allows the user to look at plots related to the various components of the hydrodynamic forces, such as the hydrostatic drag, added mass, and wave excitation.

2.3.1 Model Validation Objectives

Until the current series of tests with SWIM, the WAFAC model had been checked using the single and hinged ellipsoid tests conducted previously at IMD (McKenna, 1994). The current exploratory testing with SWIM was designed to evaluate the simulation model using the full manikin shape and point out areas where additional improvements would be needed or better definition of input data required. Some of the information that was expected from the testing was:

1. Develop experimental error margins for different initial conditions, based on repeat tests. This provides a lower limit on the accuracy required from the simulations.
2. Obtain effective drag coefficients for the whole manikin in different orientations. It may be possible to use the single, effective drag coefficient in place of the individual drag coefficients for each ellipsoid.
3. Determine which part of the manikin kinematics is modeled well and which part is not. Reasonable replication of the motion of some parts will be considered essential for the program to be treated as a valid model. For example agreement in the position and orientation of the torso as function of time (within acceptable limits) will be an important aim of the model. Since the joints were locked in almost all the tests, these would not be able to resolve how well the kinematics of each individual segment was being predicted.
4. Determine if there is better agreement of such variables as freeboard, repose angle, submerged volume, etc. when examined over longer time periods. That is, does the model make better predictions of the kinematic state of the manikin after initial transient motions are over. For evaluation of PFDs, the long term behavior of the manikin is of great interest and the model should be able to do this well, even if it shows discrepancies during the initial motion.
5. Evaluate which components of the water forces are being simulated well and which are not. There are five principal components comprising the water forces, namely: buoyancy, drag, added-mass, wave damping and wave excitation. The results from the tests should tell us the following about these components:
    a. It is expected that the buoyancy or hydrostatic force should be modeled fairly well, and if any discrepancy arises it would be from miscalculations in the actual volume being submerged.

b. The hydrodynamic coefficients for drag, added mass, and wave damping are based on a number of simplifying assumptions and the simulation of the tests should point out how well these assumptions are working.

c. Simulations of the tests in waves will provide an indication of the suitability of the assumptions used in modeling the wave excitation forces.

2.3.2 Preliminary Simulations

Prior to the simulations of the actual SWIM, a series of preliminary simulations with WAFAC were carried out using characterization data for a Hybrid II dummy, (similar data for the SWIM was not yet available). The overall inertial characteristics of the dummy, which is meant to represent a 50th percentile adult male, was expected to be similar to that of the SWIM. Simulations were performed for the bottom release tests with the different initial configurations, i.e. vertical, horizontal, and right-angled.

In all of these configurations, all of the joints of the dummy were locked. Different values of the drag coefficient (CD); added mass (Ca); and release depth (D), (of the lower torso's center of gravity (CG) from the water surface) were used to see the how these influenced the motion. The same drag and added mass coefficients were used for all segments. The principal output parameters that were watched were: the velocity of the head at the time it reached the surface, the rise time for the head to reach the surface, the maximum displacement of the lower torso, the maximum displacement of the head CG above the water surface (freeboard), the approximate heave period, the maximum rotation angle achieved by the dummy, and the pitch rotation period. All units given below are in inches and inches/sec.

<u>The results from the simulations indicate:</u>

- The time to rise to the surface from a given depth, is relatively constant for various configurations: with a drag coefficient of 0.5 (for all segments) the following was obtained:
    - depth of 100 in (of lower torso CG): rise time = 4 - 5 sec
    - depth of 50 in: rise time = 2- 3 sec
    - depth of 30 in: rise time = 0.5 sec

- The rise time increases with increasing drag, as expected. Doubling the drag coefficient from 0.5 to 1.0, increases the rise time by about 20 – 25 percent.
- Equilibrium velocities, when the drag forces roughly balance the buoyancy forces, are reached only for sufficient release depths. E.g., at release depth of 100 inches, equilibrium velocity is reached, but at release depth of 50 inches it is not.
- Equilibrium velocities are in the range of 25 - 30 in/sec.
- For releases from depths >50 inches in the horizontal and vertical configurations, the maximum displacement of the head CG above the water surface was in the range of 10 - 13 inches. The heave period averaged about 2 sec. For the bent configuration, the body rotated to a position where the lower torso was higher than the legs, and the head stayed under the water surface. The heave period for this configuration was also about 2 sec.
- There is significant horizontal displacement of the dummy for both the horizontal and vertical release configurations. These motions arise because the center of buoyancy is separated from the CG of the body. For the bent configuration, the horizontal displacement is less.
- There is significant rotation for the horizontal and vertical releases. The body continues to perform rotational oscillations after it encounters the water surface. The typical rotation period is about 2 sec. For the bent configuration, there was significant initial rotation, but little after an equilibrium position was obtained. The rotation period was about 4 sec.

2.4 Data Requirements for WAFAC

2.4.1 Integration of SWIM Instrumentation with DYNAMAN Post-Processor

One of the features of the DYNAMAN post-processor, used to view the kinematics predicted by the simulations, is the capability of comparing it with the experimental data obtained from an equivalent test. The experimental data are the output of the sensors in the SWIM, which are acquired by the Data Acquisition System (DAS). This includes the accelerometers, roll, pitch, yaw sensor, rotary potentiometer sensors, and four pressure transducers. The accelerometer data were intended to be used to obtain displacements of the CG of the dummy relative to a laboratory coordinate system (by twice integrating the accelerations). The roll, pitch, and yaw sensors were to be used to obtain the orientation of the upper torso (where these sensors were located) in time. The orientation would actually be used with the acceleration data to track the motion of the CG, since the accelerations are being measured in the body

coordinate system which is rotating over time. The rotary potentiometer data could be used to describe the relative motion of each of the movable segments in the SWIM. Finally, the pressure transducers could be used to define the depth of the dummy relative to the water surface. Thus, with all the sensor data, it would be possible to describe completely the motion of the SWIM in water.

During preliminary testing in September 1998, the software was checked out against the sensor data, and the dummy position was successfully reconstructed. During this testing, it was found that data from the roll and the pitch sensors could not be acquired at the same time. It was decided that for the test configurations planned for the SWIM, the pitch angle measurement was more important. The checkout of the software required proper definition of the initial values of all the sensors, and the relative polarity of the rotation sensors, i.e. which direction of rotation resulted in increasing or decreasing angle values.

2.4.2 Initial SWIM Data

The necessary data, which describes the SWIM, were supplied to the U.S. Coast Guard by Veridian and included:

1- Mass and moments of inertia data of the various segments, including the location of the center of gravity.

2- Geometrical data describing the sizes of the segments constituting SWIM. The model requires the various segments to be approximated by ellipsoids, and the data consists of the semiaxes of these ellipsoids along with the location of their centers.

3- Locations and properties of joints connecting two adjacent segments. The joint properties include the resistive torque generated when the relative angle between the segments is changed, as well as frictional and viscous torque at the joint.

The SWIM was modeled using 16 segments corresponding to the following dummy regions:

1. Lower torso: includes the pelvis and associated flesh and half of the lumbar spine
2. Upper torso: includes the chest up to the base of the neck and the remaining half of the lumbar spine; includes all the region between the shoulders and down to the hips
3. Neck: the segment between the upper and lower neck joints
4. Head: the segment above the upper neck joint
5. Right upper leg: segment between the right hip and the right knee
6. Right lower leg: segment between the right knee and right ankle
7. Right foot: segment below the right ankle

8. Left upper leg: segment between the left hip and the left knee
9. Left lower leg: segment between the left knee and left ankle
10. Left foot: segment below the left ankle
11. Right upper arm: segment between the right shoulder and the right elbow
12. Right lower arm: segment between the right elbow and wrist
13. Left upper arm: segment between the left shoulder and the left elbow
14. Left lower arm: segment between the left elbow and wrist
15. Right hand: segment beyond the right wrist
16. Left hand: segment beyond the left wrist

These segments correspond to actual hardware segments and also include the flesh/skin that covers the corresponding segment. The inertial and geometric measurements were made on these individual segments. The data were supplied for both the ballasted and non-ballasted configurations. As originally delivered, ballast weights were added to the upper torso (thorax), left and right upper arms, left and right lower arms, left and right upper legs, and left and right lower legs. The total ballast weight was approximately 17.5 lbs. (8 kg). Based on these initial data, initial simulations were performed with the WAFAC model. From these simulations, the initial estimates of the center of gravity and center of buoyancy were determined for both the fully ballasted and non-ballasted cases. Table 1 shows the distribution of masses and ellipsoid sizes as initially supplied for the fully ballasted case. Table 2 shows the equivalent data for the non-ballasted case.

Table 1. Distribution of masses and ellipsoid sizes for SWIM segments (ballasted).

No.	Segment	Symbol	Mass (LB)	Semiaxis X (in)	Semiaxis Y (in)	Semiaxis Z (in)	Ctr Off X (in)	Ctr Off Y (in)	Ctr Off Z (in)
1	Lo Torso	LT	14.22	4.9	6.94	6	0	0	-0.27
2	Up Torso	UT	55.4	5.6	7.16	9	0	0	0.5
3	Neck	N	3.86	2.7	2.28	4	-0.1	0	-1.1
4	Head	H	10.36	4	3.1	5	0.5	0	0.4
5	Rt Up Leg	RUL	16.25	3.3	3.5	11.4	0.15	0	1.4
6	Rt Lo Leg	RLL	9.47	2.36	2.23	9.45	0	0	0.8
7	Rt Foot	RF	1.82	5.22	1.6	1.52	0	0	-0.9
8	Lt Up Leg	LUL	16.25	3.3	3.5	11.4	0.15	0	1.4
9	Lt Lo Leg	LLL	9.47	2.36	2.23	9.45	0	0	0.8
10	Lt Foot	LF	1.82	5.22	1.6	1.52	0	0	-0.9
11	Rt Up Arm	RUA	4.19	2.07	1.64	6.88	0	0	0
12	Rt Lo Arm	RLA	3.46	1.775	1.775	5.8	0	0	1.2
13	Lt Up Arm	LUA	4.19	2.07	1.64	6.88	0	0	0
14	Lt Lo Arm	LLA	3.46	1.775	1.775	5.8	0	0	1.2
15	Rt Hand	RH	0.66	1.87	1	3.65	0	0	0
16	Lt Hand	LH	0.66	1.87	1	3.65	0	0	0

Based on the preceding data, the following characteristics for the whole dummy, in fully ballasted condition, were obtained.

Total Full Ballast Wt = 155.5 LB
Total Height = 68.8 in
Total Vol. (separate ellipsoids)= 4760 in^3
Total Displaced Wt (sep. ellip) = 172.2 LB
Net Buoyancy = 16.7 LB

Estimated CG = X = 2.11 in, Y = 0, Z = -38.5 in
(from bottom corner of heel)
Estimated Buoyancy ctr = X = 2.20 in, Y = 0., Z = -37.6 in
(from bottom corner of heel)

NOTE 1: The total displaced volume, for a fully immersed dummy, was based on the assumption that there was no overlap between the ellipsoids. This was not totally true for the ellipsoids as defined above. Modifications to the initial ellipsoid sizes were done to bring the expected buoyancy closer to the measured value.

NOTE 2: The SWIM data supplied to the Coast Guard was in English units. These units were retained for all the simulations. Most of the graphical plots were converted to metric units.

Table 2. Distribution of masses and ellipsoid sizes for SWIM segments (non-ballasted).

No.	Segment	Symbol	Mass (LB)	Semiaxis X (in)	Semiaxis Y (in)	Semiaxis Z (in)	Ctr Off X (in)	Ctr Off Y (in)	Ctr Off Z (in)
1	Lo Torso	LT	14.22	4.9	6.94	6	0	0	-0.27
2	Up Torso	UT	49.03	5.6	7.16	9	0	0	0.5
3	Neck	N	3.86	2.7	2.28	4	-0.1	0	-1.1
4	Head	H	10.36	4	3.1	5	0.5	0	0.4
5	Rt Up Leg	RUL	13.96	3.3	3.5	11.4	0.15	0	1.4
6	Rt Lo Leg	RLL	7.46	2.36	2.23	9.45	0	0	0.8
7	Rt Foot	RF	1.82	5.22	1.6	1.52	0	0	-0.9
8	Lt Up Leg	LUL	13.96	3.3	3.5	11.4	0.15	0	1.4
9	Lt Lo Leg	LLL	7.46	2.36	2.23	9.45	0	0	0.8
10	Lt Foot	LF	1.82	5.22	1.6	1.52	0	0	-0.9
11	Rt Up Arm	RUA	3.55	2.07	1.64	6.88	0	0	0
12	Rt Lo Arm	RLA	2.78	1.775	1.775	5.8	0	0	1.2
13	Lt Up Arm	LUA	3.55	2.07	1.64	6.88	0	0	0
14	Lt Lo Arm	LLA	2.78	1.775	1.775	5.8	0	0	1.2
15	Rt Hand	RH	0.66	1.87	1	3.65	0	0	0
16	Lt Hand	LH	0.66	1.87	1	3.65	0	0	0

Based on the preceeding data, the following characteristics for the whole dummy, in fully ballasted condition, were obtained.

No Ballast Wt = 137.9 LB
Total Height = 68.8 in
Total Vol. (separate ellipsoids) = 4760 in^3
Total Displaced Wt (sep. ellip) = 172.2 LB
Net Buoyancy = 34.3 LB
Estimated CG= X = 2.18 in, Y = 0, Z = -39.0 in
(from bottom corner of heel)
Estimated Buoyancy ctr = X = 2.27 in, Y = 0., Z = -37.5 in
(from bottom corner of heel)

These preliminary estimates would have to be verified by actual measurements at IMD.

2.5 Test Plan Overview

Three types of tests were conducted with the SWIM. For each type of test, a number of configurations were used to vary the initial conditions. The basic types of tests and their initial configurations are:

1. Bottom release tests from equilibrium

The manikin was released from measurable initial conditions below the water's surface Two underwater cameras tracked reflective tape on the manikin for post-test digitization. The manikin's joints were locked. The manikin was released from the following initial positions; as depicted in figure 10.

Configurations:

1.1a from a face-up and flat-on-the-back position with all joints locked, (figure 10, configuration 1).

1.1b from a face-up and flat-on-the-back position with all joints locked and with greater weight redistributed to lower limbs, (figure 10, configuration 1).

1.2a from a vertical stand-up position with all joints locked, (figure 10, configuration 2).

1.2b from a vertical stand-up position with all joints locked and with more weight redistributed to the upper body, (figure 10, configuration 2).

1.3 from a bent-at-the waist position with all joints locked, (figure 10, configuration 3).

The buoyancy of specific components of SWIM were adjusted using the foam/Delrin/lead plug inserts to assess the sensitivity of buoyancy over drag effects. SWIM's Data Acquisition System (DAS) collected

data from these tests. The tests were repeated a minimum of three times to develop a repeatability envelope. At least two different depths were used for configurations 1.1 and 1.2 to provide information for estimating an effective drag coefficient for the whole manikin

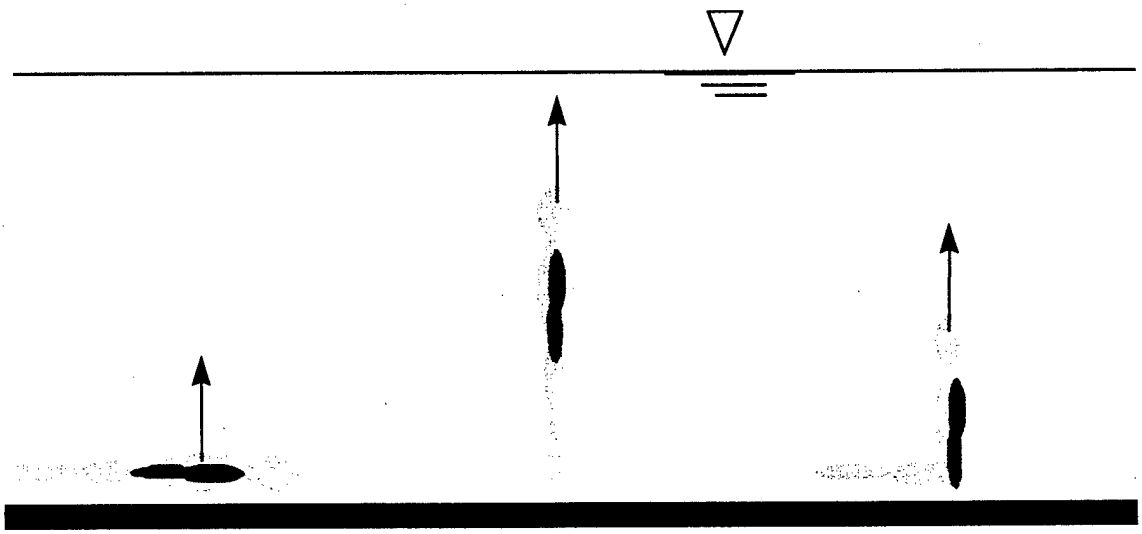

Test Configuration 1
o joints locked
o 1(a) normal outfit
o 1 (b) redistribution of weight to lower limbs

Test Configuration 2
o joints locked
o 2(a) normal outfit
o 2 (b) redistribution of weight to lower limbs

Test Configuration 3
o joints locked

Figure 10. Bottom release tests from equilibrium (IMD tow tank)

2. Push-glide tests at the water surface

The push-glide tests consisted of a push of the manikin along a horizontal path parallel to the water's surface, allowing the manikin to glide along the surface several feet before its inherent buoyancy begins to right itself. SWIM was pushed by the wave tank carriage. The carriage was brought to a stop which allowed the manikin to float free. Two in-air digital cameras were used to track the trajectory of SWIM for post-test digitization. The manikin was face down and parallel to the water-plane with all joints locked. The manikin was released from the following initial positions.

Configurations:

2.1a head forward with all joints locked

2.1b head forward with all joints locked and with more weight redistributed to lower limbs

2.2a feet forward with all joints locked

2.2b feet forward with all joints locked and with more weight redistributed to lower limbs

Figure 11 illustrates the test configurations. SWIM's DAS collected data from these tests. The tests were repeated a minimum of three times to develop a repeatability envelope.

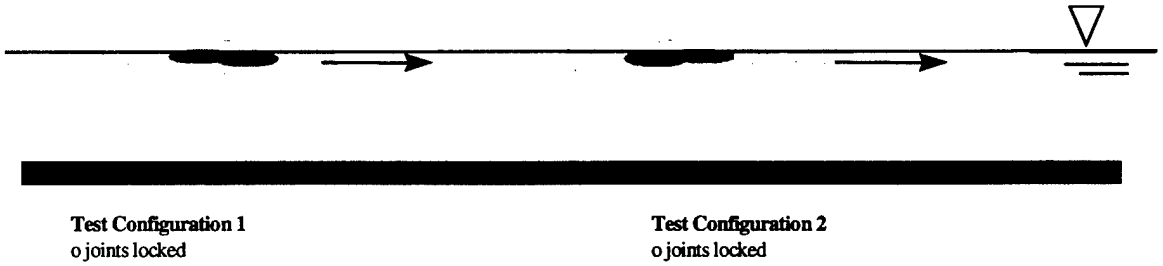

Figure 11. Push-Glide Tests (IMD Tow Tank)

3. Whole body tests in waves

This test requires the use of the wave-making towing tank at IMD. Whole-body testing with the joints locked and unlocked were performed for the following manikin positions,

Configurations:

3.1 from a face-up and flat-on-the-back position with all joints locked

3.2 from a vertical stand-up position with all joints locked

3.3 from a slightly bent-at-the waist position with all joints locked

3.4 from a slightly bent-at-the-waist position with all joints unlocked

3.5 from a slightly bent-at-the-waist position with all joints unlocked and with joint recoil springs installed

Figure 12 illustrates the test configurations. SWIM's DAS collected data from these tests. The tests were repeated a minimum of three times to develop a repeatability envelope.

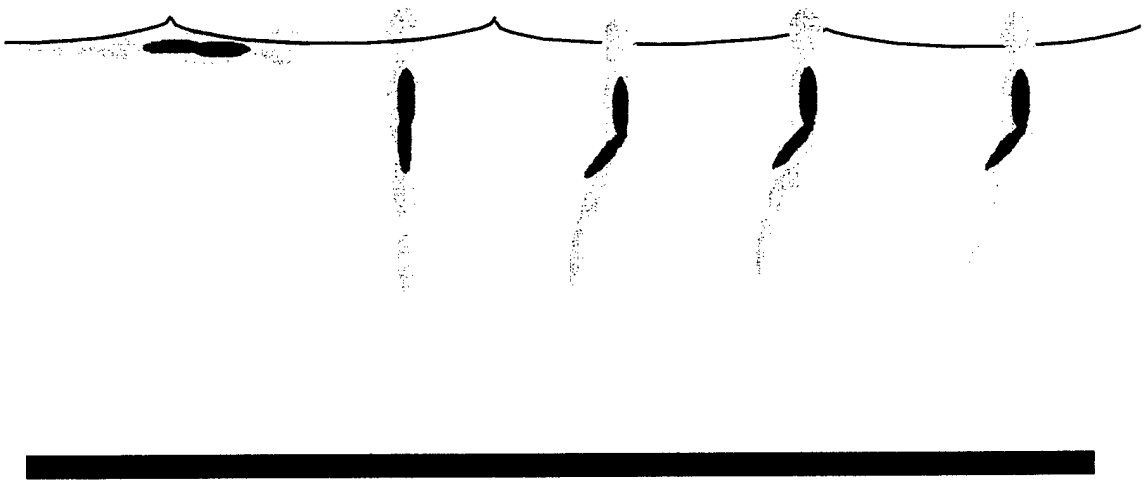

Test Configuration 1	Test Configuration 2	Test Configuration 3	Test Configuration 4	Test Configuration 5
o joints locked	o joints locked	o joints locked	o joints unlocked w/o recoil springs	o joints unlocked w/o recoil springs

Figure 12. Whole Body Tests in Waves (IMD Tow Tank)

2.6 IMD Test Facilities

The Testing for SWIM was performed at the Institute for Marine Dynamics (IMD) in St. John's, Newfoundland, Canada. IMD is a branch of the National Research Council of Canada, the principal science and technology agency for Canada. IMD was established in 1985 to provide solutions and technical support to Canadian ocean technology industries. The towing tank used for the testing of SWIM is a rectangular tank 200 meters (656.17 ft) in length, 12 meters (39.37 ft) in width and seven meters (22.97 ft) deep. A computer controlled dual flap hydraulic wave generator is supported at one end of the tank, which can create one-meter high regular waves or 0.5 meter irregular waves. A 10.5 degree beach is supported on the other end for wave absorption with two trim dock areas for additional testing. An 18-ton carriage spans the tank supported on both sides of the tank by railroad type tracks. The carriage contains computer control for the wave maker and carriage propulsion, with additional computers to support the measurement systems and sensors for the testing of model hulls as well as the mechanical support and interface for the models or devices under test. The Institute contains two other very large testing tanks, as well as mechanical, model making, painting and testing areas and all the support capabilities required for this work. IMD has a technical staff of approximately 90 people.

3.0 PRE-CALIBRATION TESTS

R&D Center staff performed some in-water calibration tests with SWIM from 19 through 21 February in preparation to the actual preliminary testing involving the IMD staff. Actual testing took place between 22 February and 5 March 1999. The following in-water tests were performed.

1- A visual inspection of individual segments and sensor system check was performed on SWIM. SWIM was shipped from the CG Research & Development Center three months before testing.
2- In-water and in-air overall SWIM weights.
3- Using the trim dock, load cell, and crane, a normal outfit test configuration and an off-normal outfit test configuration were determined.
4- Validation of volumetric measurements by incremental immersion of the whole-body SWIM manikin was completed in the trim dock.

3.1 Weights and Buoyancy Calibration

During the preliminary set up and testing a number of discrepancies were discovered which effected the test weight of the SWIM. A brief background and discussion of the solutions imposed follows. Using the Air Force ATB model, two test cases for manikin weights were defined for our preliminary testing which best represented a 50th percentile person. One weight was that of a normal 50th percentile manikin and the second was that of a lighter manikin or off-normal. These two test configurations for the normal weight manikin include all additional weights and for the off normal manikin no additional weighting (table 3). The SWIM was manufactured with pre-positioned voids in the torso and appendages called ballast pockets (figure 13). These pockets are used to modify the manikin's buoyancy by filling with weights, to make the manikin heavier and less buoyant, or flotation discs to make the manikin lighter and more buoyant. The lead weights were provided in the form of 1.5-inch disks of varying thickness, the floatation discs were made of Styrofoam. The total weight difference for the manikin from heavy to light was designed to be approximately 10 percent. These weights are distributed on the appendages at or near the center of gravity of each segment. The Upper Torso has two sealed ballast compartments which hold

up to 1250 grams (2.76 lbs.) each, while the Upper Leg, Upper Arm, and Lower Arm each have two compartments, and the Lower Leg has three. Each ballast compartment holds one or more discs depending on the volume of the segment.

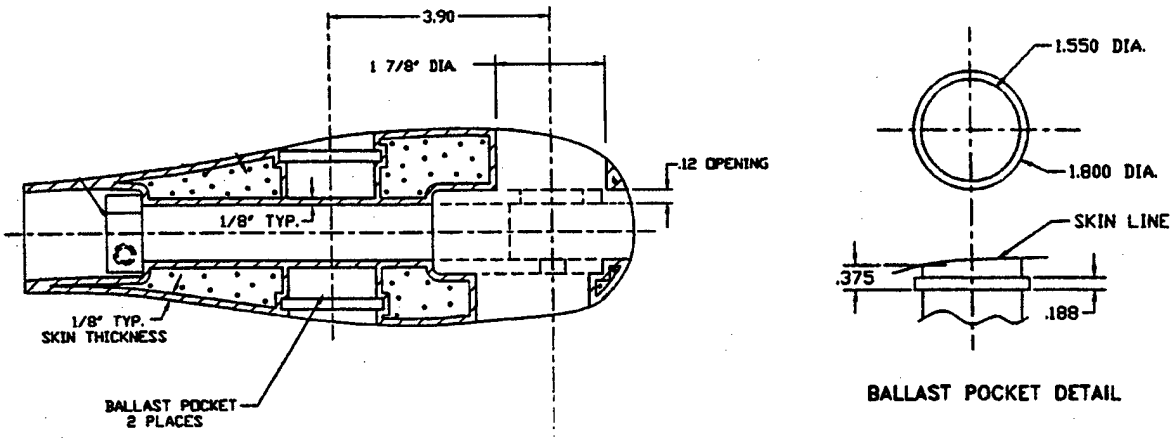

Figure 13. Example of ballast pocket in lower arm.

Additional buoyancy is added to the SWIM in the form of the floatation vest and inserts which add to the overall weight as well. The back vest, front vest and buoyancy pads are constructed of 5/16 inch neoprene. The front and back vest include pockets on the inside to hold up to a total of five floatation pads each originally also to be made of neoprene. The normal outfit for the SWIM is nine inserts, five in the front and four in the back. These are 11-3/4 in square. The front vest is secured to the back vest with zippers and laces. The total weight of the front vest, back vest and nine inserts dry is 9.7 lbs. Individual neoprene pad weights are 163 grams (0.36 lbs.). Table 3 lists the requirements for the original Air Force normal and off normal manikin weight distribution and the final normal and off normal weighting devised for these tests.

Table 3. Original Manikin Weights and Final Test Weights (Dry)

	Original Weight			Final Test Weights	
	Normal Weight (lbs.)	Off Normal Weight (lbs.)	CG & CB Intermediate Weight (lbs.)	Normal Weight (lbs.)	Off Normal Weight (lbs.)
SWIM Weight	138	138	138	138	138
Added weight to each Segment in Pockets					
Upper Torso (UT)	5.53	0.0	0.0	0.0	0.0
Right Upper Leg (RUL)	2.29	0.0	2.29	2.29	0.0
Right Lower Leg (RLL)	2.01	0.0	2.01	2.01	0.0
Left Upper Leg (LUL)	2.29	0.0	2.29	2.29	0.0
Left Lower Leg (LLL)	2.01	0.0	2.01	2.01	0.0
Right Upper Arm (RUA)	0.64	0.0	0.0	0.0	0.0
Right Lower Arm (RLA)	0.68	0.0	0.0	0.0	0.0
Left Upper Arm (LUA)	0.64	0.0	0.0	0.0	0.0
Left Lower Arm (LLA)	0.68	0.0	0.0	0.0	0.0
Front Buoyancy Vest	2.7	2.7	2.7	2.7	2.7
Rear Buoyancy Vest	3.8	3.8	3.8	3.8	3.8
Float Pads Neoprene(9)	3.23	3.23	3.23	---	
Float Pad Styrofoam (4 pad replacement)	----	----	----	0.242	0.242
Float Pad Styrofoam (5 pad replacement)	-----	----	----	0.339	0.339
TOTAL WEIGHTS	164.5	147.53	156.33	153.68	145.08

In preparation for the start of testing, the SWIM was loaded with the weights in table 3 (Original Normal), for a maximum weight set of 164 lbs. The front and back skin was filled with nine buoyancy pads and the SWIM was slowly lowered into the water at the test dock. The manikin became negatively buoyant at this heavier weight. The negative buoyancy of the SWIM was measured with a spring scale and it was found to be 4.5 lbs. negatively buoyant. Calculations were made to find out how many weights had to be removed to give the SWIM a positive buoyancy of 4.5 lbs. The two calculated test weight values for our simulated manikin (from the U.S. Air Force ATB model input files), were for all weight and no weight. It was concluded for ease of computer modeling that rather than remove some weight from all segments,

it would be more prudent to remove all the weight from specific segments. The weights from the torso, upper and lower arms were completely removed. This accounts for slightly over 14 lbs. The resultant buoyancy would then be about a positive 10 lbs. The SWIM was again lowered into the test pool and the buoyancy measured with a spring scale was 8.5 lbs. Final testing weights for the two test cases of a normal and off normal manikin are found in table 3, marked as Final Test Weights (dry). Discrepancies in weights are normal due to water absorption and captive water in crevices of the SWIM. The discrepancies between some test weights (wet) and dry weights were substantial. This added weight results in small changes to the overall CB and CG measurements which effect larger changes in the WAFAC simulations.

3.2 Water Intrusion

During the preliminary testing cracks were observed in the right and left hip segments (figure 14). As the SWIM was more closely inspected cracks were found as well in each foot. These cracks or weak points seemed to be prominent at places where the skin of the manikin was cast at a right angle to fit around the stainless steel frame of the SWIM. In the feet the cracks were hidden and the feet had to be removed to squeeze out the water. The water was pressed out of each segment and attempts were made to seal the crack by melting them together with a soldering iron, room temperature vulcanizing rubber (RTV), and inner tube type patches. Usually, not more than a few ounces of water could be squeezed out of each segment. The right and left hip segments were easily removed and they were measured at one point after the water was squeezed out. The right hip segment weight was 1283 grams (2.83 lbs.) and the left segment was 1409 grams

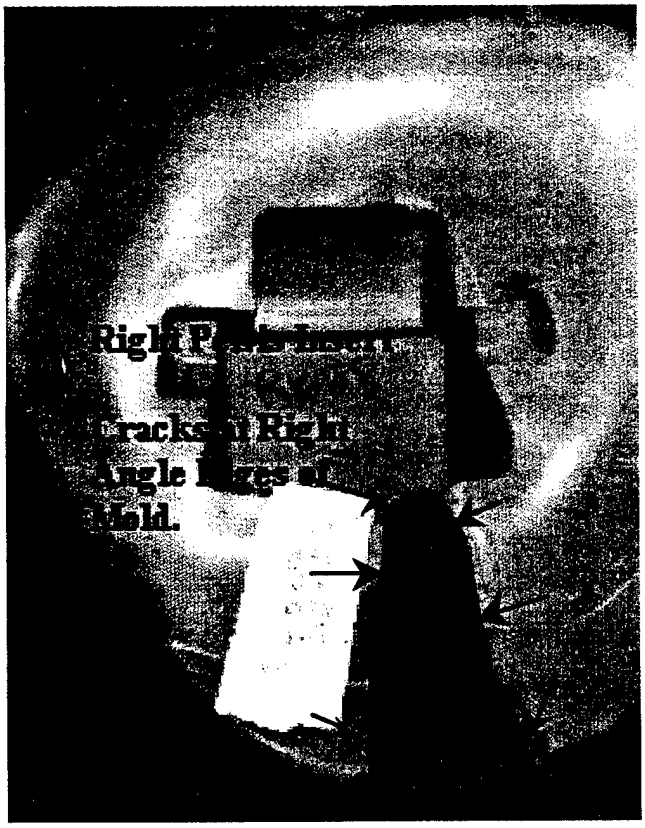

Figure 14. Seam crack on right pelvis insert.

(3.10 lbs.) a difference of 126 grams (0.28lbs). If this were all due to captive water and one segment is completely dry this accounts for 4.4 ounces of water. The original weight for each of these two segments was 2.13 lbs. / 966 grams. If this were the original weight each segment had absorbed a significant amount of water. These cracks continued to be a problem throughout testing.

3.3 Floatation Pads Neoprene/Styrofoam

The back and chest vest which supports the buoyancy pads is constructed of 5/16 inch neoprene with a pocket inside the front and back to hold additional pads of neoprene, five in the front and four in the back. At the start of the seven meter bottom release tests at the original normal weight the SWIM failed to rise to the surface on its own. It was discovered that the vest with the nine inserts all made from neoprene lost much of the buoyancy it has near the surface. At a depth of about 10 feet the neoprene compressed causing the SWIM to become negatively buoyant. This problem was solved by replacing the neoprene inserts with a high density Hygrofoam® a product of DOW Chemical Company which did not compress at the test depths used nor absorb water. Solid inserts were made to replace the pads used in the front and back vests. These inserts were sized so the buoyancy was exactly the same as the neoprene pads replaced. Two additional inserts were made with the same buoyancy as a single pad. The weight of the front and back vest together is 6.5 lbs. and each of the nine neoprene pads were 167 grams/0.368 lbs. each. The total weight for the combination of vest and nine pads dry is 9.73 lbs. The replacement Styrofoam inserts, one replacing four pads, measured 11 inches square x 1-inch thick and weighed 109.7 grams (0.242 lbs.); the second insert, which replaced five of the old pads, measured 11 inches square x 1-3/8 inch thick and weighed 153.8 grams (0.339 lbs.); or a total weight for both of 0.58 lbs. The overall weight for the final floatation vest and inserts is 7.08 lbs.; this reduced the overall weight by 2.65 lbs.

3.4 Final SWIM Test Weight

The changes in weight distribution due to the partial removal of ballast weights, the changes in floatation pad material, and the water absorption of the two foot and two pelvis segments all play a part in changing the basic attributes of the SWIM as prescribed for the WAFAC model. The resultant modified weights for our testing purposes would include: 1) Normal weight with the SWIM vest filled with the five pad foam insert in front, and four pad foam insert in back with no weight in the torso, upper arms or lower arms, and full weights in the upper and lower legs as in table 3; the weight of Normal outfit SWIM dry

is 154 lbs.; and 2) Off Normal Outfit weight with the SWIM vest filled with the four and five pad foam insert and no additional weighting in any segment, dry 145 lbs.

4.0 TESTING AND CALIBRATION

4.1 Calibration of SWIM Data Acquisition System

The SWIM contains a miniature, expandable, high speed data acquisition system DAS 32 series manufactured by EME Inc. (figure 15). The SWIM data acquisition system (DAS) drives a suite of sensors to translate the manikin's movement into engineering data. The DAS contains 32 analog channels and 16 digital inputs; it requires a PC/AT computer and a DOS operating system. The DAS is powered by a 12VDC, 5 ampere hour (Ah), rechargeable NICAD battery pack. The DAS, battery pack, accelerometers, yaw sensor, and roll and pitch sensors are housed in the chest. Four pressure sensors are on the out board sides of the torso, two at the shoulders and two at the hips. Joint position sensors are distributed throughout the SWIM body. The DAS is programmed and controlled with a computer through an RS232 interface at up to 115 kbaud. Once the DAS is calibrated and set up for sampling and acquisition, a data scan trigger is accomplished through a hard wire connection or by a remote transmitter. This transmitter is also used to re-trigger additional data scans or to shut off the DAS when the number of data runs are completed to conserve batteries. The DAS has a programmable sample rate between 10 Hz and 20,000 Hz. All data collected is sampled simultaneously and stored onboard in non-volatile memory of 32 megabytes. Onboard firmware and circuitry provides automatic calibration features for each sensor. Each channel is short circuit protected and has programmable gain, offsets, and filtering.

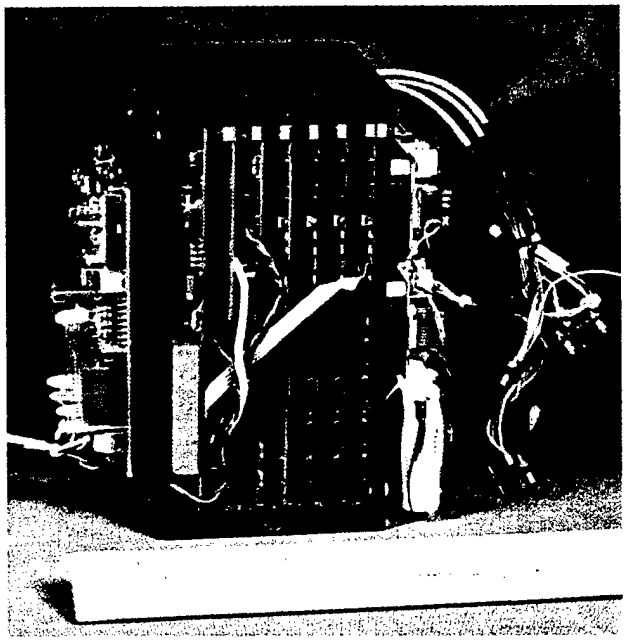

Figure 15. DAS and internal sensors.

The 32 sensors on board the SWIM are broken up into three categories of sensors, each requiring a different method of calibration. These sensors require calibration before each test sequence.
The three types of sensors and calibration techniques are:

1- RCAL Sensors. These sensors include bridge type sensors and include the four pressure transducers, three accelerometers and roll and pitch channels. RCAL sensors are calibrated electronically by selecting the sensor channel number under the DAS RCAL program screen. The sensor's offset and gain are calculated using that channel's Max and Min value and sensitivity by the DAS.

2- JCAL Sensors. These sensors are generally resistive sensors and include the 21 joint sensors used throughout SWIM. The RCAL sensors are calibrated by first selecting the RCAL calibration screen and selecting a channel. The DAS program steps through a two-point preprogrammed calibration process (table 4). The sensor, for example in the case of the SWIM, a shoulder, is moved to line up two marks for the first calibration point and the computer makes a measurement at that point, the same routine is used for the second point with a second set of alignment marks. The program then calculates offsets and gains for that channel.

3- NOCAL Sensors. These sensors include other types of sensors which do not fit into the first two types and include the compass. This sensor is selected through the NOCAL computer screen and is calibrated similarly to the JCAL sensor.

Table 4 is a table of channel numbers, sensor names, static calibration points where applicable, minimum and maximum values of travel (CH 8-20 & 25-32), or minimum maximum electronic limits (CH 1-7 & 21-24), and engineering units as compiled for the testing. Many of the SWIM sensors have mechanical limits with marked calibration points as well as electrical limits. Figure 16 relates sensors' placements and sensor channel number to the SWIM. The channels housed in the chest cavity with the DAS and battery pack are noted.

Table 4. DAS Channel Setup Data.

DAS CHANNEL NUMBER	CALIBRATION POINT 1	CALIBRATION POINT 2	MINIMUM VALUE	MAXIMUM VALUE	ENG UNITS
CH 1 Z ACCELERATION	NA	NA	-2.0	2.0	G's
CH 2 Y ACCELERATION	NA	NA	-2.0	2.0	G's
CH 3 X ACCELERATION	NA	NA	-2.0	2.0	G's
CH 4 PITCH	NA	NA	-60.0	60.0	DEG's
CH 5 ROLL	NA	NA	-60.0	60.0	DEG's
CH 6 COMPASS	NA	NA	0.0	360.0	DEG's
CH 7 UNUSED	NA	NA	NA	NA	NA
CH 8 RT SHOULDER FRONT TO BACK	-45.0	45.0	-90.0	140.0	DEG's
CH 9 RT SHOULDER SIDE TO SIDE	3.0	46.0	-5.0	150.0	DEG's
CH 10 RIGHT ELBOW	6.0	44.0	0.0	140.0	DEG's
CH 11 UPPER NECK	0.0	14.9	-5.0	20.0	DEG's
CH 12 LOWER NECK	-12.9	46.3	-15.0	50.0	DEG's
CH 13 RIGHT LOW ARM	-20.0	108.0	-25.0	110.0	DEG's
CH 14 NECK S TO S	-32.7	32.7	-35.0	35.0	DEG's
CH 15 LUMBAR SIDE TO SIDE	-7.8	7.8	-20.0	20.0	DEG's
CH 16 LUMBAR F TO B	-16.1	2.0	-20.0	20.0	DEG's
CH 17 RIGHT HIP FRONT TO BACK	-25.2	50.0	-60.0	100.0	DEG's
CH 18 RIGHT HIP SIDE TO SIDE	0.0	24.0	-10.0	60.0	DEG's
CH 19 RIGHT KNEE	21.4	76.7	0.0	125.0	DEG's
CH 20 RIGHT ANKLE	-32.7	25.1	-50.0	45.0	DEG's
CH 21 PRESS UPPER RIGHT	NA	NA	-0.1	9.5	PSI
CH 22 PRESS LOWER RIGHT	NA	NA	-0.1	9.5	PSI
CH 23 PRESS UPPER LEFT	NA	NA	-0.1	9.5	PSI
CH 24 PRESS LOWER LEFT	NA	NA	-0.1	9.5	PSI
CH 25 LEFT LOW ARM	-95.0	20.0	-105.0	25.0	DEG's
CH 26 LEFT ELBOW	5.0	55.6	0.0	140.0	DEG's
CH 27LEFT KNEE	23.6	68.3	0.0	125.0	DEG's
CH 28 LEFT HIP FRONT TO BACK	-26.3	52.6	-60.0	140.0	DEG's
CH 29 LEFT HIP SIDE TO SIDE	0.0	25.0	-10.0	60.0	DEG's
CH 30 LEFT ANKLE	-39.0	41.0	-50.0	45.0	DEG's
CH 31 LEFT SHOULDER FRONT TO BACK	-45.0	45.0	-90.0	140.0	DEG's
CH 32 LEFT SHOULDER SIDE TO SIDE	0.0	42.4	-5.0	150.0	DEG's

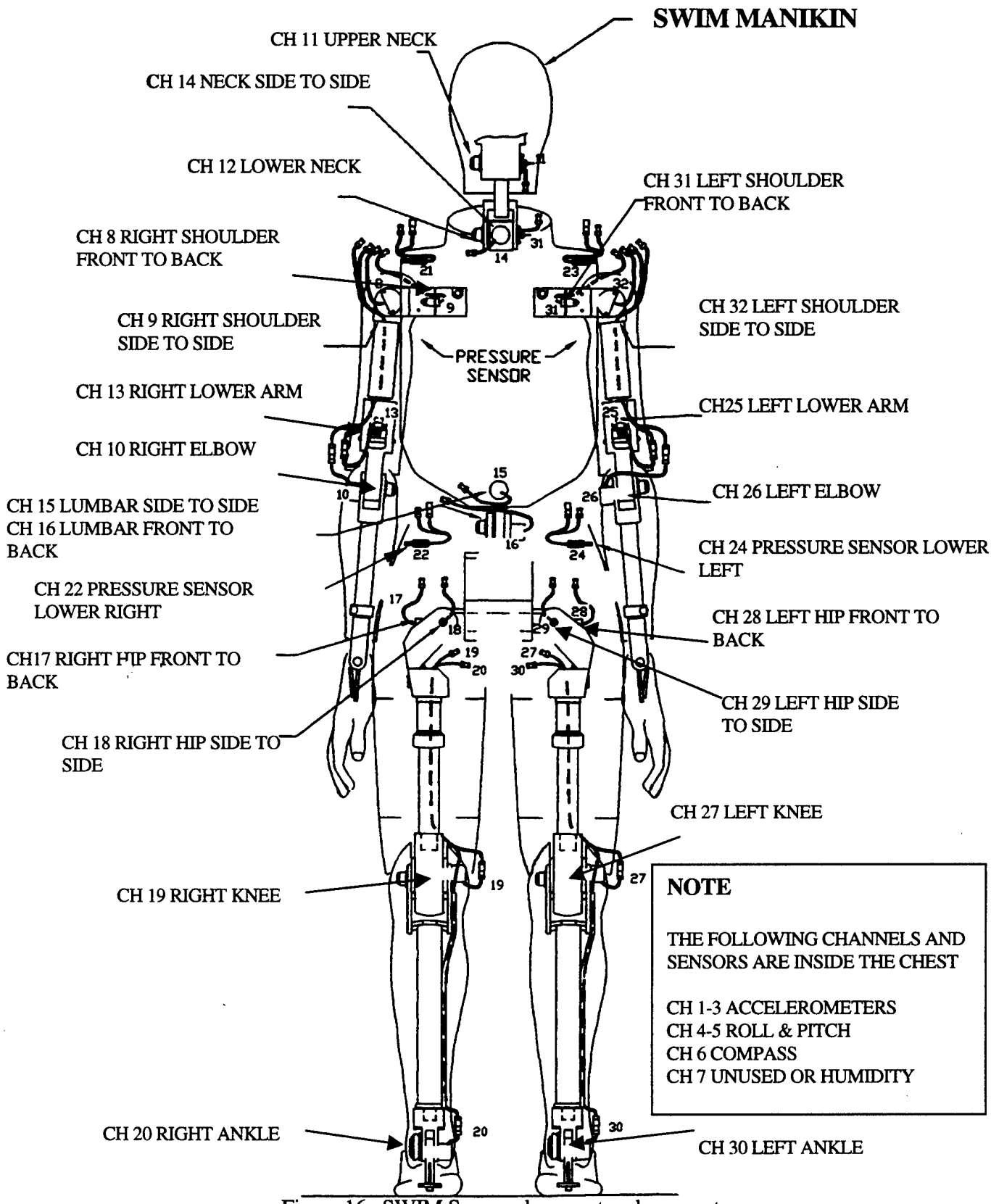

Figure 16. SWIM Sensor placement and segments

An explanation of the steps required to take a set of data follows:

A computer is connected to the DAS through the waterproof connector and the DAS is turned on. The individual sensors to be used for the test are calibrated. These calibrations are stored in memory along with all sensor sensitivities, offsets, spans and test name. The SWIM data acquisition process set up includes sampling rate, sampling delays, and number of samples, are programmed into the DAS and the DAS is armed to collect data. The wires are disconnected, capped for waterproof integrity and the SWIM is placed in the specific test posture required. The external transmitter is triggered when it is time for a test, the DAS takes the amount of data as programmed and goes into a standby mode. It is retriggered for each consecutive test using the remote transmitter. Each data acquisition sample is accomplished using the timing as originally programmed. After all tests are completed for that series the remote transmitter triggers the DAS to power down.

The SWIM is brought out of the water dried off and the computer is attached and the data is downloaded to a file along with all the setup information stored in the DAS. A new test sequence can now be started with a new calibration. The complete DAS operation, calibration and wiring is explained in the DAS 32, V7.3C Operations Manual.

4.2 Center of Gravity and Center of Buoyancy Testing

The testing of SWIM included two primary test cases or positions. The first is the straight upright position as if standing with all joints locked with arms at the sides. The second is the right angle or sitting position. Two important items of information required in these tests to verify the accuracy of the WAFAC model are the center of gravity (CG) and the center of buoyancy (CB).

The CG and CB are the points around which the SWIM weights and buoyancy rotate during testing. The CG and CB measurements were made before the compression problem with the neoprene chest inserts was realized and replaced with foam. These measurements are slightly in error due to the deviation in weight and buoyancy from the rigid foam inserts used in the final SWIM tests. Time constraints precluded retesting. These tests are discussed on the next page.

4.2.1 Center of Gravity Measurements

Two important items of information required in these tests to verify the accuracy of the WAFAC model are the center of gravity and the center of buoyancy. Center of gravity measurements were conducted for the dry SWIM in the laboratory at the normal outfit intermediate weight of 156.3 lbs. The CG tests were conducted for two positions, one the right angle sitting position with forearms locked at a right angle parallel to the legs (figure 17), and two the standing straight upright position with all joints locked (figure 18.) These measurements were made using a platform suspended from a leveled beam with needle balance points on each end. The SWIM was placed on the platform in each position and weights were added to change the angle of the platform. Using these weights and angles, vectors were calculated establishing the center of gravity for the SWIM. The center of gravity for the upright standing SWIM was calculated to be 5.300 inches measured from back of torso, 38.393 inches from the bottom of the feet on the centerline of the SWIM. The center of gravity for the sitting right angle position was calculated to be 11.90 inches from the back of the legs upward, 30.500 inches from the flat of the feet towards the chest. A brief discussion of how these calculations relate to the SWIM coordinate system is given in appendix A.

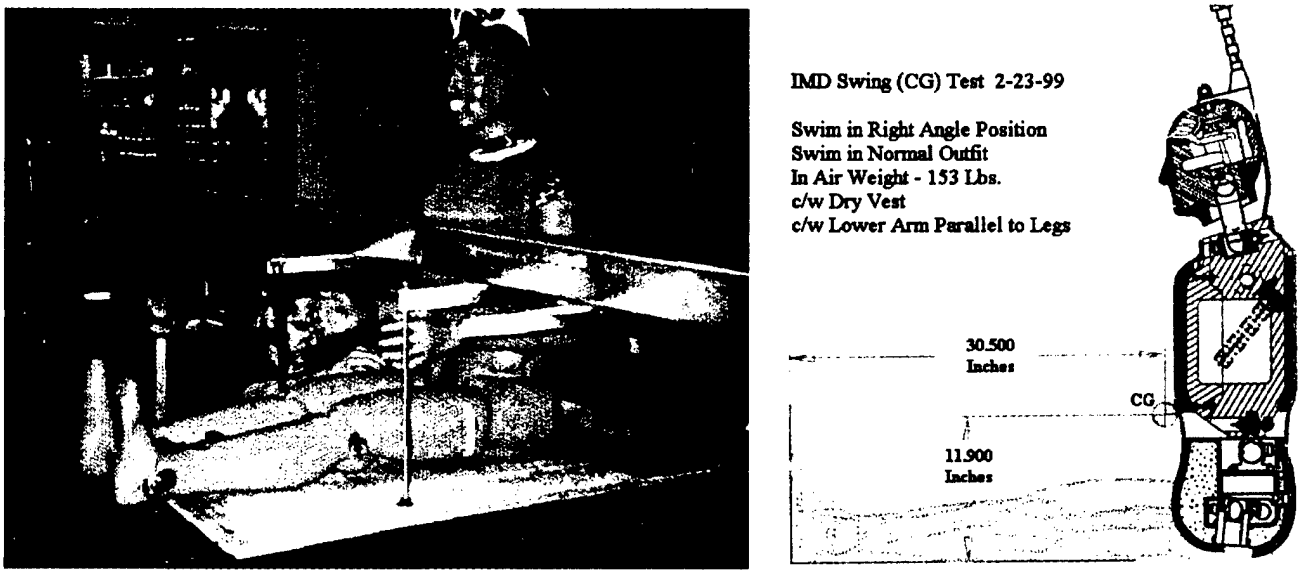

Figure 17. Center of gravity (SWING) test right angle position photo and drawing.

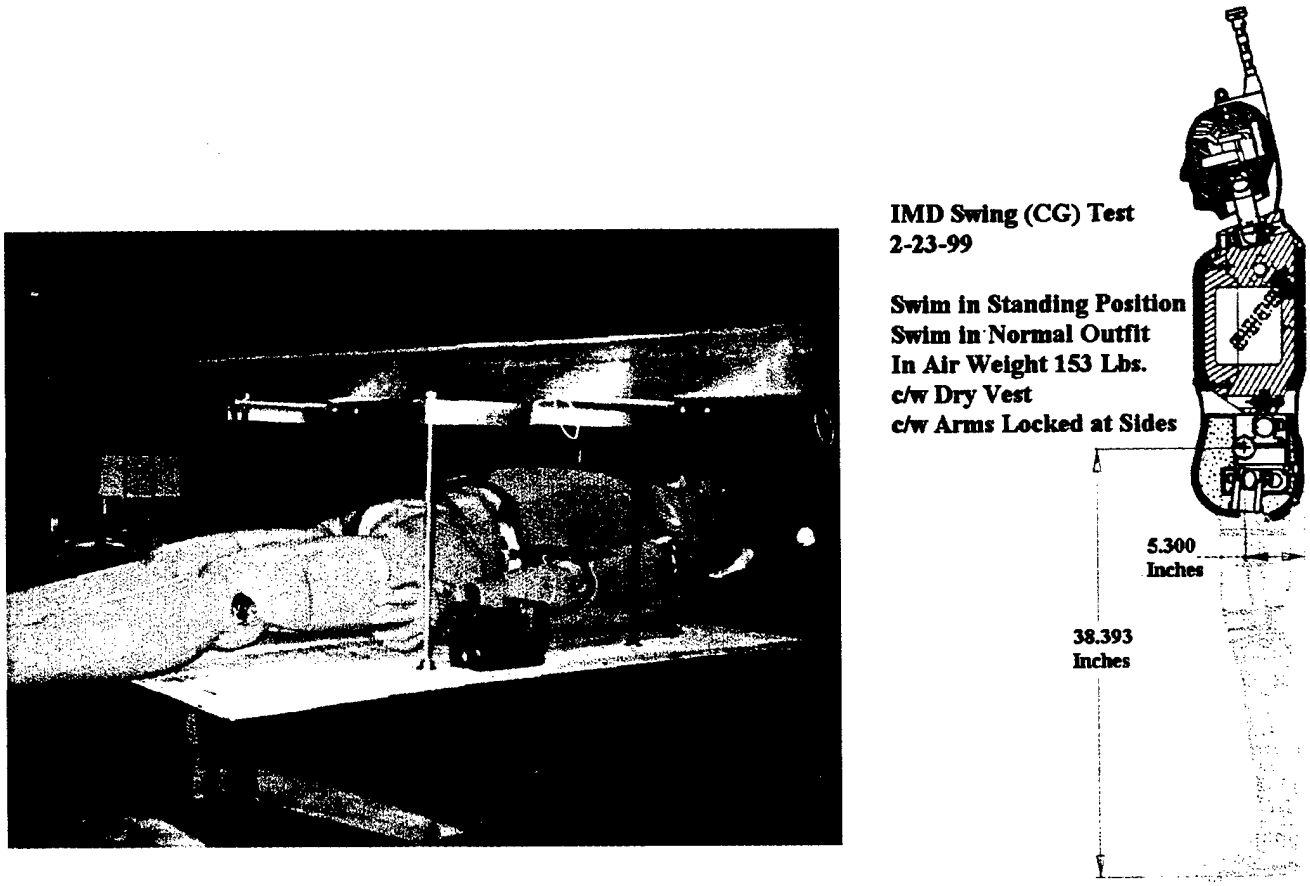

Figure 18. Center of gravity (SWING) test standing position photo and drawing.

4.2.2 Center of Buoyancy Measurements

Center of Buoyancy measurements were made in the test tank underwater at a weight of 156.3 lbs. CB measurements were made for two positions, one standing straight upright (figure 19), and the other in the right angle position with forearms locked in the right angle position parallel to the legs (figure 20.) Note for the purposes of CB measurements standing upright and laying horizontally are the same. The joints were locked as required for each position. During the CB testing a line had to be attached between the ankles and the neck to keep the SWIM joints from moving out of the right angle position. This was a problem because the locking bolts on the top of the thigh joints are too small to secure the weight of the legs when the SWIM was lifted from the floor into the water with the overhead crane. Center of buoyancy tests were made by pulling the SWIM under water from various points along the SWIM as listed below from feet to head and measuring the pitch angle for the SWIM. The CB measurements assumed no roll during the testing. The attachment points on the SWIM were as follows:

1 CB ATTACHMENT POINTS FOR STANDING POSITION NORMAL WEIGHT

A. At rear side center of ankles three inches from the bottom of the feet.

B. At the rear side center of knees, 17.5 inches from bottom of the feet.

C. At the rear side of the shoulders in the center, 55.75 inches from bottom of feet.

D. At the Head bolt 68.25 inches from the bottom of the feet.

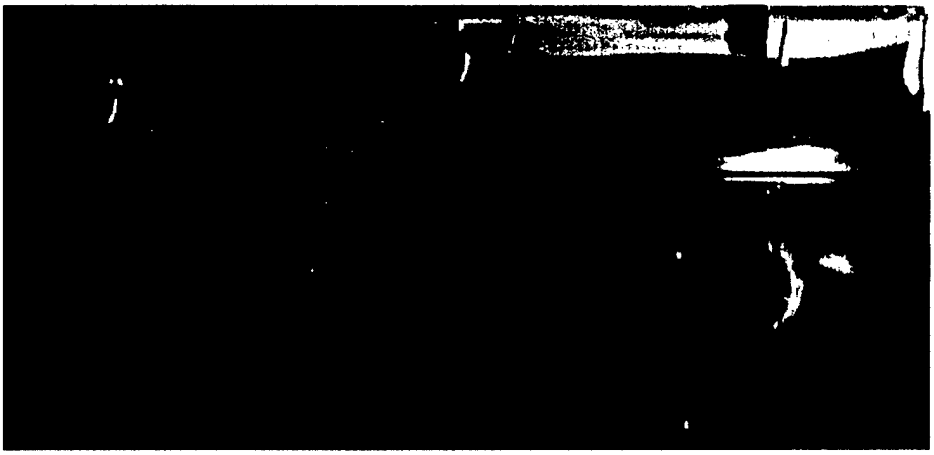

Figure 19. Center of buoyancy measurements, horizontal/vertical position underwater.

2 CB ATTACHMENT POINTS RIGHT ANGLE POSITION NORMAL WEIGHT

A. At front side center of ankles, 4.13 inches from sitting position.

B. At back center of knees 0.78 inches from sitting position.

C. At front center of upper torso, 23.7 inches from sitting position.

D. At front head eye bolt 38.89 inches from sitting position.

Center of buoyancy calculations were made using the measured values from the tests and the CG values from the previous test. The CB values for the standing upright position was found to be 0.17 inches forward of the CG or 5.47 inches from the back of the torso, 0.90 inches above or 39.29 inches from the bottom of the feet. The CB value for the right angle sitting position were similarly calculated to be 0.38 inches behind and 1.54 inches below the CG for mark for that position or 10.36 inches measured from the bottom of the legs, and 30.12 inches as measured from the feet. A discussion of center of buoyancy calculations is found in appendix B.

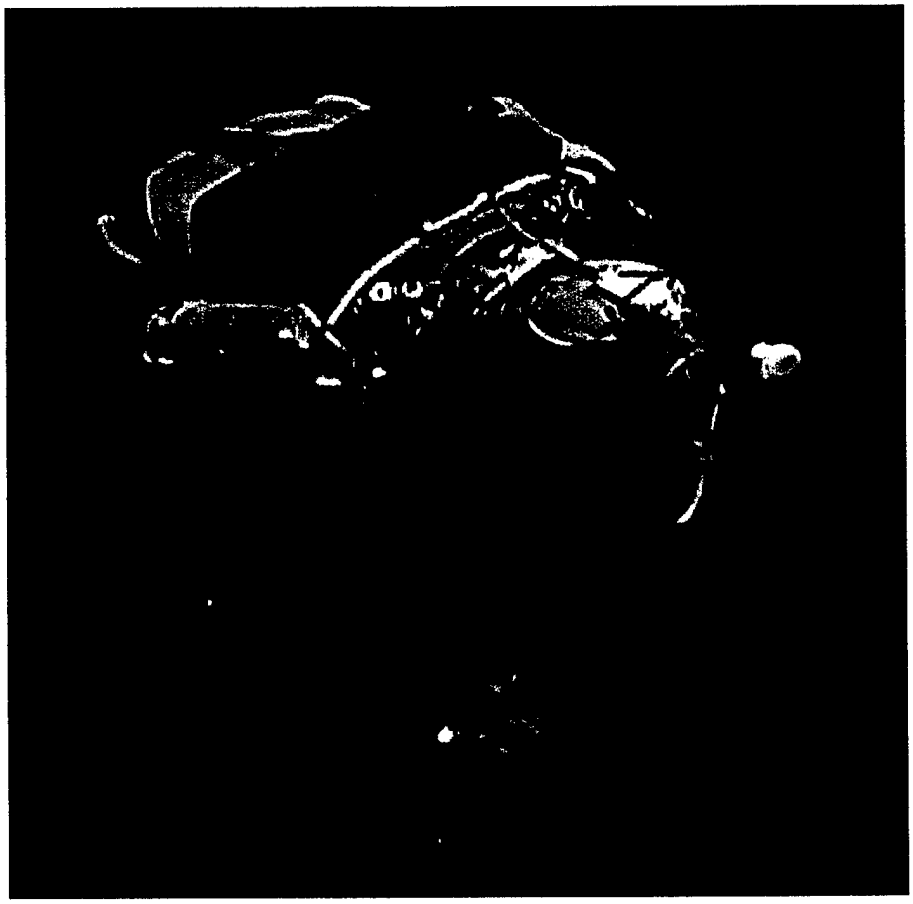

Figure 20. Center of buoyancy measurements, right angle position underwater.

4.3 Drag Testing of Swim

Drag testing of the SWIM was conducted to measure the drag coefficients through the water. This data is required to accurately model the SWIM movement through the water. Drag testing was conducted in the test tank using the towing carriage load cells as the measuring device. A test frame was constructed that would securely hold the SWIM in the siting position with all joints locked (figure 21), the horizontal position (figure 22), and the standing position. This test frame was installed on the carriage-towing fixture which would securely hold the SWIM. The carriage allowed the frame and SWIM to be lowered in the water. For testing purposes the SWIM was lowered 12 inches below the water surface. Testing was conducted on the SWIM in an upright face forward, upright back forward, upright left side forward, upright right side forward, horizontal head forward, horizontal feet forward and right angle face forward,

right angle back forward, attitudes. Testing was conducted at speeds of 0.1, 0.2, 0.3, 0.4, 0.5 and 1.0 meters per second. The forces acting on the SWIM were measured using the towing carriage load cells and recorded by the carriage instrumentation. The SWIM was removed from the fixture and the same tests were conducted to remove additional drag caused by the fixture itself. Table 5 is the resultant drag coefficients from the drag tests for the SWIM in normal weight and floatation vest inserts. Table 6 lists the drag data.

Figure 21. Drag testing forward direction locked right angle position.

Figure 22. Drag testing forward direction locked horizontal position.

The coefficients appear reasonable, except probably for the difference seen in the sideways motion, between the forward and reverse directions, since the dummy should provide a symmetrical profile towards the stream in both directions.

The drag coefficients were used as the basis for the initial estimates of the coefficients to be used in the SWIM modeling effort. The appropriate coefficient was for the principal configuration that was modeled.

Table 5. Measured drag coefficients.

Configuration	C_D Forward	C_D Reverse
Horizontal; parallel to motion	.67	.65
Vertical; perp to motion	1.20	1.24
Bent at waist;	.81	.97
Sideways; rt shoulder towards motion	.80	.90

Table 6. SWIM manikin drag data.

	(All Measurements in Newtons)				Vertical		Vertical Right	
Velocity	Horizontal Position		Right Angle Position		Face Forward		Shoulder Forward	
(m/s)	Forward	Reverse	Forward	Reverse	Forward	Reverse	Forward	Reverse
0.1	0.547	0.681	1.074	1.32	2.261	3.886	1.317	2.285
0.2	2.517	1.724	5.393	4.501	9.186	11.389	5.543	6.421
0.3	4.866	3.812	12.087	11.035	20.43	25.225	12.341	14.153
0.4	7.594	6.946	21.155	20.923	35.992	45.393	21.71	25.483
0.5	10.699	11.124	32.598	34.164	55.873	71.894	33.651	40.411
0.6	14.184							
0.7	18.046							
0.8	22.287							
0.9	26.907							
1	31.904							

4.4 Qualisys ® Video Tracking System

During the bottom release tests and the whole body in waves tests a video tracking system was used to provide a secondary method of tracking the SWIM as it moved through the water. The Qualisys® tracking system is a set of two video cameras wired to a video monitor and computer. The system also employs a series of lights near the cameras. This system was used underwater for the bottom release tests and above water for the in wave tests. The system was set up with two cameras set on underwater towers on each side of the test area. In this case the cameras were set up with a viewing path perpendicular to the assent path of the SWIM through the water. The test area that the cameras can view is limited in space and must be set up meticulously. Once the cameras are in position precise calibration is completed using balls (the size of golf balls) covered with retro-reflective material. These balls are moved throughout the viewing area to make sure distance definition throughout is uniform. The typical tracking device used with this system is called a tree (figure 23.) This tree was attached under the lifting bolt of the SWIM on the head and consists of a series of very light weight composite rods with a ball on top of each rod. The rod lengths vary, which enables tracking of roll and pitch as will as acceleration through the water. The SWIM had additional retro-reflective tape attached at predetermined locations on the body. The results from the Qualisys® system were not available for this report, and will be reduced at a later time by the staff at IMD and reported on.

Figure 23. Qualisys tree on SWIM.

5.0 MODIFICATIONS TO SWIM INPUT DATA

The following modifications were required based on the results of the preliminary testing.

5.1 SWIM Inertial Characteristics

During initial weight measurements by the Coast Guard at IMD with the actual SWIM, a number of problems were noticed with the data set that had been developed for the dummy. These are described below:

1. The total weight of the original, fully ballasted dummy was 73.2 kg (161 lb). This was 2.5 kg (5.5 lb) higher than the total weight provided in the data set. The discrepancy arose because the data set did not take into account the normal weight of the chest vest, consisting of the Neoprene outer jacket and the inner Neoprene pads. The original data set developed for the U.S. Coast Guard have to be modified to reflect the actual weights. The additional weight could be easily absorbed in the weight of the upper torso segment, but the location of the CG and of the principal moments of inertia were affected. These measurements could not be easily repeated, so it was assumed that because of the symmetric positioning of the vest about the original CG of the chest, it would not significantly change the location of the CG. The value of the moments of inertia was a more difficult proposition, but it was assumed that because the rotational accelerations encountered would be very low, it would not change the final results very much. Inertial measurements on the upper torso with the vest added should be made prior to any future test sequence. The weight of the dummy (in air) increased significantly once it was fully immersed. The weight of a wetted dummy was 76.4 kg (168 lb), an increase of 3.2 kg (7 lb). Thus, the added inertial effect would also have to be included in the data set used for the simulations. Much of this increase was due to the absorbed water in the neoprene vest. But a small amount of the increase was due to water absorbed through small holes in some of the skin segments, specifically the right and left upper thigh flaps and the right and left foot. The skin segments were treated with waterproofing material, and though the problem was not totally eliminated, the amount of water absorbed in the segments probably became negligible, and the only consequential effect was the water absorbed in the vest. Thus the increased inertia would have to be accounted for by an increase in the upper torso mass.

2. During the initial tests by the Coast Guard at IMD, it was discovered that the fully ballasted SWIM would not be buoyant. This effect could be surmised from the fact that the maximum expected buoyant force on the dummy was 78.2 kg (172 lb), as given in tables 7 and 8. This buoyant force was over-estimate, as it does not take into account the overlap of the ellipsoids used to represent the dummy, and it would be reasonable to expect that the buoyant force would be less than the wetted weight of 76.4 kg. From the measurements made, it appeared that the dummy had a negative buoyancy of about -2 kg (-4.5 lb).

3. In order to reduce the effective weight of the dummy, it was decided to set the normal ballast weight to include the additional weight in the lower extremities and not include the ballast weights in the thorax and arms. The ballast weights that were removed amounted to a total of 4.1 kg (9.0 lbs.). This reduced the original, fully ballasted, dry weight of the dummy from 73.2 kg to 69.1 kg (152 lb). This was the configuration selected for the center of gravity measurements made at IMD. The ballast weight that remained in the lower extremities amounted to 3.9 kg (8.6 lb). This modified ballast configuration was defined to be the normal ballast configuration for the SWIM.

5.2 Modifications to Segment Data in SWIM Input Data Set

Once the CG and CB measurements were available, the predictions of these locations based on the SWIM data sets were generated using the DYNAMAN program. For these comparisons, the SWIM was modeled in both the straight and bent configurations, and the position of the CG and CB was determined. Differences in the locations with the experimental data were then examined and the input data were then adjusted to provide better agreement. This procedure is described below.

5.2.1 Adjustment of Inertial Properties

As discussed the original weights of some of the segments had to be adjusted. After the final configuration was achieved with the Styrofoam inserts, it was possible to adjust only the upper torso weight from 55.4 lb to 56.5 lb to achieve the total measured wet weight of 154 lb. The SWIM weight only included the ballast weights in the lower extremities. It should be remembered that though the difference in weight of the upper torso was not large, the underlying reasons for the difference were

significant. The original upper torso weight included the thorax ballast weight, but did not include the weight of the jacket and inserts, nor did it account for the increase in weight due to water absorption. Thus it was somewhat of a coincidence that the loss of ballast weight was essentially offset by the increase in the vest weight and absorbed water.

5.2.2 Adjustment of Ellipsoid Dimensions

The sizes of the ellipsoids in the original SWIM data set generated a buoyant force of about 172 lb which was significantly higher than the actual measured buoyant force of about 157 lb. This prompted a detailed evaluation of the appropriate ellipsoid sizes based on the CAD drawings for the SWIM. The original ellipsoid dimensions are overlaid on the SWIM CAD drawings in figure 24, which show the dummy in both frontal and side views. When the drawings were checked, it appeared that the ellipsoids representing several segments over-represented the volume of the segment. The principal region where this occurred was the region between the upper torso and lower torso. In the actual dummy, a part of this region is empty, with only the region about the lumbar spine having any volume. This occurred because there was no skin to fill between the two segments in this region. There was a similar, though small over-representation of the volume around the neck region. On the other hand, there was an under-representation of the volume of the upper torso itself. This probably arose because the original data set did not utilize the outside dimensions of the jacket with all the inserts which increased the X (front-back) dimensions of the ellipsoid significantly. The new jacket with the squarish, Styrofoam inserts actually made the volume larger than could be represented by an ellipsoid shape.

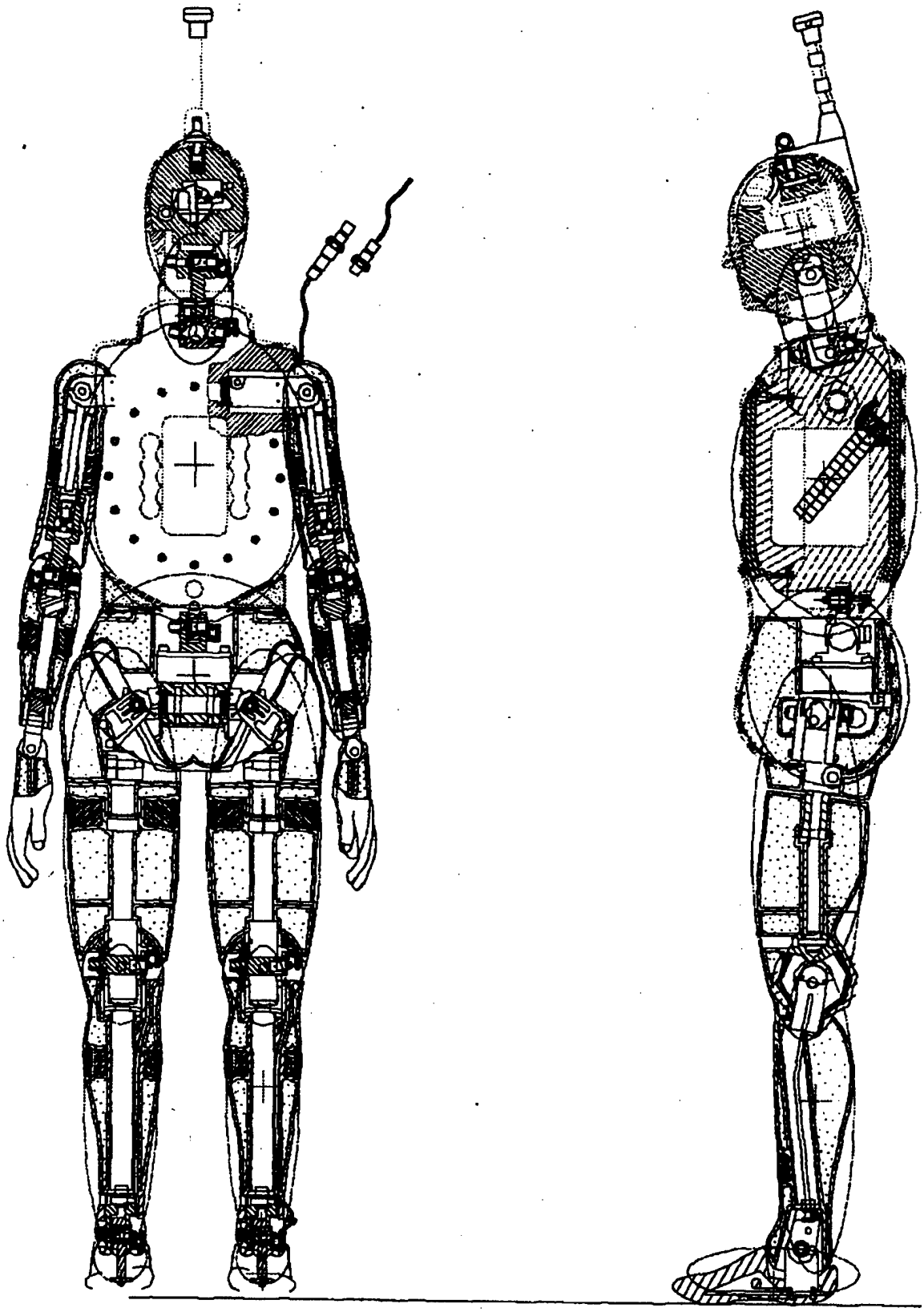

Figure 24. Front and side views of the SWIM with the original ellipsoids overlaid.

In addition to the ellipsoid dimensions of the upper and lower torso and the neck, which were not properly represented, some of the other ellipsoids dimensions were modified to minimize the overlap between neighboring segments. As indicated earlier, one limitation of the current model is that the buoyancy (and drag) is calculated for each individual ellipsoid and thus the overlap regions are counted twice. By minimizing the overlap, this error could also be reduced. After the sizes were estimated from the CAD drawing, some small tuning was done to bring the estimate of the buoyant force closer to the experimental value. The final ellipsoid sizes that were arrived at are shown in figure 25 in the front and side views.

The modifications made in the ellipsoid sizes are shown in table 7. The table provides the original semi-axes dimensions and the new ones.

Table 7. Modification of Ellipsoid Sizes for SWIM Input Data.

Segment	Original Dimension (inches)			New Dimension (inches)		
	X-axis	Y-axis	Z-axis	X-axis	Y-axis	Z-axis
LT	4.9	6.94	6	5.4	6.94	5.3
UT	5.6	7.16	9	6.7	6.8	9
N	2.7	2.28	4	1.5	1.6	1.6
H	4	3.1	5	4	3.1	5
RUL	3.3	3.5	11.4	2.8	3.4	8.2
RLL	2.36	2.23	9.45	2.36	2.23	8.15
RF	5.22	1.6	1.52	5	1.6	1.5
LUL	3.3	3.5	11.4	2.8	3.4	8.2
LLL	2.36	2.23	9.45	2.36	2.23	8.15
LF	5.22	1.6	1.52	5	1.6	1.5
RUA	2.07	1.64	6.88	2.07	1.64	6.88
RLA	1.775	1.775	5.8	1.775	1.775	5.8
LUA	2.07	1.64	6.88	2.07	1.64	6.88
LLA	1.775	1.775	5.8	1.775	1.775	5.8
RH	1.87	1	3.65	1.87	1	3.65
LH	1.87	1	3.65	1.87	1	3.65

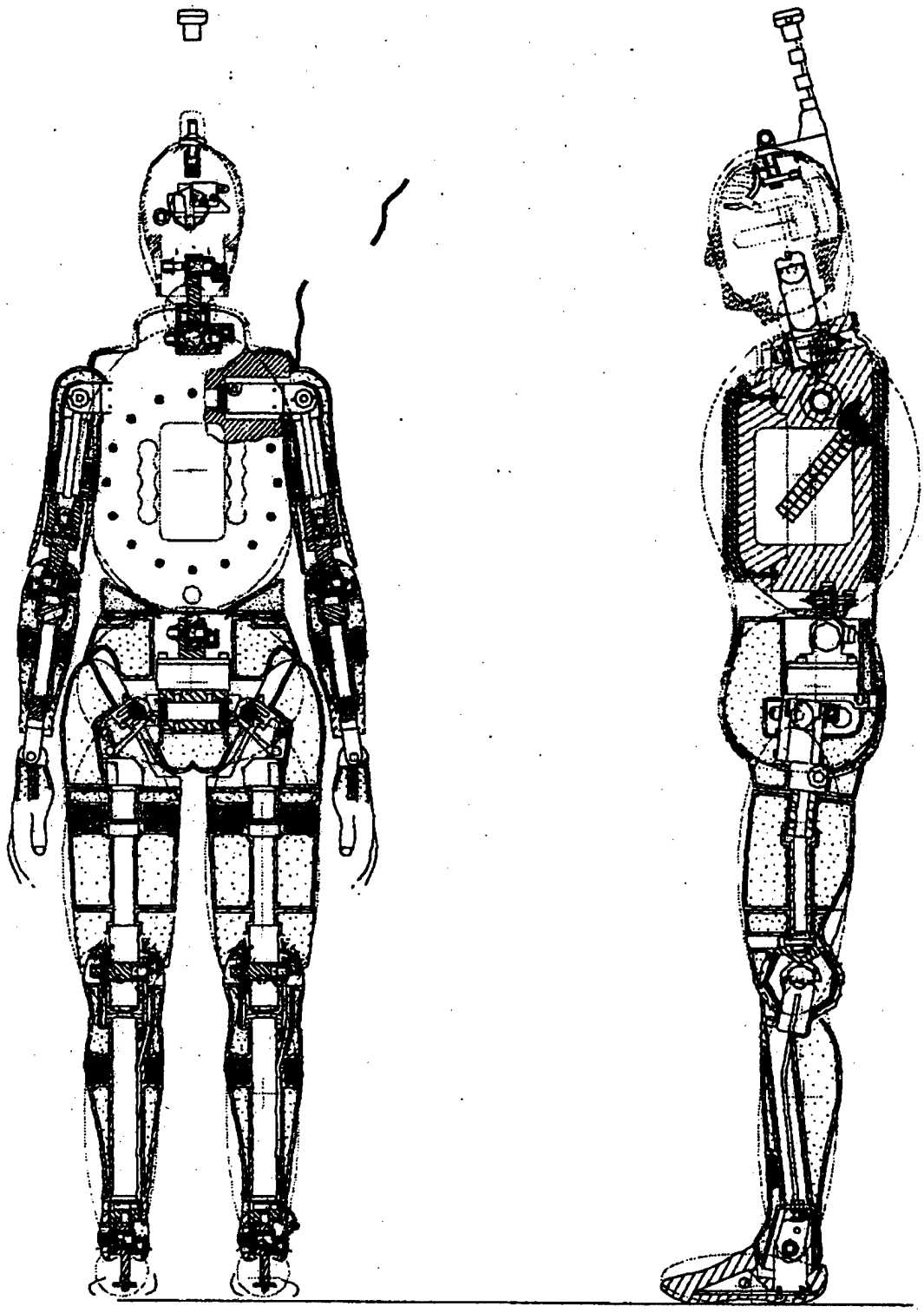

Figure 25. Front and side views of the SWIM with the new ellipsoids overlaid.

The following changes were made:

1- The dimensions of the lower torso were reduced to account for the space between the it and the upper torso.

2- The X-dimension of the upper torso was increased by about an inch to account for the jacket and the Styrofoam inserts.

3- The dimension of the neck was reduced to account for the space around the lower neck joint and to reduce overlap.

4- The dimension of the upper leg was reduced in the vertical direction to eliminate overlap with the lower leg and lower torso.

5- The dimension of the lower leg was reduced to eliminate overlap at the knee.

6- The dimensions for the head, arms, and hands were not modified.

5.2.3 Adjustment of Ellipsoid Center Locations

The position of each segment ellipsoid relative to the segment CG was also modified to reflect its correct position. The segment CG values were obtained from Veridian, and though there was some adjustment of the upper torso weight, it was assumed that these locations remained unchanged relative to the hardware landmarks. From the CAD drawings, the change in the position of the ellipsoid centers for those ellipsoids whose sizes had been modified were noted. Some additional fine-tuning was performed on the values obtained from matching the CAD drawings by requiring that the experimental CB location would be close to that predicted by the model. These changes are given in table 8.

Table 8. Modifications of ellipsoid centers for SWIM input Data.

Segment	Original Center (inches)			New Center (inches)		
	X	Y	Z	X	Y	Z
LT	0	0	-0.27	0.3	0	-0.6
UT	0	0	0.5	0.5	0	-0.6
N	-0.1	0	-1.1	0.5	0	-0.6
H	0.5	0	0.4	0.5	0	0.4
RUL	0.15	0	1.4	0.15	0	2.5
RLL	0	0	0.8	0	0	0.6
RF	0	0	-0.9	0	0	-0.75
LUL	0.15	0	1.4	0.15	0	2.5
LLL	0	0	0.8	0	0	0.6
LF	0	0	-0.9	0	0	-0.75
RUA	0	0	0	0	0	0
RLA	0	0	1.2	0	0	1.2
LUA	0	0	0	0	0	0
LLA	0	0	1.2	0	0	1.2
RH	0	0	0	0	0	0
LH	0	0	0	0	0	0

The following changes were made:

1- The lower torso, upper torso, and neck centers were changed to reflect the change in ellipsoid size.

2- The upper and lower leg center locations were changed to reflect the changes in ellipsoid sizes.

3- The foot center location was changed to reflect the location of the segment CG

4- The head, arms, and hand centers were not changed.

5.2.4 Check on Buoyancy of Single Segments

The Coast Guard estimated the buoyancy of the individual segments in the SWIM dummy by gradually immersing it to the levels of individual joints. Though this is not as accurate as testing the segments separately, it provides some backup information, which can be used to tune the buoyancy estimates from the simulation data set. Two estimates are provided to show the possible spread in measuring the buoyancy values. The first set was generated from average values obtained from immersion tests conducted at both the Coast Guard R&D and at IMD. The second set was estimated from immersion tests at IMD just prior to the actual SWIM testing (table 9). Both estimates used the older version of the chest

vest with the Neoprene pads. Thus there may be some difference in the buoyancy of the upper torso, with the introduction of the Styrofoam pads, though it probably would not be significant since the overall buoyancy was within one pound.

Table 9. Estimated buoyancy of individual segments (from immersion testing).

Segment	Buoyancy EST #1 (LB)	Buoyancy EST #2 (LB)	Buoyancy from model (LB)
LT	38.0	27	30
UT	55.8	63	62
N	0.2	0.2	0.6
H	9.5	8.9	9.3
RUL	11.5	12.3	11.8
RLL	7.0	7.8	6.5
RF	2.0	2.2	1.8
LUL	11.5	12.3	11.8
LLL	7.0	7.8	6.5
LF	2.0	2.2	1.8
RUA	3.2	3.2*	3.5
RLA	2.4	2.4*	2.8
LUA	3.2	3.2*	3.5
LLA	2.4	2.4*	2.8
RH	0 .8	0.8*	1.0
LH	.8	0.8*	1.0
	158.3	158.5	156.7

NOTE: *No separate estimation was made for these segments; assumed to be same as in Test 1
Estimated from test based on total buoyancy; upper torso could not be checked in isolation

The two estimates were fairly close and the major discrepancy was in the distribution of the buoyancy between the lower and upper torsos. It is seen that the buoyancy predicted by the model based on the segment ellipsoid sizes is fairly close to that of the measurement estimates, though there is some discrepancy in the distribution of the buoyancy between the arms and legs.

5.3 Instrumentation

A number of sensor channels were initially found not to be operational. Among the ones which would effect measurement of the dummy kinematics were the roll sensor (channel 5), the lumbar side-to-side pot (channel 15), the lumbar front-to-back pot (channel 16), the left knee pot (channel 27), and the left ankle pot (channel 30). Channels 15, 27, and 30 were replaced. Since the roll sensor would help in providing information on the complete motion of the dummy, channel 15 was ultimately used for a new roll sensor which was glued on to the outside of the dummy. It was decided that for all the important tests, the joints would remain locked, thus the original lumbar rotation would not be required.

As testing progressed, it was found that the original pitch sensor had limitation for some configurations. The sensor range was only between -60° and +60° and did not provide correct results when the dummy was close to a horizontal orientation. A new pitch sensor, which would operate over a larger range, was then attached to the outside of the chest using channel 16.

During the analysis of the results from the initial bottom release tests, it was found that the accelerometer data appeared to vary over a much wider range than would be expected for the dummy's motion in water. Also, when the accelerometer data was examined for these tests, they did not show the expected resolution, such as an indication of the damped oscillations that one would expected as the dummy performed heave oscillations at the water surface. It was originally planned to use the accelerations to derive the displacements of the CG of the dummy in the X, Y, and Z directions. For example, the graph for the accelerations in the X and Z directions for the one of the bottom release test from three meters (with normal ballast, and straight vertical configuration) is shown in figure 26. A problem with the accelerometer data may have been that its operational range was much greater than that actually seen during testing and the resolution was not high enough to pick up the small changes in acceleration during the heave oscillations.

As an alternative, the pressure transducer data was examined to see if it could be used to estimate the vertical motion relative to the water surface. For the bottom release tests, this motion would provide the most information. Examination of this data showed that when the data were differentiated twice to obtain acceleration, the output appeared reasonable, both with respect to its magnitude and the damped oscillations. The data from the lower right and left pressure transducers were seen to match well, indicating that the dummy attitude remained fairly constant during the motion (something that was also seen in the video coverage of the event). The accelerations derived from the pressure transducer data are shown in figure 27.

The accelerometers show about the same magnitude of change in the Z acceleration (it should be remembered that the accelerometer is measuring the body system and there will be some change due to the pitching of the dummy). But the time interval for the change is about twice in the case of the accelerometer, which will make the change in velocity, twice as much which would make it too high. It would appear that the accelerometer is not able to pick up the sharper change seen in the pressure transducer data.

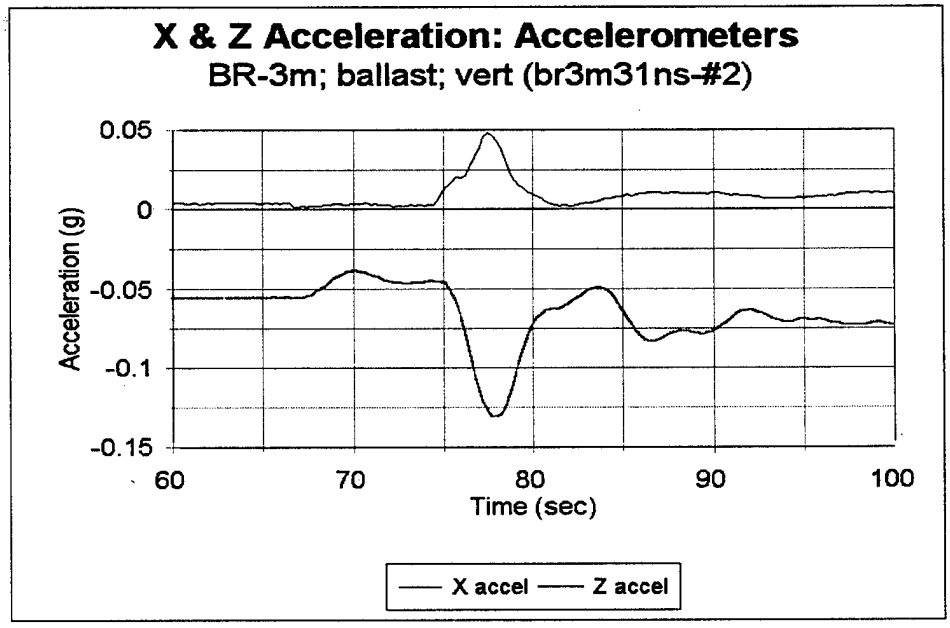

Figure 26. X and Z accelerations for 3 m bottom release, normal ballast in vertical configuration, as measured by the accelerometers.

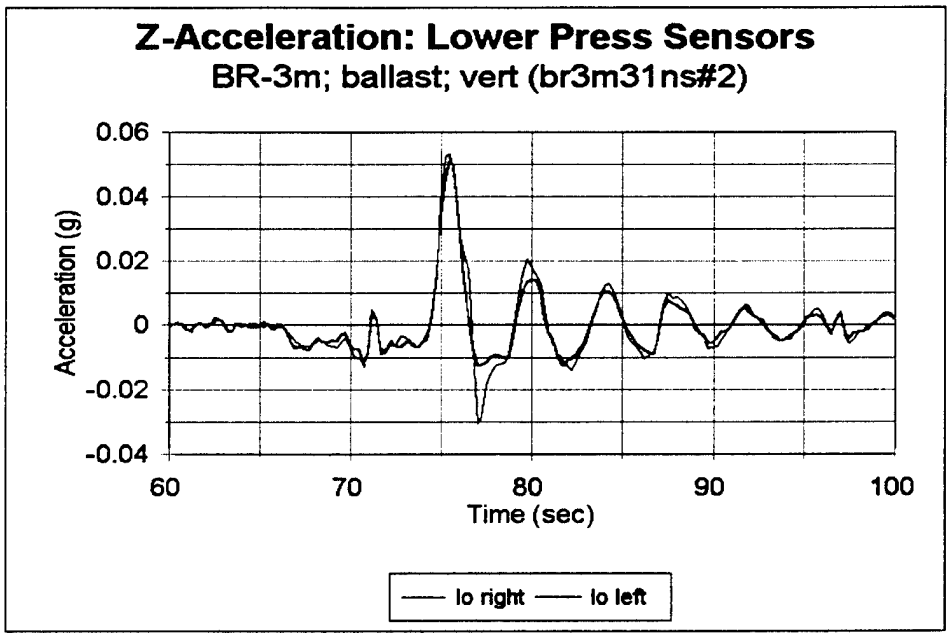

Figure 27. Vertical accelerations obtained from pressure transducer data for 3 m bottom release, normal ballast, vertical configuration.

An approximate estimate of the desired peak acceleration and the time interval over which it acts can be made based on the buoyancy force and the visual estimate of the rise time. The buoyancy force is about four lbs., which would result in an average acceleration of about 0.03 g of the dummy if there was no drag force. The rise time to the surface was about eight seconds. For the dummy to come to a stop in its vertical motion, the acceleration actually increases from zero and reaches a maximum, and then decreases below zero and reaches a negative minimum, so that the net velocity at the end is zero. Assuming that the rate of increase or decrease of acceleration is constant, then one would estimate about four seconds for the period when the acceleration is above zero, with a peak at about twice the average, or 0.06g. As mentioned earlier the magnitudes from the two sources are not different, but the time period when the acceleration is positive is about the right range for the pressure transducer, but about twice as broad for the accelerometer.

Examining another test, the 3 m-bottom release with no ballast and vertical configuration, a similar situation is encountered. Figure 28 shows the output from the accelerometers and figure 29 shows the acceleration computed from the lower pressure transducers.

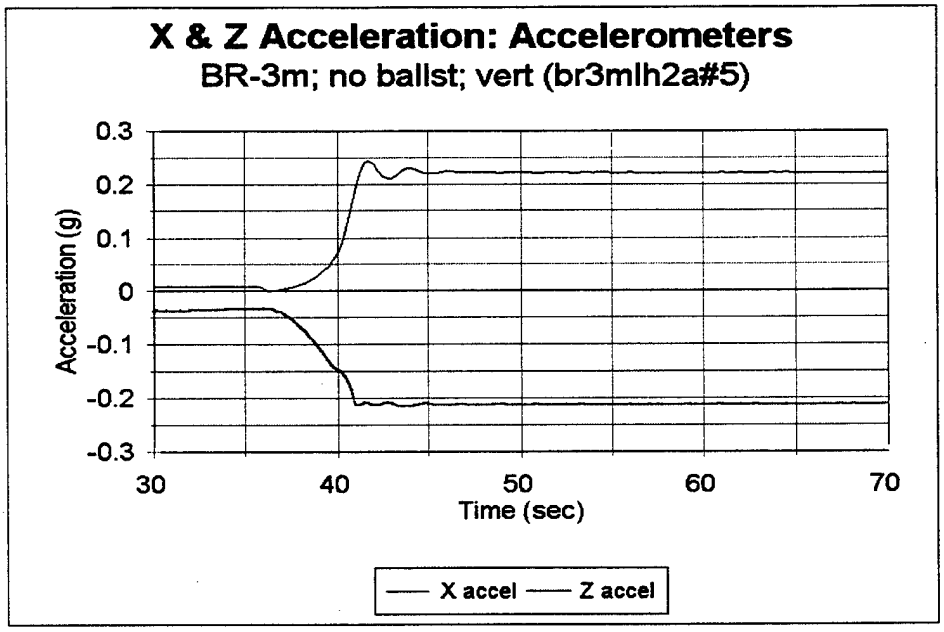

Figure 28. X and Z accelerations for 3 m bottom release, no ballast in vertical configuration, as measured by the accelerometers.

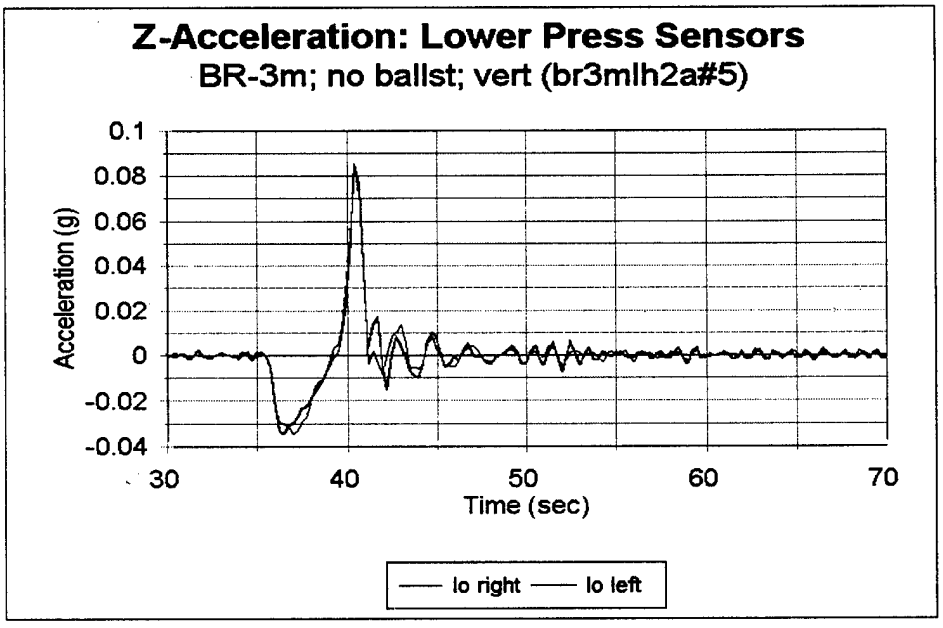

Figure 29. Vertical accelerations obtained from pressure transducer data for 3 m-bottom release, no ballast, vertical configuration.

It is seen that in this case as well, the magnitude of the acceleration change recorded by the accelerometer is too high and there is very little information on the heave oscillations.

The accelerometer data appeared to be reasonable for the wave tests. Figures 30 and 31 show the acceleration output from the accelerometers and the computed accelerations from the pressure transducers for the case of the test in waves with frequency = 0.3 Hz (with normal ballast and straight configuration).

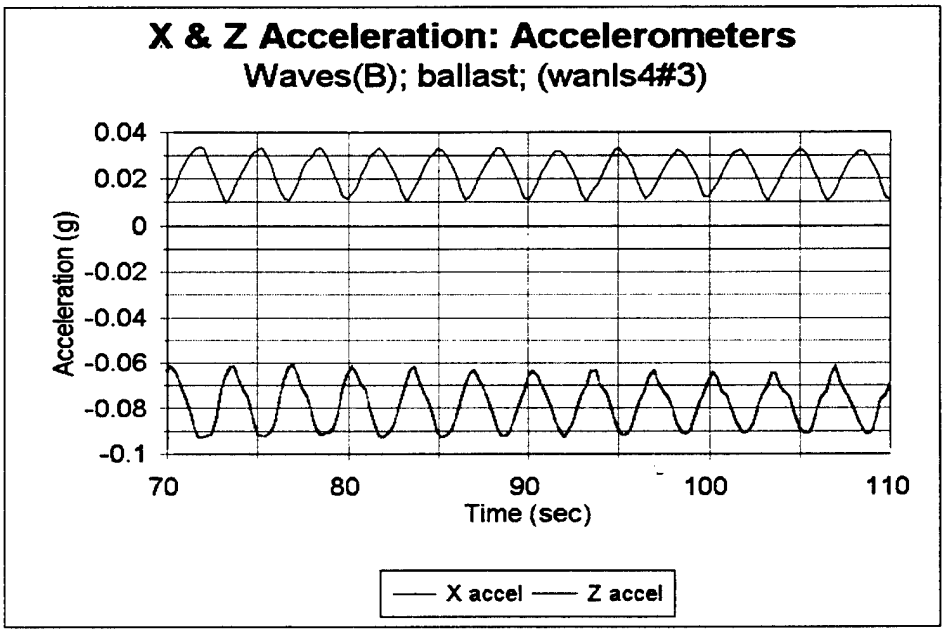

Figure 30. X and Z accelerations for wave tests (frequency = 0.3 Hz), normal ballast in straight configuration, as measured by the accelerometers.

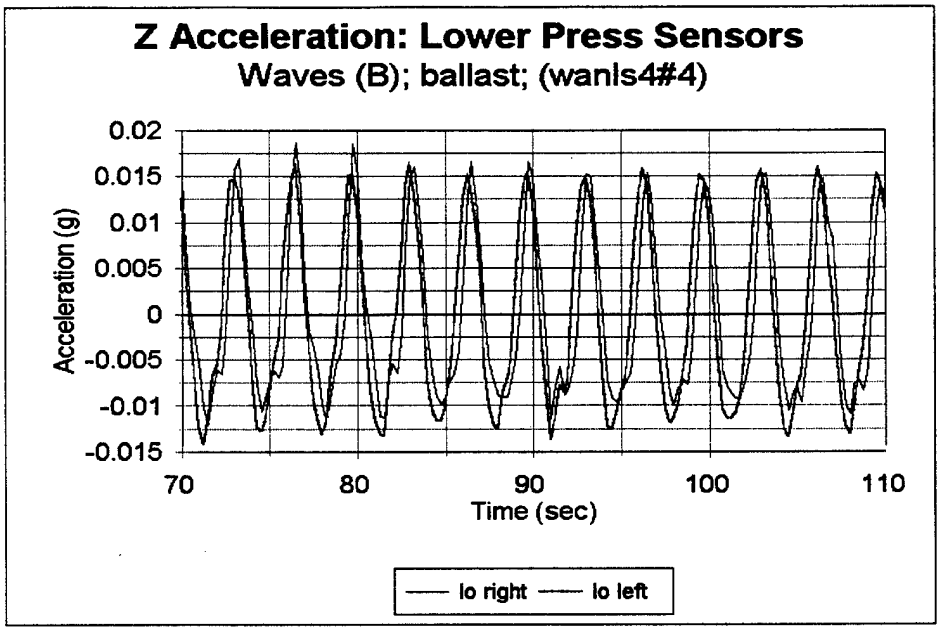

Figure 31. Vertical accelerations obtained from pressure transducer data for wave tests (frequency = 0.3 Hz), normal ballast, straight configuration.

A critical part of the validation of the WAFAC model centered around whether the model could predict the basic characteristics seen during a bottom release, namely: the time to rise to the surface; the period of heave oscillation; and the relative decrease in the amplitude of oscillations or the damping. It is believed that the pressure transducer data could be used for this purpose, and the bottom release tests were analyzed using these data. A limitation of the data, of course, was that motion in the X and Y directions could not be tracked. The computer model predicts some amount of horizontal drift, and this cannot be verified using this data. This part of the model may have to be verified during a follow-up evaluation.

5.4 Locations of Pressure Sensors

The positions of the four pressure transducers were an important input. The initial depth information was obtained from these sensors. The locations of the transducers were not available at the start of the testing and their estimated locations relative to the CG of the upper torso were obtained from direct measurement. The locations for the four sensors are listed in Table 10.

Table 10. Pressure sensor X,Y, Z locations.

Location (rel. to up torso)	Channel No	X (in)	Y (in)	Z (in)
Upper right	21	1.7	5.7	-5.8
Lower right	22	1.5	4.5	9.2
Upper left	23	-0.2	-5.9	-6.3
Lower left	24	0.2	-4.5	10.0

All measurements were relative to the upper torso CG, though the lower pressure transducers are actually located physically in the lower torso. Since the lumbar spine was locked for all the tests, both segments could be considered as rigidly connected and the location of the lower transducers relative to the lower torso CG (which is defined to be the reference segment for the SWIM in the model) could be obtained. The vertical separation, when the dummy is erect, between the CG of the upper torso and the CG of the lower torso is about 13 inches. Thus, the typical location of the lower torso CG is about four inches below the depth found from the pressure transducers. The correction due to the pitch angle was made when the dummy was at intermediate pitch angles.

5.5 CG and CB Predictions from the SWIM Model

After making all modifications to the SWIM data set, the DYNAMAN program was run to estimate the CG and CB locations for the four basic configurations:

i. Normal ballast and straight configuration

ii. Normal ballast and right-angled configuration

iii. No ballast and straight configuration

iv. No ballast and right-angled configuration.

The results from the simulations are provided in the table 11. Comparisons are made with the experimental data for the CG and CB for configurations (i) and (ii) which were the two setups that were measured.

Table 11. Comparison of CG and CB values from test and simulations.

Configuration	Measurement	Test	Simulation
Normal ballast, straight	CG - X (wrt back)	5.28	5.66
	CG - Z (wrt heel)	-38.4	-38.7
	CB - X (wrt CG)	+.17	+.15
	CB - Z (wrt CG)	-.90	-1.00
Normal ballast, rt-angle	CG - X (wrt heel)	-30.5	-30.48
	CG - Z (wrt heel)	-11.86	-11.75
	CB - X (wrt CG)	-.38	-1.13
	CB - Z (wrt CG)	+1.54	+.25
No ballast, straight	CG - X (wrt back)	-	5.61
	CG - Z (wrt heel)	-	-39.77
	CB - X (wrt CG)	-	+.20
	CB - Z (wrt CG)	-	+.02
	CG - X (wrt heel)	-	-31.06
	CG - Z (wrt heel)	-	-12.29
	CB - X (wrt CG)	-	-.55
	CB - Z (wrt CG)	-	+.78

It is seen that for the normal ballasted, straight configuration, there is a small discrepancy in the X location of the CG relative to the back of the torso. This may arise from an error in the final assignment of the torso ellipsoid or from the compression of the jacket when the dummy was laid down on the CG measurement fixture. (It should be remembered that the CG measurements were made using the original Neoprene pads whose use was discontinued). The location of the CB (relative to the CG) was fairly close. If the CB measurements are accurate, this should lead to a close prediction of the equilibrium repose angle.

For the right-angled configuration (with normal ballast), there is a close agreement in the CG location (relative to the bottom of the heel), but their is a significant divergence in the location of the CB relative to the CG. The relative location, i.e. behind and below the CG, is the same for both the test and simulation. But the magnitudes are quite different. It is not known if this discrepancy arose because of error in the measurement process, or in the possible realignment of the segment ellipsoids when the legs were bent. The comparison of the motions predicted by the simulation with those seen in the tests will be the real judge of the accuracy of the CB values. If the final repose angle of the dummy is similar, then it will indicate that the simulation estimates are reasonable.

6.0 SWIM SIMULATIONS

Simulations of all the principal configurations were generated based on the available input data. The simulations were meant to be an exploratory evaluation of the performance of the WAFAC model with different initial conditions. In this study, no detailed examination was made of the sensitivity of the output parameters to different values of the important hydrodynamic coefficients. As indicated in the previous section, there were some areas of uncertainty in the SWIM data set to be used for the simulations. These centered around the precise location of the CG and of the CB relative to the CG. The test data for the bottom release from three meters were used to tune the input data set so that we were able to get the closest agreement between the simulation and test results. The principal coefficients were the drag coefficient, the added mass coefficient, and to a lesser extent the wave-damping coefficient. The preceeding test data were used to select values for these coefficients which appeared to provide good agreement with the test.

6.1 Determination of Initial Conditions

The initial conditions that are supplied to a WAFAC simulation consist of the initial orientation and position of the manikin, any initial motion of one or more segments, and the initial state of the joints, i.e. whether they are locked or not. In addition to the manikin data, the state of the water has to be described. For the bottom release and the push-glide tests only the location of the water plane relative to a point on the dummy has to be specified. In the current simulations, the water plane was made coincident with the horizontal plane, $Z = 0$ in the inertial coordinate system. In this case the location of the CG of the lower torso determines the depth from which the dummy starts its motion. For the wave tests, the description

of the waves are provided essentially through the wavelength, wave amplitude, and its direction relative to the dummy. For the push-glide test, the initial speed with which the dummy is moving in water is also inputed.

For all the test conditions, it is important to ensure that the initial conditions are maintained up to the moment the test is initiated. Any forces arising from the imbalance between the gravitational and buoyancy forces have to be controlled by constraint forces (such as by using wires or other mechanisms) which will keep the manikin in equilibrium until it is released. If any off-balance forces are initially present, they will tend to make the motion of the dummy different from the simulation predictions, especially during the early stage of the simulation. It is expected that as equilibrium is achieved when the dummy reaches the surface of the water, the differences will be less.

The tests were designed such that the motion would be basically in the vertical, X-Z plane. All forces were arranged to achieve this result. Because of small asymmetries in the left and right sides of the dummy, some off-axis motions entered into the results, especially over longer time periods and some roll and yaw motions enter into the picture. In the case of the simulations, all the data with respect to the dummy and the initial conditions are symmetrical, so there is no motion outside the X-Z plane. (In reality, there are small numerical errors that creep in which generate non-zero values for yaw and roll, but these are very small with respect to the change in the pitch angle.)

6.2 Estimates for the Hydrodynamic Coefficients

The initial estimates for the drag, lift, and added mass coefficients were made based on the results of the computer simulations performed to predict the motion of the initial ellipsoids tests done by IMD (Shams, 1996). From these tests, the range of values for the drag coefficient ranged from 0.4 - 2.0. The added mass coefficients ranged from 0.3 - 1.0. In addition, wave damping coefficient values were in the range of :

$$a_0 = 0.1 \text{ to } 0.3; \qquad a_1 = 0.25 \text{ to } 0.54$$

From the IMD drag tests, we also had information on the full-dummy coefficients, which ranged from about 0.6 when the dummy was parallel to the flow to 1.2 when the dummy was perpendicular to the flow.

The right-angled configuration fell approximately in-between.

For most of the simulations, an initial set of values were used, based on the initial ellipsoid study and on the IMD drag testing. If there was significant disagreement in the result with those from the test, then some parameter variation was performed to see if a closer agreement could be achieved. No detailed variation was performed during this study.

6.3 Summary of Simulations

The principal simulations, along with the initial configurations, and the corresponding test data sets are given in the table 12. Test file names are listed and are abbreviated notations for tests. For each condition, the test data were examined. As noted in the previous section, the accelerometer data were not usually reliable. The pressure transducer data were used to examine the vertical motion of the dummy in water. Usually all four pressure transducer locations were used, but normally, the lower transducers were more consistent. Since these motions were meant to occur mainly in the vertical plane, the average of the left and right side readings were used as the basis for comparing the simulation results. From the time history data, the time point at which release occurred was located. Usually the simulations were performed for about 30 seconds, which would allow the dummy to oscillate about 4 - 5 times.

6.4 Validation Procedure

The principal parameters that were examined to evaluate the 'goodness of fit' of the simulation results with the test were:

1. the depth location of the CG of the lower torso over time. Agreement in time history would ensure that the rise time to the surface and the vertical velocity of travel would also agree.

2. the pitch angle of the body over time. This would indicate whether the CB was located correctly relative to the CG and also provide information on the rotational drag of the body.

3. For the bottom release tests, the amplitude and the time period of the heave oscillations.

4. For the push-glide test, the time required for the body to come to a stop and for it to become upright was also compared.

Table 12. Description of SWIM simulations.

Configuration	Test File	Run No	Test Start Pt (sec) (relative to run)	Simulation File
Bottom release 3 m; norm ballast; vertical	br3m31ns	2	67.0	br3mns1
Bottom release 4 m; no ballast, vertical	br4m31ls	3	92.5	br4mls1
Bottom release 3 m; no ballast, vertical	br3mlh2a	5	36.0	br3mls1
Bottom release 3 m; norm ballast, horiz.	br3mnh32	3	78.0	br3mnh1
Bottom release 3 m; no ballast, horiz	br3mlh2a	2	62.75	br3mlh1
Bottom release 3 m; norm ballast, bent	br3mnr32	3	42.0	br3mnr1
Bottom release 3 m; no ballast, bent	br3mlr32	1	33.75	br3mlr1
In waves; f =0.3 Hz; norm ballast; vert.	wanls4	4	40.0	Wans1
In waves; f=0.5 Hz; norm ballast; vert	wanls4	9	40.0	Wbns1
In waves; f=0.7 Hz; norm ballast; vert	wanls4	11	40.0	Wcns1
In waves; f=0.5 Hz; no ballast; vert	wbljls3	2	40.0	Wbls1
In waves; f=0.5 Hz; norm ballast; bent	wbnlr4	4	40.0	Wbnr1
In waves; f=0.5 Hz; norm ballast; jts unlocked; vert	wbnju	3	70.0	Wbnsj1
Push-glide; v=1 m/s; norm ballast; face fwd & down;	pgnjls	4	30.0	Pgnjls1

7.0 TESTING RESULTS

7.1 Bottom Release Tests

Bottom release testing was completed for depths of seven, five, four, and three meters, with joints locked in the upright and right angle positions. These release points are measured to the bottom of the SWIM feet and are nominal but repeat-able depths. The joints were locked to prevent move-ment of the seg-ments to make modeling easier. The release mechanism was attached to a Styrofoam float. This mechanism/float was attached to a rope which went through a pulley attached to an underwater tower and back to the surface at the side of the test tank. The use of this underwater tower allowed the release mechanism to be moved to different depths during testing. The SWIM was fastened to the mechanism and pulled underwater to the stop on the tower. When the SWIM was stable and at equilibrium under water the data acquisition systems were triggered, a string was pulled to release the SWIM to float to the surface. Data were

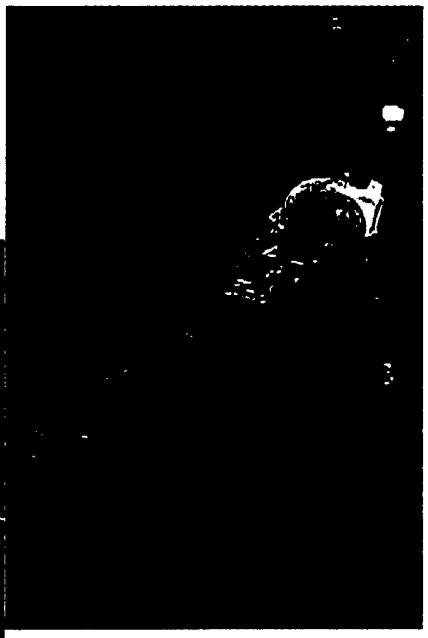

Figure 32-A. Above 7-meter bottom release test on surface, end of test.

Figure 32-B. Left 7-meter bottom release test breaking surface.

Figure 32-C. Left 7-meter bottom release test halfway to surface.

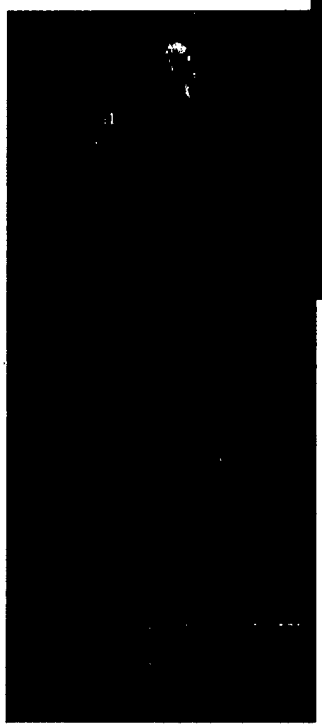

Figure 32-D Left 7-meter bottom release test, test start 7 meters below surface.

taken a few seconds before the release, figure 32-D; during the rise to the surface of the water, figure 32-C; breaking the surface, figure 32-B; and for a time, while floating on the surface, figure 32-A. These data later are used as input data to the WAFAC model program and are compared to the simulation information using the same weights, buoyancy and characteristics of the SWIM for each series of tests. Each set of tests was completed three times. The measure of this effort is to determine how closely these two systems match.

7.1.1 Bottom Release Tests Summary

The bottom release tests conducted at three and 4 meters depth were used to compare the SWIM sensor output data to the WAFAC computer simulation. Bottom release tests at five and seven meters were lost due to sensor problems and are not recoverable.

The three and four meter bottom release tests with normal ballast and no ballast in both the straight and right angle configuration generally showed very good repeatable for the sets of three tests conducted with the SWIM. In comparison with the WAFAC model simulations the profiles for the depth and rise time to the surface, for those tests, were also good. The simulation usually predicted a slower response by one or two seconds in the rise of the SWIM to the surface than the actual test showed. For the pitch angle general wave form comparisons between the test and simulation were good but the actual angle of pitch response between the two was not. The test always showed a higher pitch angle and a more dampened frequency than that of the simulation. Various adjustments were made to the drag and added mass coefficients to correct the response of the simulation to the actual test data. These changes reflected an even closer match between the simulation and test for the depth and rise times for the tests but had only moderate success in correcting the pitch angle response. It is apparent that better measurements of the CG and CB need to be made at exact test weights which would include captive water. More accurate measurements of all the base data will aid future simulations. The replacement of the accelerometers and pitch and roll sensors with sensors of the proper sensitivities will positively effect future simulations.

Appendix C contains a more detailed explanation of the incremental changes made to the coefficients for drag, lift, added mass and wave damping for the bottom release testing.

7.2 Push Glide Tests

The push glide tests were originally to be conducted at velocities of 0.3, 0.6, and 0.9 m/s, making 3 runs each with head forward at normal and off-normal weights, and again with feet forward at both weights. The push glide tests were conducted last because these were the least critical tests. A frame constructed in an 'H' pattern was used and affixed to the tow carriage assembly. The frame had 1- inch tapered pins toward the outboard side of each leg of the H at shoulder width on the front side and knee width on the back side. The attachment brackets were mounted to the SWIM shoulders and knees and a small line was tied through each with a 4-inch loop in the end. The frame was lowered to about three inches above the SWIM as it floated horizontally in the water face down (figure 33), in normal outfit weight. The loops in the string were attached over each pin, but it was impossible to keep the SWIM on the frame because the feet tend to sink. To overcome this, a tether line was attached to the ankles. This solved three problems: one, it allowed us to pull the feet up level with the water until the carriage could move forward; two, it helped orient the SWIM exactly in the direction of the test; and three, it allowed reverse pressure on the loops and pins and held the SWIM in place at the shoulders until the test started. During the final testing only the shoulders were attached to the pins. The towing carriage was programmed for speeds as above and tests were conducted first at 0.3 m/s. The result when the carriage stopped was that the SWIM moved forward very little and when the feet sunk and it righted it bumped the frame. The same test was run at 0.6 m/s and 0.9 m/s with similar results. It was obvious that push glide tests of less than one m/s would yield little useful data. One of the problems occurring was the deceleration of the carriage. At 18 tons it was not programmed to decelerate quickly. The deceleration was adjusted as short as deemed safe and three tests were conducted again at one m/s. These results were good. The SWIM glided forward about one SWIM length, about six feet, it gently turned toward the right front and righted itself in a face up attitude of about 15 degrees with the bottom of the nose in the water, figure 34. Further push glide testing was not completed due to time restrictions.

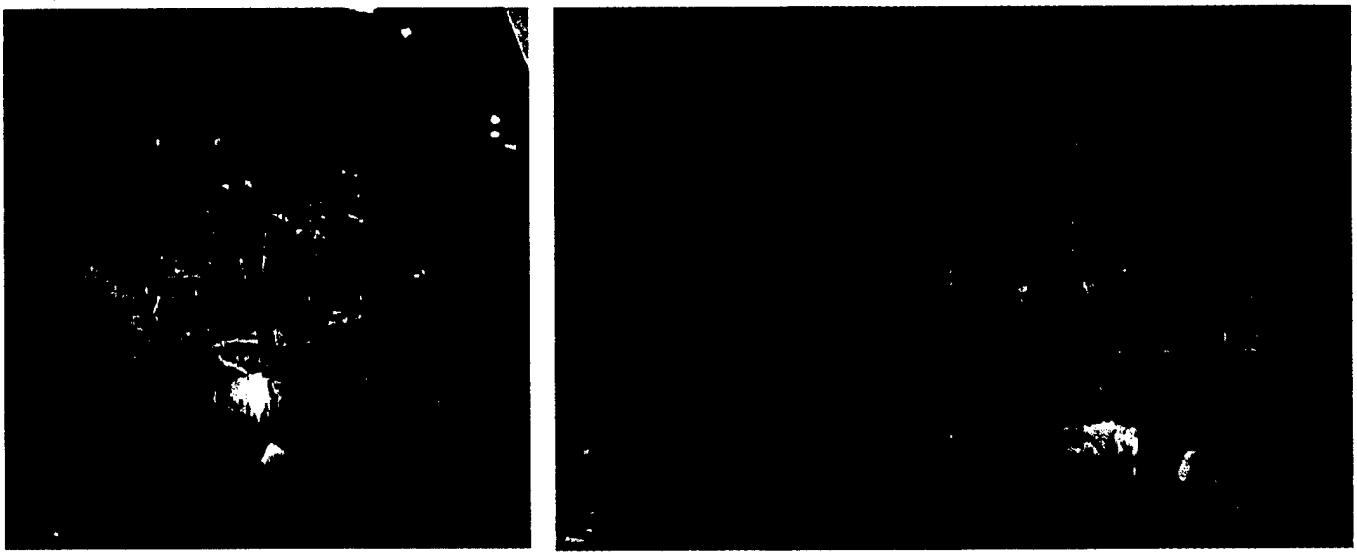

Figure 33. Push glide tests forward and side view.

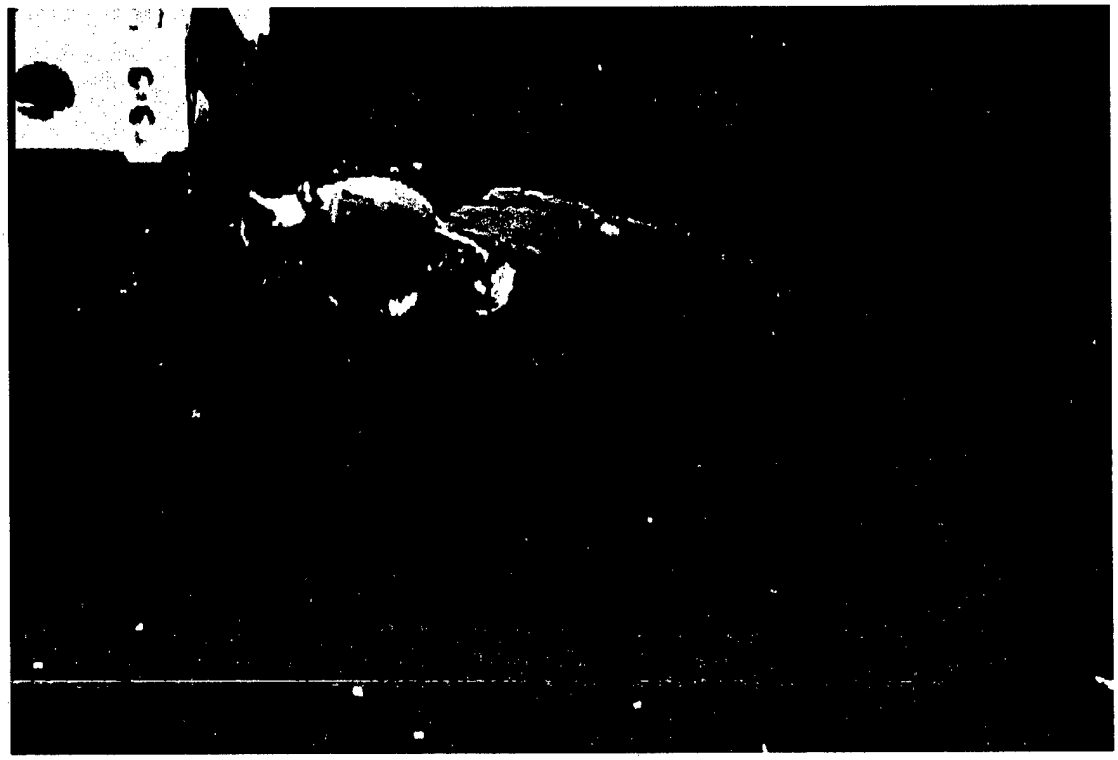

Figure 34. Final attitude of SWIM during push glide tests.

The data from test PGNJLS (run #4) was used for comparison. The pressure transducer and pitch time-histories were checked to determine the depth and pitch angle to be used for the initial condition in the simulation. The initial conditions from the pressure and pitch sensors from this run provided the following initial conditions:

Depth (mean depth from avg. of right and left pressure transducers): 14 inches (0.36 m)
Pitch (from auxiliary pitch sensor-channel 15) -90 deg.

The position of the lower torso CG based on the depth was taken to be 12 inches. The coefficient values used in this simulation were:

drag coefficient:	$C_D = 0.6$	
added mass:	$A_i = 0.3$	(for all directions)
wave damping:	$a_0, a_1 = 0.25, 0.5$	

No significant changes were made to the coefficients, these values were similar to those used for the case with the ballasted dummy in bottom release tests. The drag coefficient was similar in magnitude to that obtained from the IMD towing tests.

The results are shown in figure 35 and figure 36.

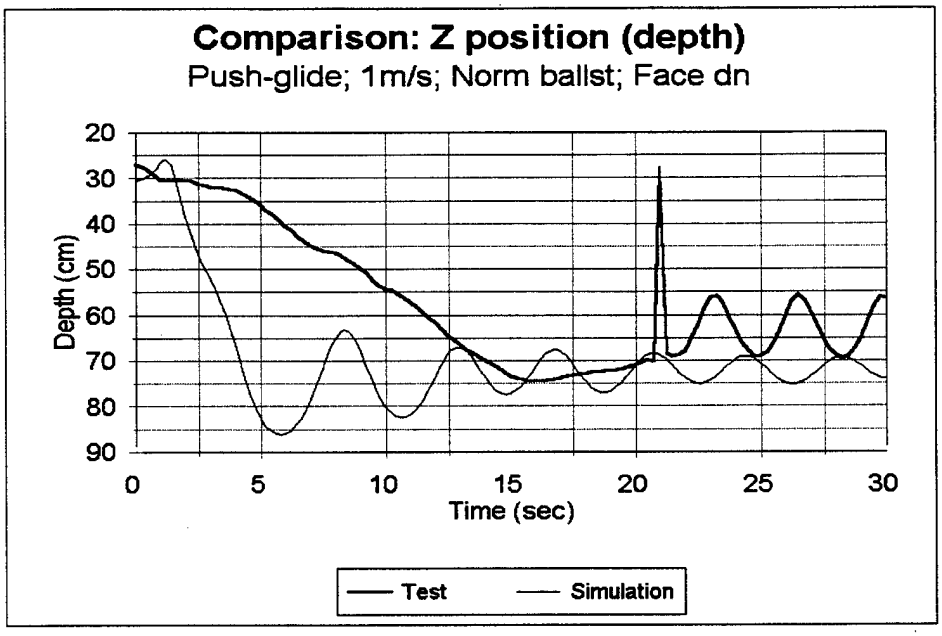

Figure 35. Comparison of depth from test and simulation: push-glide test; normal ballast; horizontal; face down.

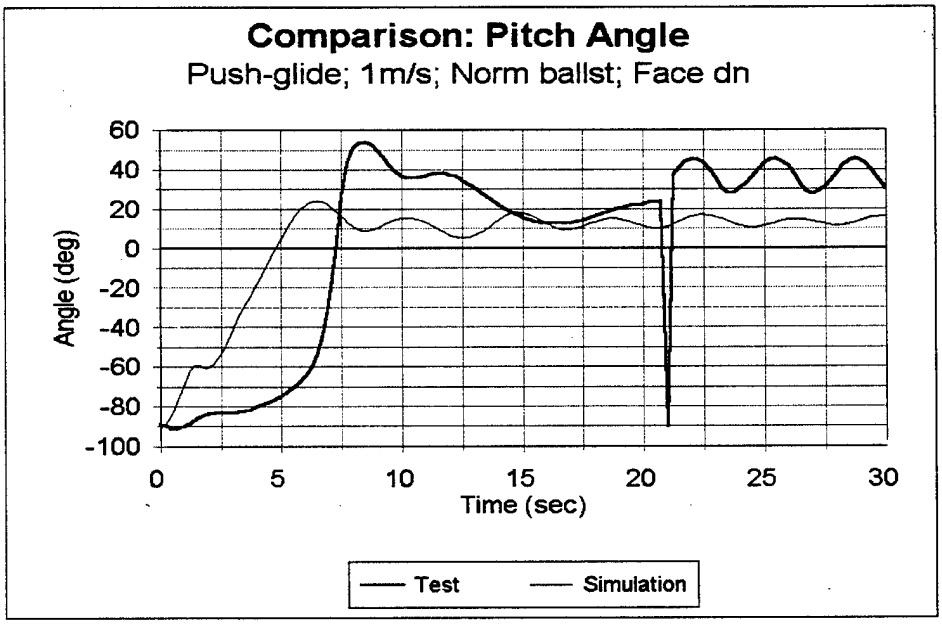

Figure 36. Comparison of pitch from test and simulation: push-glide test; normal ballast; horizontal; face down.

It is seen that the simulation shows a much faster response than seen in the test, but the magnitude of the change in depth and in pitch is predicted fairly well. There is a small glitch in the sensor data from both

the pressure sensor and the pitch sensor, which may have been due to some background electrical spike. From the pitch sensor data, it is seen that the simulation predicts that the dummy will upright itself about 2 sec. earlier than actually seen in the test. This time can probably be controlled by proper adjustment of the rotational drag as the dummy rotates into its equilibrium position. The amount of glide predicted by the program was about 50 inches. This appeared to be similar in magnitude to what was observed visually. The actual distance could not be directly compared to test data since the X accelerometer information showed anomalous behavior.

7.3 Whole Body In-Wave Tests

The SWIM whole body in wave testing was to be completed at various attitudes using the wave making capability of the towing tank. It became apparent after an initial test sequence that it was difficult to hold the SWIM in some of these initial starting positions without imparting movement to the manikin at the start of the test. Tests were completed for the SWIM in the following configurations:

1. Swim outfitted for Normal and Light weight in the vertical position, joints locked.
2. Swim outfitted for Normal weight in the right angle position, joints locked.
3. Swim outfitted for Normal weight in the vertical position, all joints unlocked.

The wave sets used for test purposes were:

Wave Set A = Frequency 0.3 Hz, Length 17 meters, Height 25 cm (10 inch)

Wave Set B = Frequency 0.5 Hz, Length 6.2 meters, Height 25 cm (10 inch)

Wave Set C = Frequency 0.7 Hz, Length 3.2 meters, Height 25 cm (10 inch)

Wave Set D = Frequency 0.5 Hz, Length 6.2 meters, Height 30 cm (12 inch)

Testing in wave front A or C appeared to impart little movement to the SWIM for these preliminary tests. Wave front B and D seemed to provided the stimulation which would yield the best data overall. The SWIM was moved to a point slightly forward (toward the wave maker) of the halfway mark of the tank and lowered into the water. The halfway mark was used to permit the longest data run possible before waves were reflected back into the tank from the beach and still allow a small amount of data to be taken in the still water before the first wave encounter. It was also thought that the SWIM would be pushed back toward the beach with each wave encounter. Small tag lines were attached to the SWIM in order

to orient the manikin properly to the oncoming wave set and to aid in moving the SWIM back to the same starting position between test series. One line was threaded over the side of the carriage to the SWIM head lifting eye and the other on one shoulder. At the start of each test SWIM was oriented perpendicular to the front of the tank and allowed to reach absolute equilibrium in the water with the lines slackened. Each test sequence included three tests and started with a perfectly calm water surface. With still water data acquisition was initiated.

1- Test 1, Data was gathered during the transition from still water to the wave set.

2- Test 2, Data was gathered while under the forces of the wave set.

3- Test 3, Data was gathered while under the forces of the wave set.

As each test progressed the tank carriage was moved backwards as the SWIM moved and returned to the same starting position after each set of three tests. The following summaries for each test describe the attitude changes of the SWIM in general terms for tests conducted in 0.5 Hz waves with either 25cm (10 inch) or 30 cm (12 inch) waves.

SWIM VERTICAL, JOINTS LOCKED, NORMAL WEIGHT

- CHEST FACING AWAY FROM WAVES, FACE UP, HEAD FORWARD

As the test started the SWIM Floated with a chest up attitude at about 20 degrees with the face out of the water to the mouth. As the waves encountered the SWIM the head went under water on the crest and out of the water at the troughs to the middle of the neck.

- CHEST FACING WAVES, FACE UP, HEAD AFT

At the start of the test the SWIM floated in the chest up attitude of about 20 degrees with the face out of the water up to the mouth. As the waves encountered the SWIM the manikin slowly turned to the right approximately 90 degrees, over a period of two minutes and ended up with the right shoulder into the waves. The SWIM then would then waffle back and forth between 85 and 95 degrees from its starting point as the waves washed by. With the SWIM on the crest of a wave the water was usually covering the head to the middle of the forehead. When the SWIM was in the trough, the water was below the jaw to the mid neck level. This was the final non-resting position while in the wave front.

SWIM RIGHT ANGLE POSITION, JOINTS LOCKED, NORMAL WEIGHT

- BACK FACING WAVES, FACE IN WATER, HEAD AFT

At the start of the tests, the SWIM floated in an attitude with face down in water with only about one inch of the back of the head above the surface with the angle on the back about 20 degrees to the surface of the water, figure 37-A. As the waves washed by the SWIM, the SWIM stayed in the same back-toward waves attitude and rocked front to back over about 20 degrees, alternately with the head under and the lower back just touching the surface (figure 37-B), to half of the head and top of the shoulders breaking the surface (figure 37-C), to the head under and the lower back just touching the surface (figure 37-B).

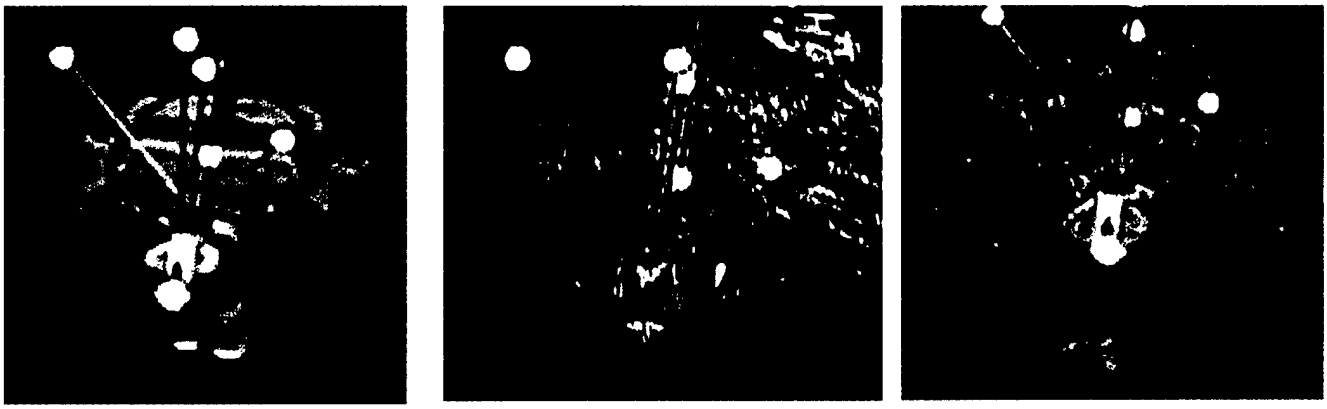

A B C

Figure 37. Wave test right angle, A – start of test, B – head under (wave crest), C – head above water (wave trough).

SWIM VERTICAL, JOINTS UNLOCKED, NORMAL WEIGHT

- BACK FACING WAVES, FACE IN WATER, HEAD AFT

At the start of the test the SWIM's legs hung straight down in the water with approximately a 35-degree angle to the back. The SWIM was face down in the water up to the ear line with the back toward the surface of the water. As the waves encountered the SWIM the water moved to alternately completely cover the head to having the neck and shoulders out of the water. The SWIM stayed with the back toward the waves.

SWIM VERTICAL, JOINTS UNLOCKED, NORMAL WEIGHT

- CHEST FACING WAVES, FACE UP OUT OF WATER, HEAD FORWARD

At the beginning of the test the SWIM's legs hung down at about a 15-degree angle to the chest with the face out of the water up to the chin and the chest facing the water surface. As the waves encountered the SWIM the SWIM turned 180 so that the feet were forward. The waves alternately move the SWIM between a head underwater position to the front chest and most of the head above water.

7.4 A Summary of Whole Body In-Wave Tests

The whole body in-wave tests were of special interest in the use of the WAFAC mode, as this is the first time the software has been tested against this condition. It should be noted again that the pressure transducers were used for the acceleration and depth characteristics and this was a disadvantage. The pressure transducers measure depth to the surface of the water. In a periodic wave set this varies as the waves pass by and we do not get exactly the same effect as if the wave form were measured by accelerometers.

1. In the case of the 0.3, 0.5 and 0.7 Hz wave front, with normal ballast and straight configuration there was good frequency match between the WAFAC simulation and the test output for both the depth and pitch of the SWIM. The magnitude of the depth was lower for the test than the simulation and the pitch magnitude was higher in the test.

2. In the case of the 0.5 Hz wave front, with no ballast and straight configuration the frequency match between the test and simulation was good for the depth. The magnitude of the depth was lower in the test. The pitch sensor over ranged at 90 deg.

3. In the case of the 0.5 Hz wave front with normal ballast in the right angled position the frequency match for the depth was good but the magnitude was significantly off with the test lower than the simulation.
4. In the case of the straight unlocked joints, 0.5 Hz wave front with normal ballast there was good agreement between the test and simulation for the frequency of the depth and pitch. The magnitudes however were considerable off, both the depth and pitch were much higher in the test than the

simulation. For this test we also looked at the right hip and right shoulder movement. The result is that the test data show very little movement as compared to the simulation. The lack of movement of these two segments was observed during the tests. There appears to be a certain amount of binding of the skins with each other which reduces movement.

5. In summary, it was learned that making do with sensors which do not have the sensitivity or range required is not an adequate solution. Also the CG and CB need to be defined more accurately. The weights of a wet and dry SWIM need to be better defined so the solutions, which depend on these data, is more accurate. The in water tests were the first chance to use the WAFAC model for this type testing and with the baseline data collected the outcome is encouraging. There was consistency in waveforms and frequency in some cases between the test data and the simulations for those same runs. Some comparisons were close and some were not. With more testing of a fully functioning suite of sensors in SWIM the outlook for a closer comparison is reasonable.

8.0 RESULTS

8.1 Discussion and Conclusions

Simulations using the WAFAC model and DYNAMAN were performed to model the testing conditions set up during test sequence at IMD. The simulations included bottom release tests, wave tests and one push-glide test. The main results obtained from the simulations are summarized below.

1. The rise time to the surface was predicted well by the model for the bottom release tests for all test conditions. Some adjustment of the initial drag coefficient was necessary to make the agreement better. But this feature meant that on the whole the buoyancy and drag forces were being modeled correctly. For the unballasted cases, the simulation usually placed the final equilibrium position slightly closer to the water surface than seen in the test. This was probably due to small difference in the buoyancy being estimated by the program and the actual buoyancy. (No separate CB measurement was made with the unballasted dummy.)

2. There was approximate agreement in the heave amplitude and frequency, the agreement getting worse for the cases with no ballast and when the dummy was placed in a right-angled configuration.

3. The simulation model generally followed the shape of the pitch time history. The model predicted correctly the final configuration for the vertical and horizontal cases with and without ballast. The normally ballasted right-angled case was also well duplicated. The simulation predicted shallower equilibrium pitch angles than seen in the test. This is probably due to simulation placing the CB slightly off from the actual position. The only serious mismatch was with the unballasted, right-angled case. In this case, the simulation predicted that the dummy would pitch away in an opposite direction than seen in the test. It is not clear what may have produced this effect.

4. For the wave tests, the model predicted the general frequency and shape well. For the wave test with the 0.5 Hz frequency and normal ballast, the more complex motion seen in the test, of the head being submerged every other wave could also be duplicated, by proper adjustment of the coefficients. There was usually a mismatch in the amplitude of the forced oscillation, with the simulation predicting much higher amplitudes. The simulation and the test data used different frames of reference for measuring depth, so from this initial evaluation it was not clear the degree of agreement that actually occurred.

5. The push-glide simulation indicated motion similar to that seen in the test, but did not show a good numerical match with the limited test data. The amount of glide predicted by the program could not be directly compared because of the lack sensor data.

6. For the unlocked joint condition the model indicated that the rotation of the arms and legs was greater than seen in the test, but was still relatively small for the wave condition used.

8.2 Recommendations for Future Modeling

The current simulations were intended to provide a fairly detailed view of the performance of the WAFAC model in different conditions. As summarized, there was general agreement in the gross motion characteristics such as rise time, heave oscillation frequency, amount of expected pitch rotation, etc. For some conditions, especially those involving the unballasted dummy, the agreement was not as good and pointed out the need for improvement in several areas.

8.2.1 SWIM Input Data

As indicated in the earlier sections, there were certain limitations in the input data used for the SWIM simulations. These included:

1. The original data did not take into account the weight of the vest.
2. The original data did not take into account the slightly different weight distribution resulting from a wet dummy.
3. The ellipsoid data had to be revised to more closely represent the actual surface geometry of the SWIM. This was done using the CAD files for the SWIM, but were not verified on the actual manikin.

8.2.2 SWIM Measurements

The center of gravity measurements were taken with a dry manikin while the actual testing was with a wet manikin which had a slightly different weight distribution. Also the center of gravity measurements and the center of buoyancy measurements were taken on slightly different dummy setup. The center of gravity measurements were taken with the original neoprene pads, while the center of buoyancy measurements were with the revised Styrofoam inserts. Since the Styrofoam inserts produced a slightly different surface geometry this may have lead to an error in the location of the CB relative to the CG, especially since the CB is very close to the CG location. The correct position of the CB relative to the CG is crucial in predicting the correct repose angle of the dummy.

The sensitivity of the buoyancy data to the correct measurement of the tie-point application indicated that these measurements require a more precise procedure. In addition, for a thorough validation of the model, the buoyancy of the individual segments had to be thoroughly determined. Only then can the input data used in the model be reliably verified.

8.2.3 Instrumentation

The inability to use the accelerometer data limited the information that could be extracted from the tests. For this initial investigation, this limitation was not critical, since the pressure transducer data appeared to work correctly and could be used to analyze the bottom release tests fairly thoroughly. But for future

testing, the data from the accelerometers would be necessary to estimate the amount of horizontal drift expected in different water conditions.

The lack of reliable accelerometer data also meant that the motion of the dummy with respect to the laboratory coordinate system could not be fully established. Reliance was made on the pressure transducer data which provides information relative to the water plane, which in the case of waves is always changing. This made it difficult to directly compare the output from the simulation with the test data. It may be possible to modify the simulation program, to allow output relative to the water plane. For a few tests, the lack of pitch data meant that the rotational motion of the dummy could not be tracked properly. Only a very rough comparison could be made between the predictions of the model and the data from the test.

8.2.4 Modeling Enhancements

From the results, it appeared that the SWIM model performed well in predicting the gross motions of the SWIM dummy. The time of rise, the heave frequency, and even the equilibrium repose angle were fairly well predicted. But the model can be improved with a number of modifications:

1. One area is a closer definition of the surface area than the current ellipsoid model. A fair representation of the surface area, and hence the volume of water displaced, is achieved with the correct ellipsoid sizes. But with the capability of modeling the surface forms more closely, e.g. by the use of cylindrical shapes, it should be possible to improve the predictions for the buoyant force and the drag force.

2. The overlap between adjacent ellipsoids should be accounted for. In the present simulations, the overlap was minimized by a thorough evaluation of the appropriate ellipsoid sizes that should be used. However, there were still areas where either there was some residual overlap or there was a volume that was not represented.

3. The capability of modeling different drag coefficients in different directions, as well as, for rotation should be introduced. The original single ellipsoid tests indicated that the drag coefficient depended

on the aspect ratio presented in the direction of motion. Intermediate directions may be modeled by some form of interpolations between the coefficients used along two different orthogonal directions.

4. Rotational added mass coefficients should be introduced to account for the inertial effects during rotation of the dummy. For some configurations, there was a significant difference in the time to reach equilibrium, one reason being a mismatch in the rotational inertia of the body.

5. The results from the wave tests at different frequencies show that there is a difference in the optimum coefficients required. Further examination of this effect is necessary and it may be necessary to provide an option to have some frequency dependent coefficients, especially regarding the wave damping coefficients.

6. One area of the model that needs more careful checking is the unlocked joint case in waves. The dynamics of the dummy as a whole is working correctly and the standard joint model has been verified in normal dynamic conditions. But there were some anomalous results, and it is not clear at present whether they are due to problems in the calculations of the moments generated by the hydrodynamic forces on the individual segments. A simpler test such as a release from a horizontal position, with unlocked joints may be useful in identifying the problem.

Since a fairly close agreement was reached for many of the primary response parameters, it is expected that none of these modifications would result in any significant change in the model. These changes should make the model more robust and capable of handling unusual motions of the dummy in water, and not merely translational motions.

8.3 SWIM Enhancements

A number of deficiencies were found with the SWIM during testing, and have been reported on in this report. These deficiencies some in the form of initial data some in the form of hardware problems need to be resolved before further testing continues. The following items are identified for these purposes and are in no particular order of importance.

- The CB and CG measurements need to be remeasured using a dry and wet SWIM where applicable, for the ballasted and unballasted conditions.
- SWIM test weights while wet and dry need to be well defined.
- The SWIM floatation vest needs to be 'pinned' in some manner to the chest and back so that it adheres to the SWIM exactly the same at each application.
- The SWIM internal accelerometers need to be replaced with accelerometers with the proper sensitivity to detect the small accelerations in water.
- The Roll and Pitch sensors should be replaced with sensors that can detect and measure as close to 360 degree rotation as possible.
- A better Yaw angle indicator should be installed which has more repeatable calibration features.
- Thought should be given to an integrated 6 degree of freedom sensor package, which would include all these sensors.
- Present placement of lower pressure transducers makes modeling very difficult, as the transducers change attitude with the flexing of the lower torso. Changing placement of the two lower pressure transducers should be considered.
- A close look at the interaction of the skins of the major segments with the torso, looking at freedom of movement should be examined. Consideration should be given to coating those portions of the segments that rub together with Teflon or a similar material.
- New skins for the right and left pelvis insert should be made, because of leaking due to cracks.
- New feet should be made, because of leaking due to cracks.
- A patch kit of suitable materials and glues should be purchased to insure the timely repair of tears and cracks during future testing.
- The present SWIM chest cavity is machined to exactly fit the batteries and sensor package. In the event additional machining is necessary, thought should be given to machining out all the useable space in the chest and preparing an insert to hold the instrumentation securely. In this manner making room for different or additional sensors would require only replacing the insert.
- Locking bolts for the major segments should be changed to a hex head bolt. The bolts used to tighten the thigh joints presently use an Allen wrench format and cannot be tightened enough to prevent movement of those joints. Larger bolt sizes may solve this problem.

9.0 CONCLUSIONS

These preliminary tests showed that the general floatation attitudes of the SWIM in the water can be adjusted to reflect those of a human. Although there was general agreement between experimental and analytical results using the WAFAC program, it became apparent that many of the problems discussed in section 8.2.4 and 8.3 must be resolved before testing continues.

The next step in the development of the SWIM and WAFAC model will be to fix the deficiencies identified in the preliminary testing and conduct new measurements on SWIM to establish better baseline data. This new baseline data will in turn be used to improve the performance of the WAFAC model. The objectives of the initial SWIM and WAFAC tests were met. These were the first systematic tests of the SWIM and WAFAC and showed the potential for both tools to emulate the other. The total validation of each tool will facilitate future work within the U.S. Coast Guard and Transport Canada, in the broad general area of PFD performance improvements. The SWIM will provide a better mechanism for the no risk testing of life jackets in rough water. The WAFAC model will provide a mechanism to simulate and refine new PFD designs without water testing. Further testing will be coordinated through the U.S. Coast Guard Headquarters Office of Design and Engineering Standards (G-MSE), and Office of Boating Safety (G-OBP) and Transportation Development Center, Canada. Testing is scheduled to start in FY 2000.

10.0 REFERENCES

McKenna, R., Gareau, G., and Macesker, B. (1994). Experiments with Ellipsoids to Simulate Human Body Hydrodynamics,. SAFE Conference.

Macesker, B., Gareau, G., "New Tools for Coast Guard Research of the Rough Water Performance of Personal Floatation Devices (PFDs)," U.S. Coast Guard R&D Center No. CG-D-19-97.

Manikin Calibration Experiments in Still Water: Drop Tests and Bottom Release Tests, NRC IMD, TR-1993-24.

Newman, J.N. (1989), Marine Hydrodynamics. The MIT Press, Cambridge, MA.

Reynolds, D. (1993), A case study of the water force analysis capability for the ATB model with emphasis on improved added mass and damping. Final Report, AL/CFBV, Bolling AFB.

Reynolds, D.B., "A Study of the Water Forces Analysis Capability for the ATB Model with Emphasis on Improved Modeling of Added Mass and Wave Damping," Sponsored by the Air Force Office of Scientific Research, 1992.

Shams, T. (1996), "WAFAC Ellipsoid Simulations, Prepared for the U.S. Coast Guard R&D Center.

Technical Operating Report (TOR) for the Sea Water Instrumented Manikin – A Flotation Manikin Mechanical Subsystems and Sensors, Systems, Veridian, Inc., Draft Report Prepared for Wright Patterson Air Force Base, 1998.

United States Department of Transportation/Transport Canada Joint Research Project Agreement Number 6 for the Performance Research of Personal Floatation Devices dated November 14, 1991.

Weerappuli, D.P.V., Development of Water Forces Analysis Capability (WAFAC) for the Articulated Total Body Model," GESAC, Inc., Prepared for WPAFB, 1992.

Wright-Patterson Air Force Base, "Recommended Characteristics of Anthropomorphic Manikins for Use in Testing Effectiveness of Personal Flotation Devices," dated January 1990.

10.1 Additional References of Interest

Note: Although the following references have not been specifically referred to in this report, they are of direct interest to this project.

(A) "Sea Water Instrumented Mannequin (SWIM) Preliminary Experiments" Institute for Marine Dynamics, NRC, St. John's, Newfoundland, Canada 1999.

(B) Girton, T.R. and Wehr, S.E., "An Evaluation of the Rough Water Performance Characteristics of Personal Floatation Devices," USCG-M-84-1 Report January 1984.

(C) Hart, C.S., "A Study of the Factors Influencing the Rough Water Effectiveness of Personal Floatation Devices," DTRC-88/026 Report July 1988.

(D) Steinman, A.M. CDR, "A Comparison of the Protection Against Immersion Hypothermia Provided by Coast Guard Anti-Exposure Clothing in Calm versus Rough Seas, "USCG Report CG-D-17-85, June 1985.

(E) Mannikin/ATB Validation Assessment, Melville Shipping Ltd., Prepared for Canadian Coast Guard, 31 March 1995.

(F) McConville, J.T., "Anthropometric Relationships of Body and Body Segment Moments of Inertia," AFAMRL-TR-80-119, December 1980.

(G) DAS-32 Data Acquisition System Operations Manual, Version 7.3C, EME Corporation, Arnold, MD.

(H) "Volume Tests of Manikin Components and Photogrammetric Analysis of Human Subjects," Melville Shipping, Inc. Prepared for Transport Canada, 31 March 1996

(I) Generation of Body Data (GEBOD) Report, Wright Patterson Air Force Base

(J) McKenna, R., Gareau, G., and Macesker, B. 1994. "Experiments with Ellipsoids to Simulate Human Body Hydrodynamics," SAFE Conference.

APPENDIX A

CENTER OF GRAVITY MEASUREMENTS

IMD performed CG measurements on the whole dummy in two configurations, namely, with the dummy completely straight and with the legs bent at right angles at the hip. The measurements were made on the dry, normally ballasted dummy (i.e. with the dry weight of 69 kg). The results from these measurements were:

i. Straight configuration:

As measured relative to the IMD reference frame:

Longitudinal (in X direction of dummy system) position:	0.134 m (5.28 in)
Vertical (in Z direction of dummy system) position:	0.0097 m (0.38 in)

NOTE: It should be remembered that in the dummy coordinate system, the +Z axis is directed from the head to the feet, and the +X direction is directed from the back to the front (posterior-anterior).

For the purposes of comparison with the CG calculated from the SWIM model, these positions were translated to a reference frame tied to the bottom of the heel . In this frame, the positions were:

CG - X: 0.134 m (5.28 in)

CG - Z: -0.975 m (-38.4 in)

ii. Right-angled configuration:

As measured relative to the IMD reference frame:

Longitudinal (in X direction of dummy system) position:	0.0291 m (1.15 in)
Vertical (in Z direction of dummy system) position:	0.301 m (11.85 in)

Again, in terms of a reference frame with the origin at the heel:

CG - X: 0.774 m (30.5 in)

CG - Z: -0.301 m (-11.86 in)

After the CG measurements were made, and during the initial bottom release tests, a problem with the Neoprene pads was discovered. It was found that when the dummy was released from a depth of seven meters, it sank. This was probably due to the increased hydrostatic pressure resulted in a compression of the pads and a resulting loss of buoyancy. In order to circumvent the problem, the pads were replaced

with Styrofoam pads which would remain stiff under water. The approximate volume of the upper torso remained about the same upon replacement, but the shape was somewhat more squarish with the stiffer Styrofoam pads. Also the weight dummy remained essentially unchanged with the replacement. Because of this the CG measurements were not repeated, since it was expected that it would be close to the original values.

The weight of the dry SWIM (with normal ballast) with the Styrofoam inserts was 69 kg (152 LB), while the weight in the wet state was 154 lbs. The net buoyancy of the complete dummy was found to be 1.7 kg (3.7 LB). These values were used to finalize the inertial characteristics of the SWIM data set.

APPENDIX B

CENTER OF BUOYANCY MEASUREMENTS

CB measurements were taken in both the straight and the right-angled configurations. For each configuration, the dummy was held under water, using a cable tied to four specific locations on the dummy. For each tie location, the dummy would rest a specific pitch angle. Using the pitch data at the four locations, the relative position of the CB from the CG was estimated. It was assumed that the tie-point was placed symmetrically along the Y axis, thus producing no roll or yaw motion. The pitch was measured using the pitch sensor. For the straight configuration, the pitch sensor attached to channel 4 on the DAS was used. For the right-angled configuration, it was found that the angle could go past 60 deg., which was the range on the sensor. For this configuration, the new roll sensor, which has a full 180° range, and which had been attached to DAS channel 16 was converted to measure pitch.

The calculation used is based on a simple balance of moments of the buoyant force and the tension force on the cable about the body CG. This is shown in figure B-1.

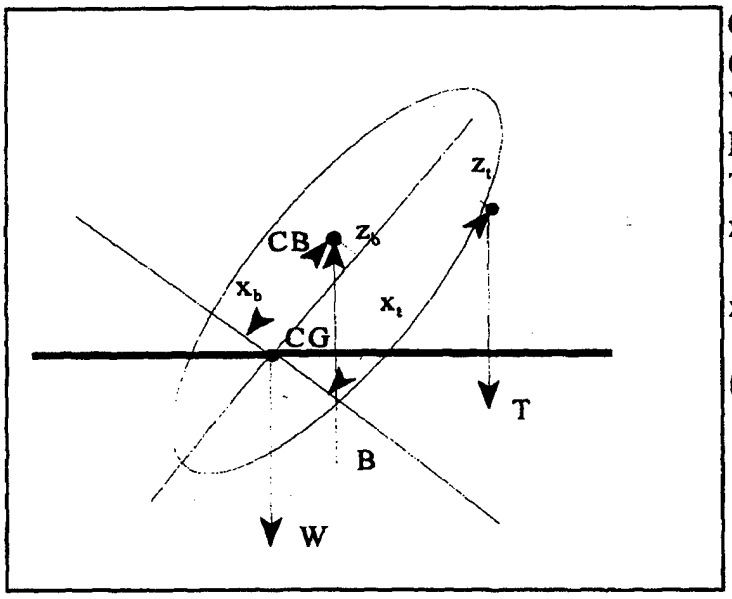

CG = center of gravity
CB = center of buoyancy
W = weight of system
B = buoyant force
T = cable tension force
x_b, z_b = X, Z coordinates of CB relative to CG
x_t, z_t = X, Z coordinates of cable tie-pt relative to CG
θ = angle of pitch of dummy in equilibrium

Figure B-1. Diagram showing setup of CB location calculations.

The balance of forces, of course, lead to:

$$B = W + T \qquad \text{and } T = B - W \tag{1}$$

i.e. the buoyant force will equal the sum of the body weight and the tension force.

The balance of moments of B and T about the CG leads to:

$$B(z_b \cos\theta - x_b \sin\theta) = T(z_t \cos\theta - x_t \sin\theta)$$

$$z_b - x_b \tan\theta = \frac{T}{B}(z_t - x_t \tan\theta) \tag{2}$$

where the symbols have been defined above. In the second equation, all the terms except for x_b and z_b are measured and hence are the two unknowns. B and T are known from direct measurements in air and water. The location of the tie-points are also measured with respect to the CG that was measured for a specific configuration, and finally, the pitch angle θ is measured using the pitch sensor. Thus, this equation is in the form of a linear equation with two unknown parameters:

$$y = ax + b; \tag{3}$$

and there are four points at which x and y have been measured. This gives us a minimum number of measurements to allow us to use a regression fit to evaluate x_b, z_b. Additional measurements would make the fit better.

i. Straight configuration:

The equilibrium pitch angles which were achieved are shown in figure B-2. The section of the time history data where effective equilibrium was achieved is also shown for the four locations.

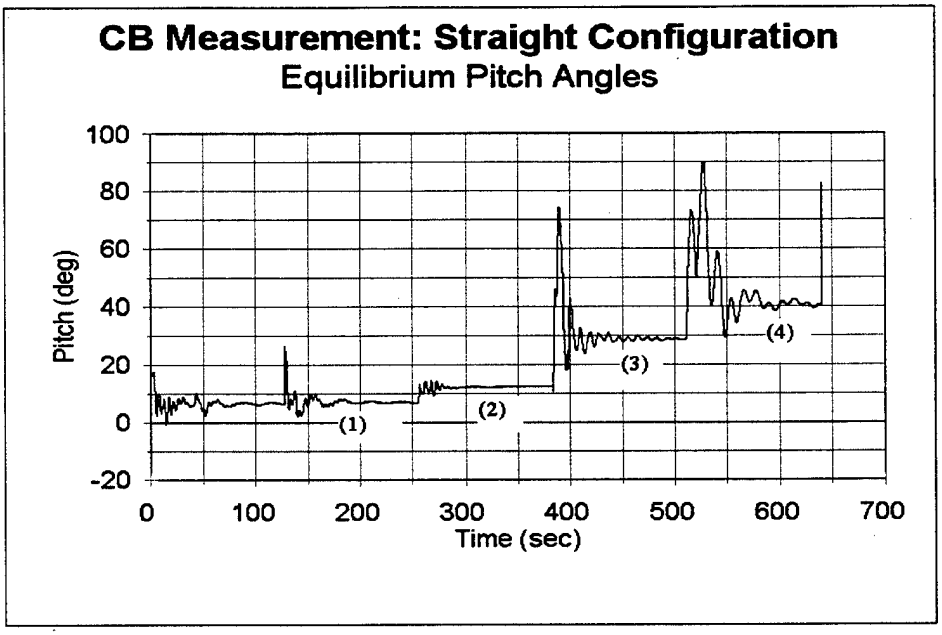

Figure B-2. Time history of pitch angles during CB measurement of straight configuration.

The four locations, relative to the CG, at which the SWIM was tied for this configuration, and the estimated equilibrium pitch angles were:

1. at head: $x_t = -2.9$ in, $z_t = -29.9$ in, $\theta = 7°$

2. at shoulder: $x_t = -5.2$ in, $z_t = -17.4$ in, $\theta = 12°$

3. at knee: $x_t = -3.3$ in, $z_t = +20.9$ in, $\theta = 29°$

4. at ankle: $x_t = -2.3$ in, $z_t = -35.0$ in, $\theta = 41°$

Using the regression fit for equation (2), the CB location was found to be:

$x_b = 0.17$ in
$z_b = -0.90$ in

This indicates that the CB is very close to the CG and slightly above and forward of the CG. The small magnitude of the values indicates that it will be sensitive to any errors in the measurement of the tie-point locations. From the values for the CB location, it would be expected that the body would try to reach an equilibrium angle (when fully submerged) of:

$\tan^{-1}(.17/-.90) = -11°$ (i.e. approximately upright and leaning back)

ii. Right-angled configuration:

The equilibrium pitch angles which were achieved are shown in figure B-3. The section of the time history data where effective equilibrium was achieved is also shown for the four locations.

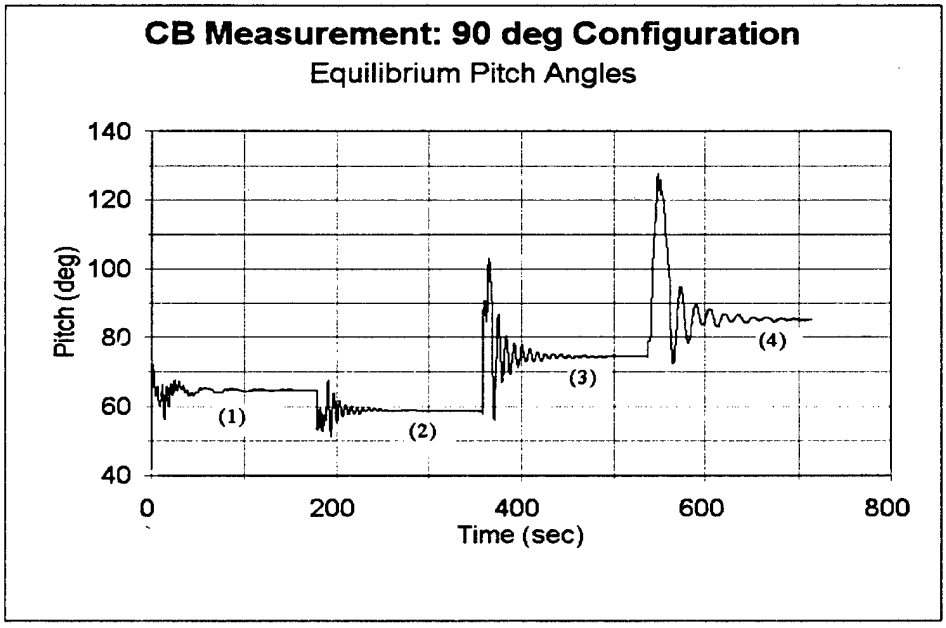

Figure B-3. Time history of pitch angles during CB measurement of right-angled configuration.

The four locations, relative to the CG, at which the SWIM was tied for this configuration were:

1. at head: $x_t = -7.9$ in, $z_t = -27.0$ in, $\theta = 65°$

2. at shoulder: $x_t = -2.2$ in, $z_t = -11.8$ in, $\theta = 59°$

3. at knee: $x_t = +12.6$ in, $z_t = +10.8$ in, $\theta = 74°$

4. at ankle: $x_t = +25.3$ in, $z_t = +7.8$ in, $\theta = 85°$

Using the regression fit for equation (2), the CB location was found to be:

$x_b = -.38$ in
$z_b = 1.54$ in

This indicates that the CB is close to the CG and slightly behind and below the CG. As for the straight configuration, any errors in measuring tie-point location would be translated to errors in the CB location. From the values for the CB location, it would be expected that the body would try to reach an equilibrium angle (when fully submerged) of:

$\tan^{-1}(-.38/1.54) = 166°$ (i.e. the body is rotated forward and the head is pointing down).

[This page intentionally left blank.]

APPENDIX C
BOTTOM RELEASE TESTING

The following provide the summary of the comparisons from the bottom release tests.

i. Three meter; normal ballast; vertical orientation

The vertical, bottom release test from three meter with normal ballast was used as the base test for identifying the principal hydrodynamic coefficients in this configuration. Experimental data for the center of gravity and center of buoyancy were gathered specifically for this configuration (and for the right-angled configuration).

The pressure transducer and pitch time-histories were checked to determine the actual depth and pitch angle from which the dummy was released. The right and left lower pressure transducers agreed well, indicating that there was little initial roll or yaw.

Several runs for this configuration were compared to examine the degree of variation expected from the tests. The plots from three tests of the output of the pressure transducers (converted to depth) are shown in figure C-1. The plots from the same three tests of the output of the pitch sensor are shown in figure C-2.

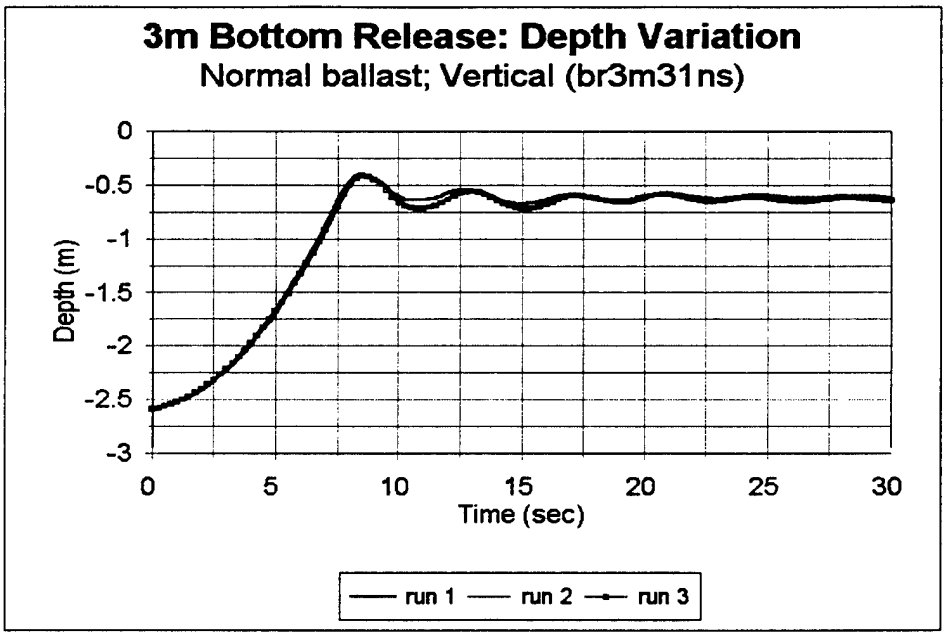

Figure C-1. Variation in-depth time history for three repeated runs (3 m bottom release with normal ballast and vertical orientation).

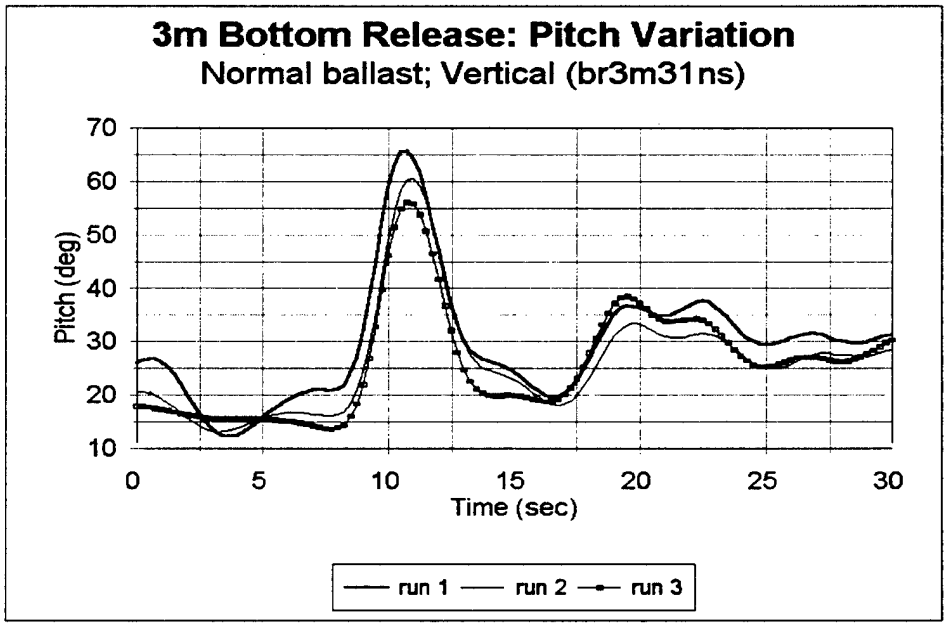

Figure C-2. Variation in pitch for three repeated runs (3 m bottom release with normal ballast and vertical orientation).

It is seen that there is good repeatability (within 2 percent) for the rise profile and for the initial heave oscillations. There is some variation in the peak magnitude of the pitch that is attained, up to about 15 percent. But the shape of the pitch time history is quite similar between runs.

Run #3 was used as the specific test run for comparison. The initial conditions from the pressure and pitch sensors from this run provided the following initial conditions:

Depth (from avg. of right and left pressure transducers):	100 inches (2.54 m)
Pitch (from pitch sensor - channel 4):	20°

The position of the lower torso CG based on the preceding depth was taken to be 104 inches. For the initial simulation the following values for the coefficients were used:

drag coefficient:	$C_D = 0.6$	(from drag test)
lift coefficient:	$C_L = 0.2$	
added mass:	$A_i = 0.5$	(for all directions, from ellipsoid simulations)
wave damping:	$a_0, a_1 = 0.0, 0.0$	

The time histories for the depths are shown in figure C-3 and for the pitch angles in figure C-4.

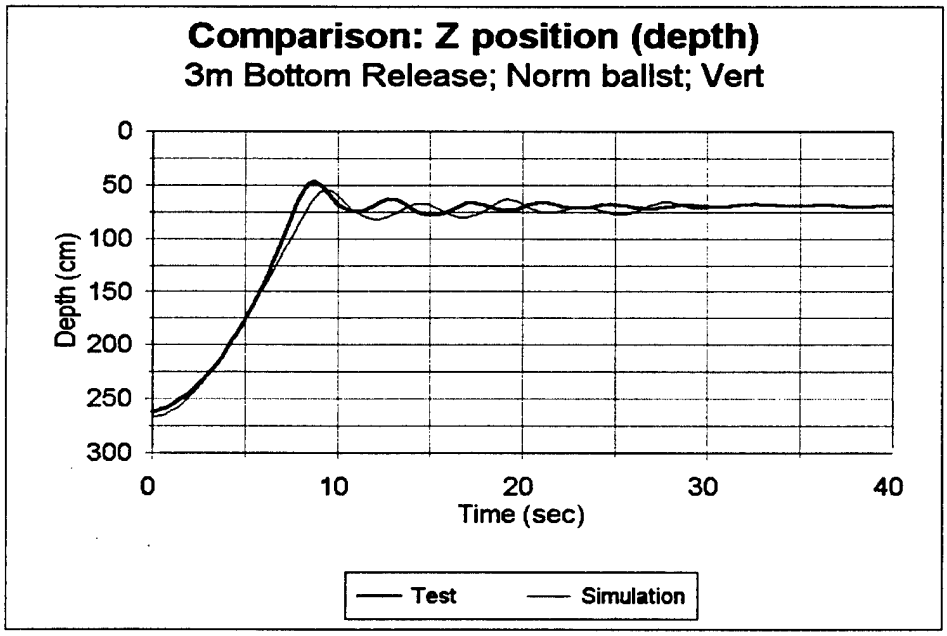

Figure C-3. Comparison of depth from test and simulation: Bottom release at 3 m with normal ballast and vertical orientation (original coeff).

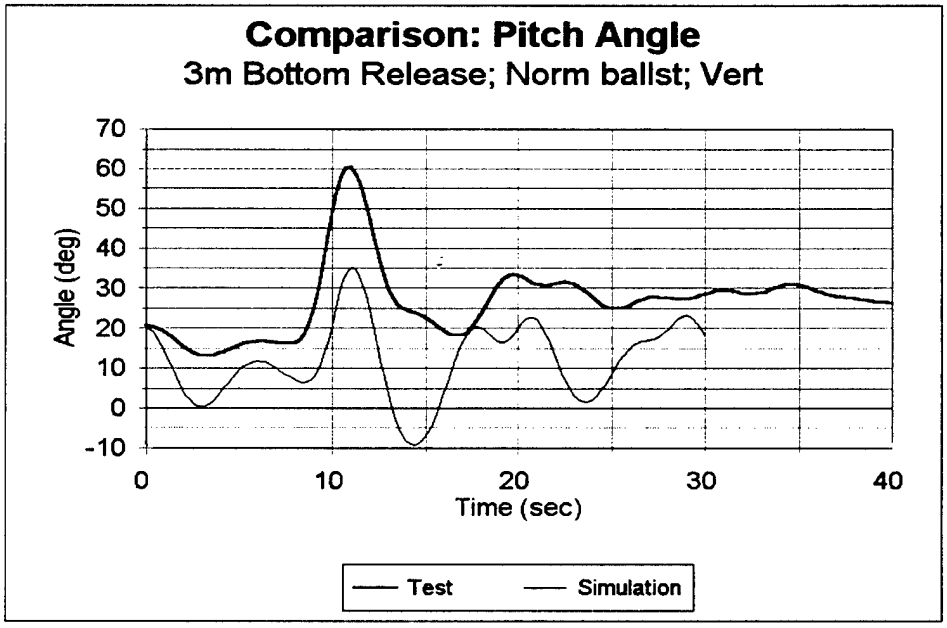

Figure C-4. Comparison of pitch angle from test and simulation: Bottom release at 3 m with normal ballast and vertical orientation (original coeff).

It is seen that there is some discrepancy in the initial rise profile, and the simulation predicts that the dummy rises somewhat slower than actually in the test. The pitch time history has about same shape as in the test, but the change in pitch as the dummy moves upwards is less in the simulation and the final equilibrium angle is also less.

To improve the agreement, the following modifications were made to the drag coefficient and added mass coefficient.

drag coefficient: $C_D = 0.5$

added mass: $A_i = 0.3$ (for all directions)

The new comparisons are shown below in figure C-5.

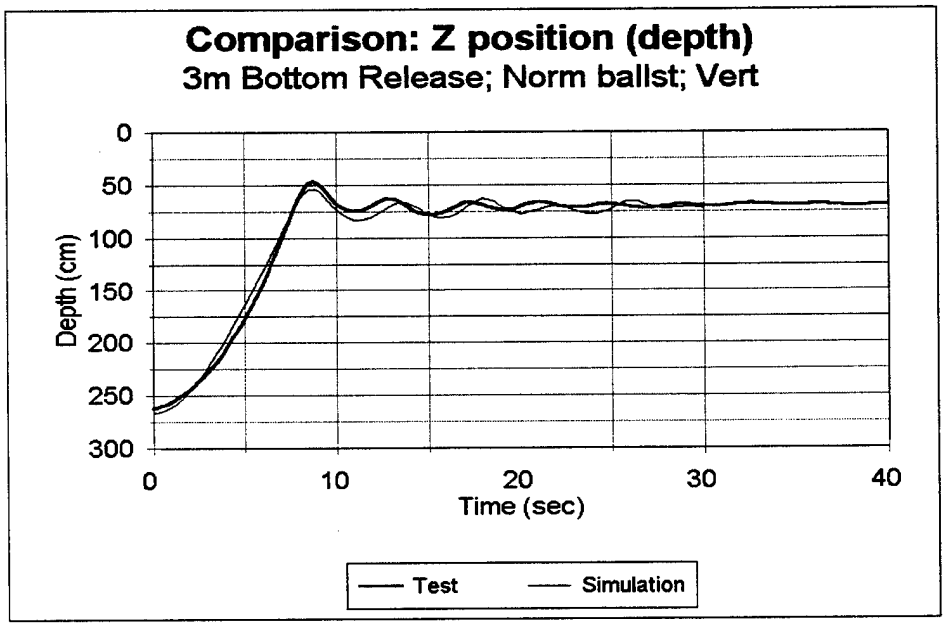

Figure C-5. Comparison of depth from test and simulation: Bottom release at 3 m with normal ballast and vertical orientation (modified coeff).

Overall, it is seen that there is now good agreement in rise time and the initial heave oscillation amplitude and frequency. The pitch angle also follows the shape seen in the test, but there is a relative discrepancy that is maintained and the basic pitch frequency figure C-6, is higher in the simulation. Over time, the difference in amplitude and frequency begin to increase. The most likely reason for the discrepancy in the pitch angle and the variation in the heave response at later times is in the exact amount of buoyancy

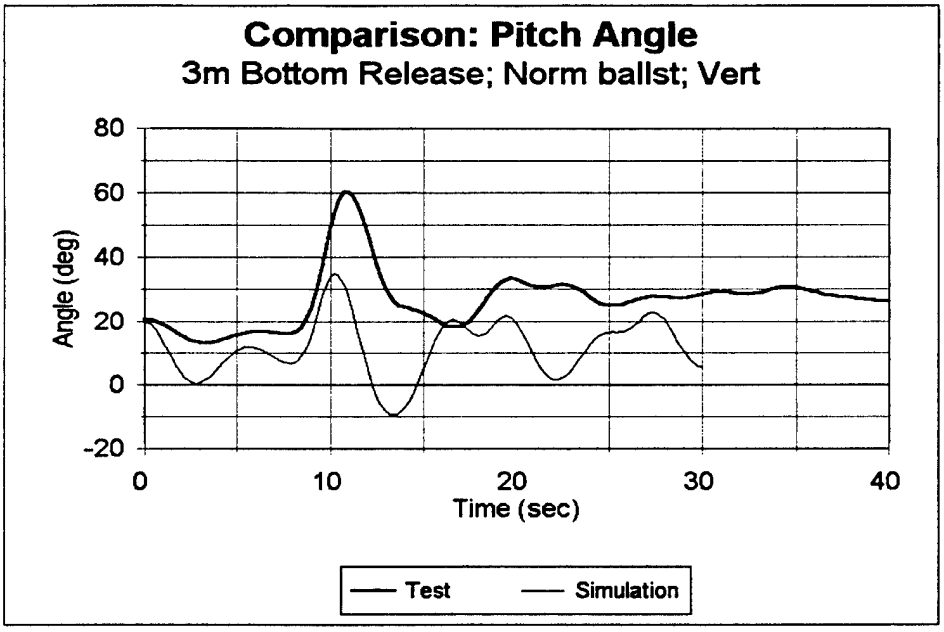

Figure C-6. Comparison of pitch angle from test and simulation: Bottom release at 3 m with normal ballast and vertical orientation (modified coeff).

and the location of the CB. Since the CB is very close to the CG, small differences in its predicted location would lead to some significant differences in the final equilibrium angle and hence the effective drag felt by the body over time.

ii. Three meter; no ballast; vertical orientation

The tests from BR3MLS2A (runs 4, 5, and 7) were used for evaluating the simulation. The pressure transducer and pitch time-histories were checked to determine the actual depth and pitch angle from which the dummy was released. The right and left lower pressure transducers agreed well, indicating that there was little initial roll or yaw.

Three runs for this configuration were compared to examine the degree of variation expected from the tests. The plots from three tests of the output of the pressure transducers (converted to depth) are shown in figure C-7. The plots from the same three tests of the output of the pitch sensor are shown in figure C-8.

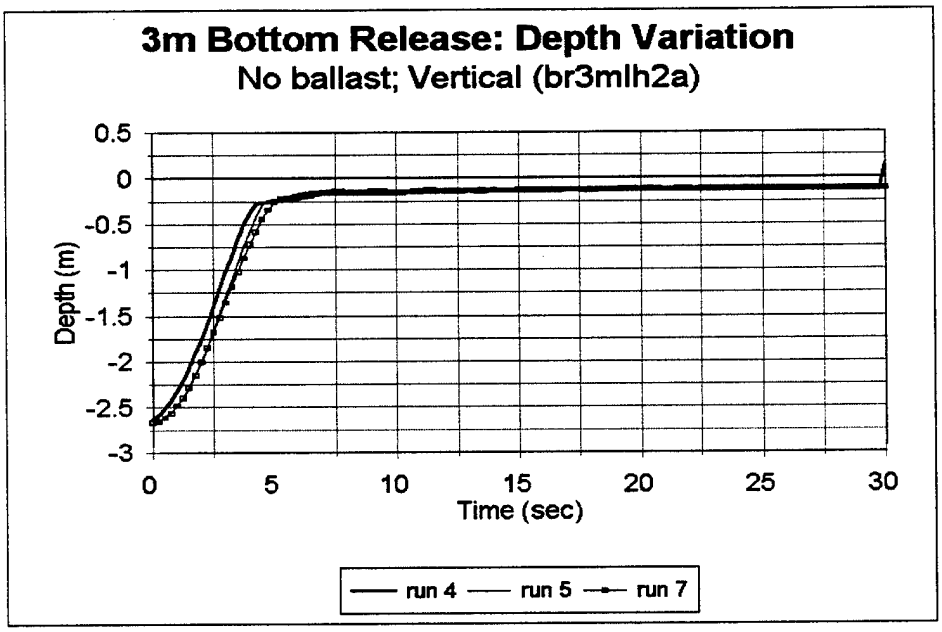

Figure C-7. Variation in-depth time history for three repeated runs (3 m bottom release with no ballast and straight orientation).

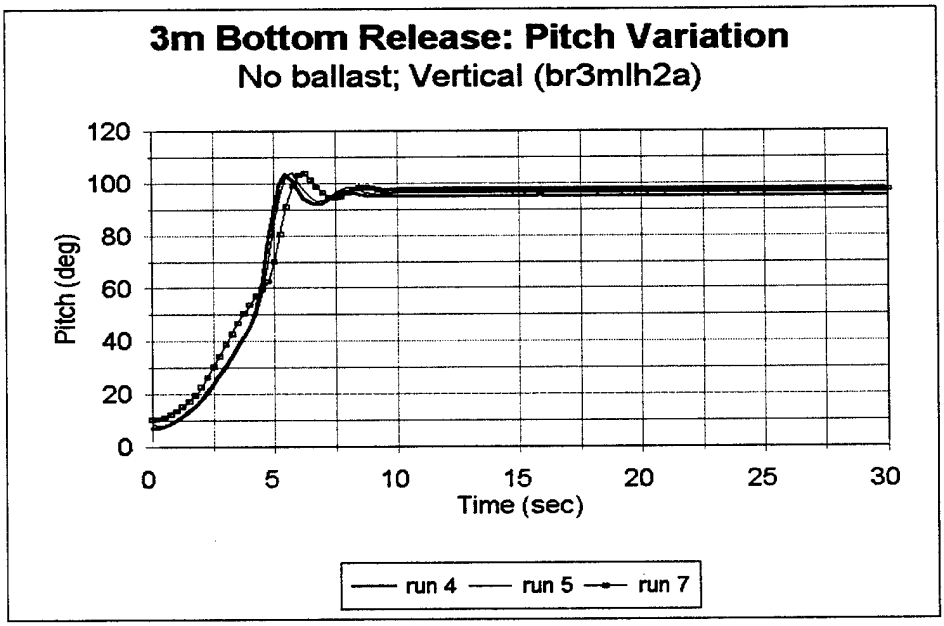

Figure C-8. Variation in pitch for three repeated runs (3 m bottom release with no ballast and vertical orientation).

It is seen that there is about a one sec. range in the rise times from the runs, but otherwise the runs agree well. There is good match in the maximum pitch achieved during the runs.

Run #5 was used as the specific test run for comparison. The initial conditions from the pressure and pitch sensors from this run provided the following initial conditions:

Depth (from avg. of right and left pressure transducers):	103 inches (2.61 m)
Pitch (from pitch sensor - channel 4):	10 deg.

The position of the lower torso CG based on the preceeding depth was taken to be 107 inches. For the initial simulation the following values for the coefficients were used:

drag coefficient:	$C_D = 0.9$	(avg. of horizontal and vertical drag coefficients)
added mass:	$A_i = 0.5$	
wave damping:	$a_0, a_1 = 0.0, 0.0$	

NOTE: The average of the drag coefficients for horizontal and vertical motions was used, since the body rotates from a vertical to a horizontal configuration at the end.

The time histories for the depths are shown in figure C-9 and for the pitch angles in figure C-10.

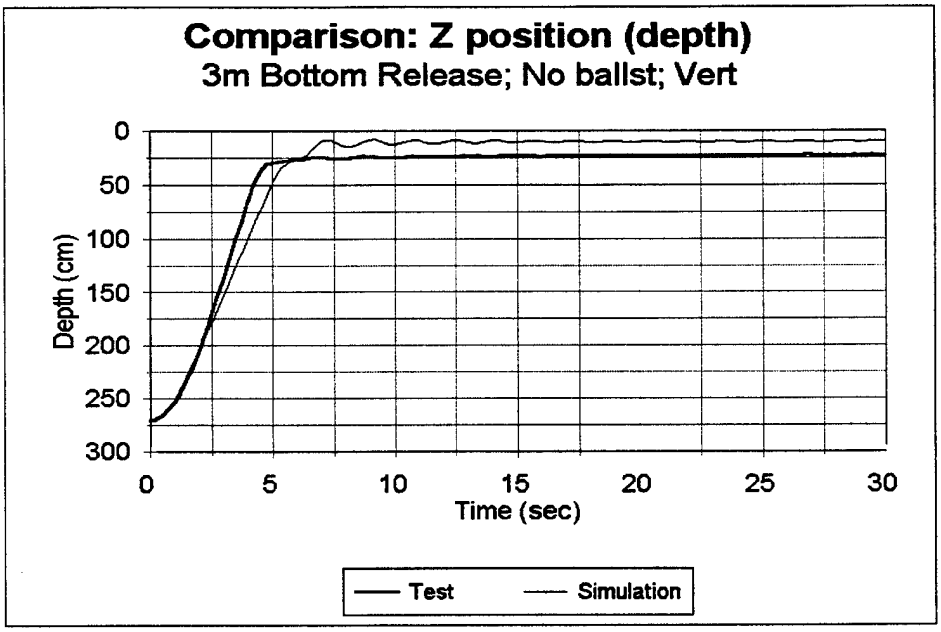

Figure C-9. Comparison of depth from test and simulation: Bottom release at 3 m with no ballast and vertical orientation (original coeff).

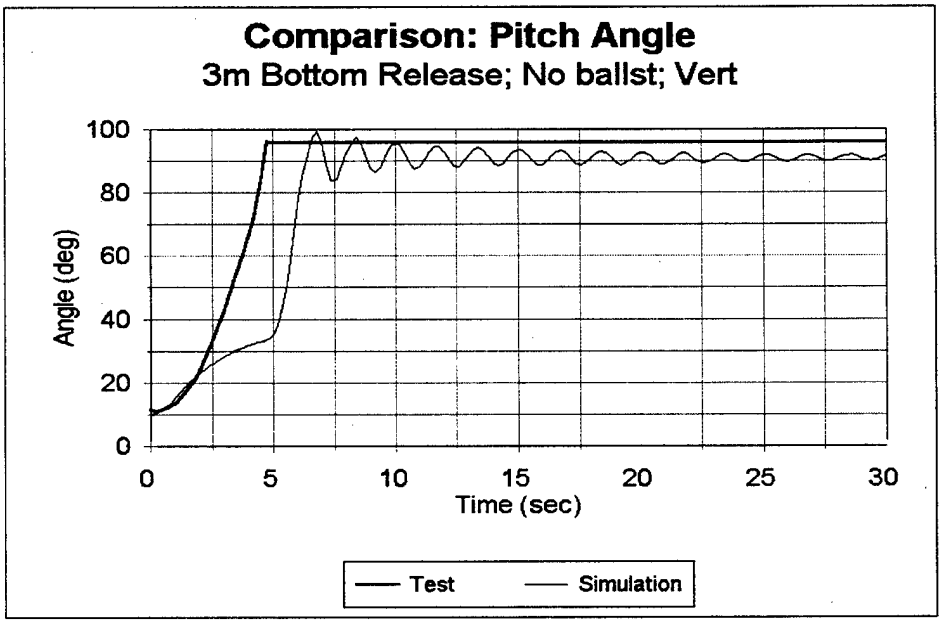

Figure C-10. Comparison of pitch angle from test and simulation: Bottom release at 3 m with no ballast and vertical orientation (original coeff).

It is seen that there is some discrepancy in the initial rise profile, and the simulation predicts the rise time to be a little longer than in the test. The pitch time history has the same shape, in this case correctly predicting that the dummy will rotate from the vertical to a horizontal configuration. But the change takes place slower in the simulation. The pitch sensor cut off at the end, so it was not possible to compare the final equilibrium angles.

To improve the agreement, the following modifications were made to the drag coefficient and added mass coefficient.

drag coefficient:	$C_D = 0.8$	
added mass:	$A_i = 0.3$	(for all directions)

The new comparisons are shown below in figure C-11 and figure C-12.

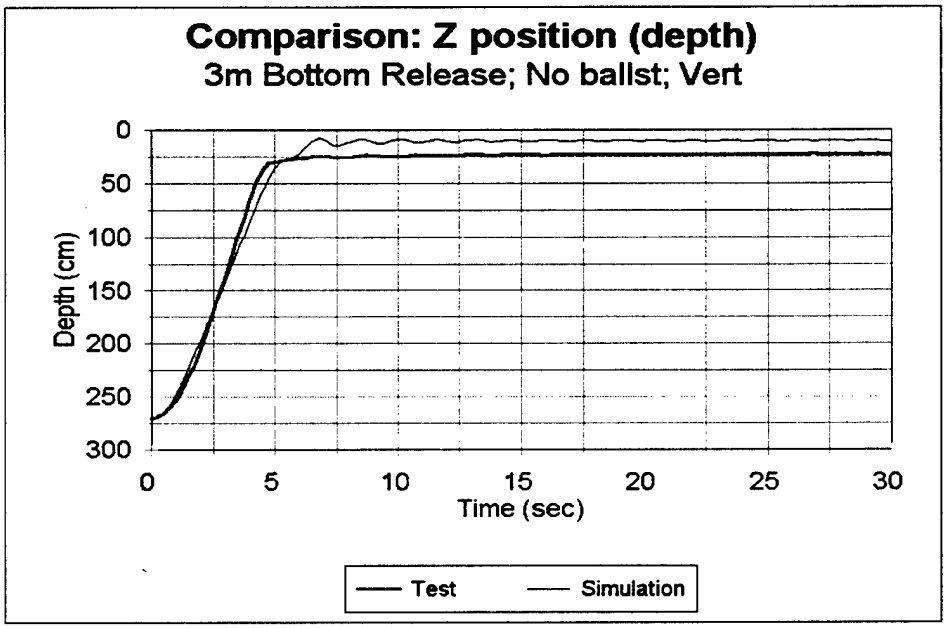

Figure C-11. Comparison of depth from test and simulation: Bottom release at 3 m with no ballast and vertical orientation (modified coeff).

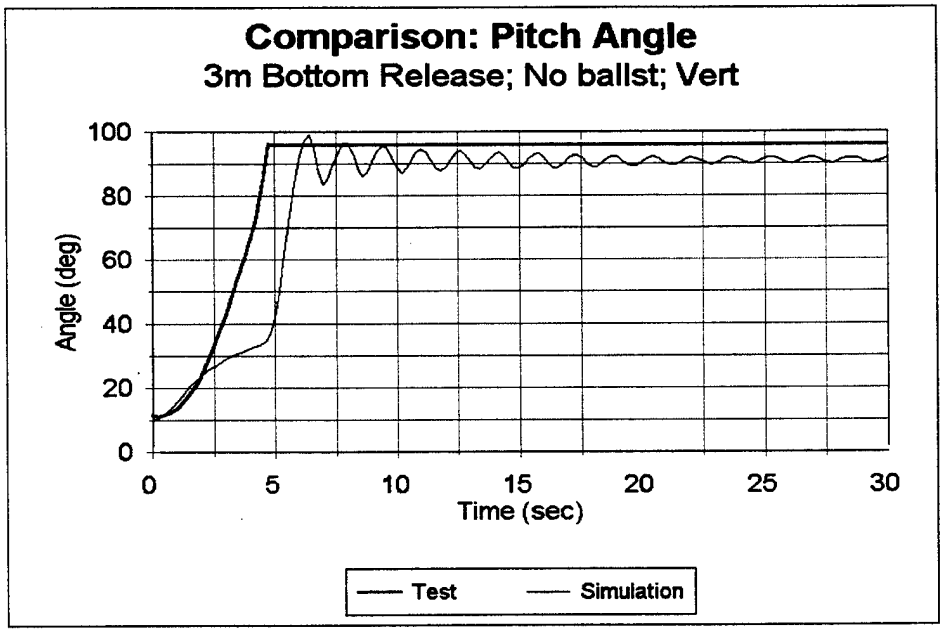

Figure C-12. Comparison of pitch angle from test and simulation: Bottom release at 3 m with no ballast and vertical orientation (modified coeff).

Overall, it is seen that there is better agreement in rise time. The pitch angle also changes a little faster than before though still trailing the test motion. There are oscillations in the pitch in the simulation, which cannot be compared since the pitch sensor locked at about 95 deg.

iii. Three meter; normal ballast; horizontal orientation

The tests from BR3NH32 (runs 2, 3, and 4) were used for evaluating the simulation. The pressure transducer and pitch time-histories were checked to determine the actual depth and pitch angle from which the dummy was released.

Three runs for this configuration were compared to examine the degree of variation expected from the tests. The plots from three tests of the output of the pressure transducers (converted to depth) are shown in figure C-13. The plots from the same three tests of the output of the pitch sensor are shown in figure C-14.

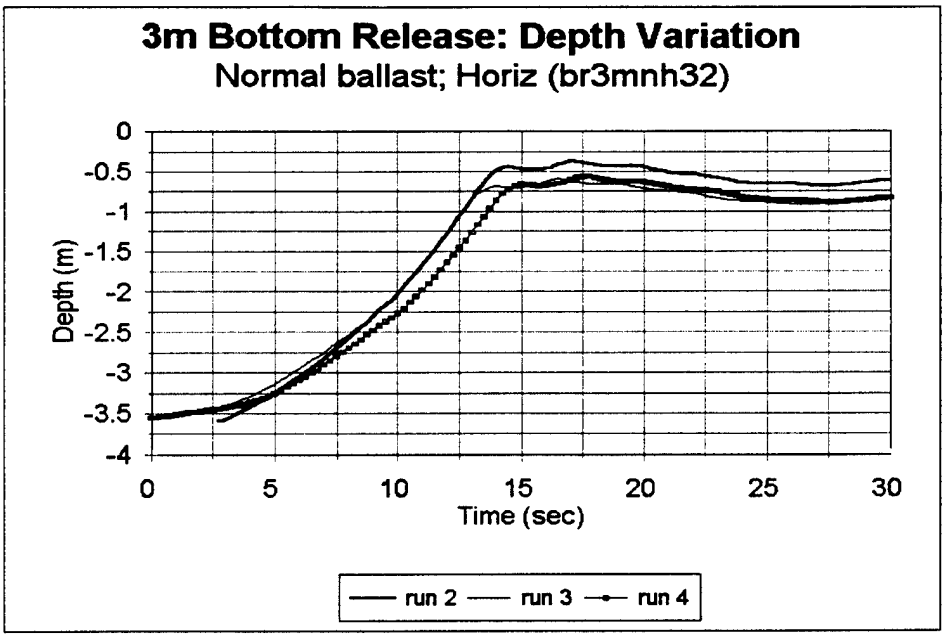

Figure C-13. Variation in-depth time history for three repeat runs (3 m bottom release with normal ballast and horizontal orientation).

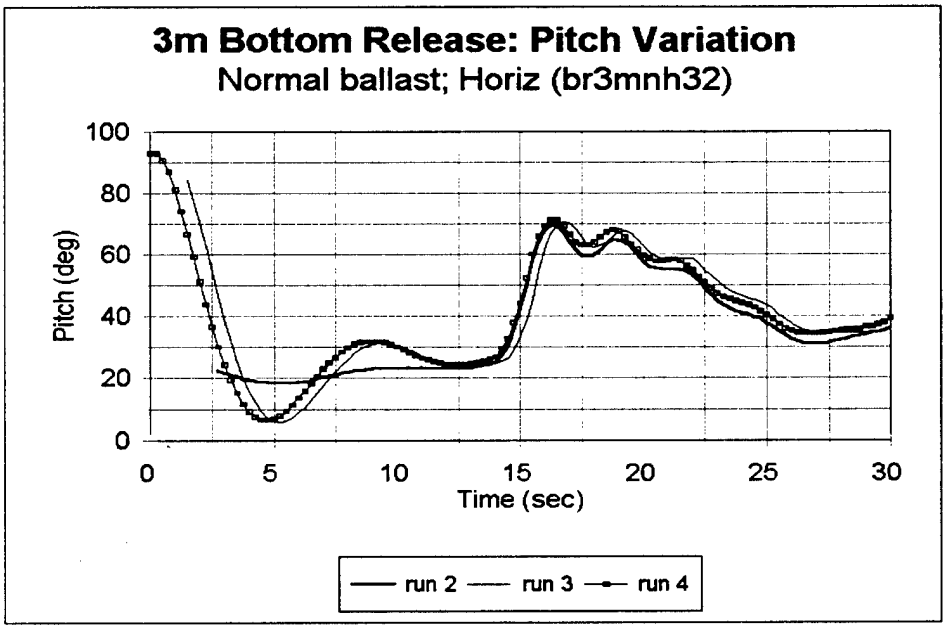

Figure C-14. Variation in pitch for three repeat runs (3 m bottom release with normal ballast and horizontal orientation).

It is seen that there is some discrepancy in the maximum height the dummy achieves (as measured by the lower pressure transducer). Two runs match each other well, but the third differs by about 25 cm (or around 10 percent). There is also about one sec. difference in the rise times between the runs. The pitch time histories match well, with about a 5 percent discrepancy.

Run #3 was used as the specific test run for comparison. The initial conditions from the pressure and pitch sensors from this run provided the following initial conditions:

Depth (from avg. of right and left pressure transducers):	128 inches (3.25 m)
Pitch (from pitch sensor - channel 15):	85 deg.

The position of the lower torso CG based on the preceeding depth was taken to be 131 inches. For the initial simulation the following values for the coefficients were used:

drag coefficient:	$C_D = 1.2$	(from test)
added mass:	$A_i = 0.5$	
wave damping:	$a_0, a_1 = 0.0, 0.0$	

The time histories for the depths are shown in figure C-15 and for the pitch angles in figure C-16.

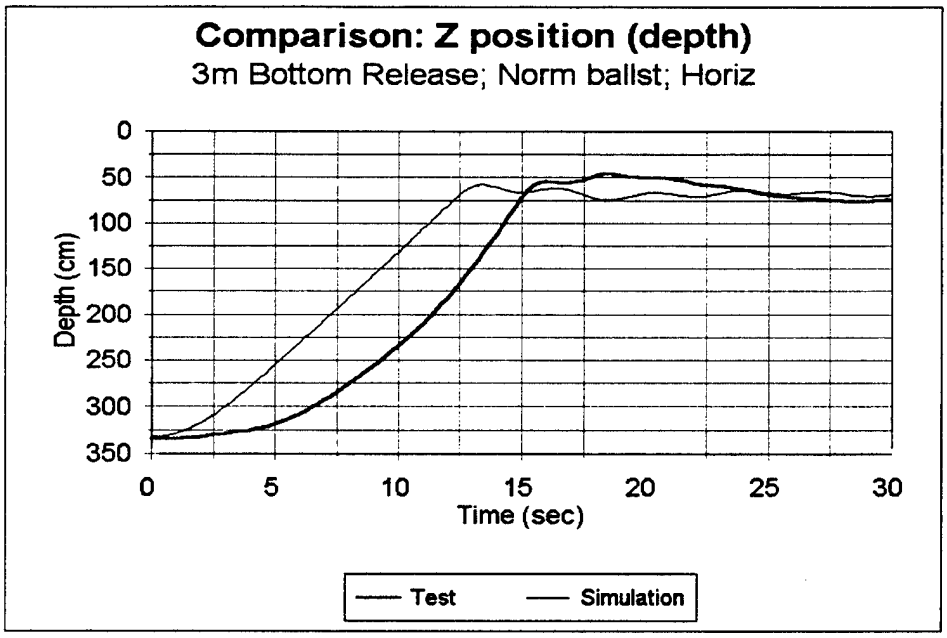

Figure C-15. Comparison of depth from test and simulation: Bottom release at 3 m with normal ballast and horizontal orientation (original coeff).

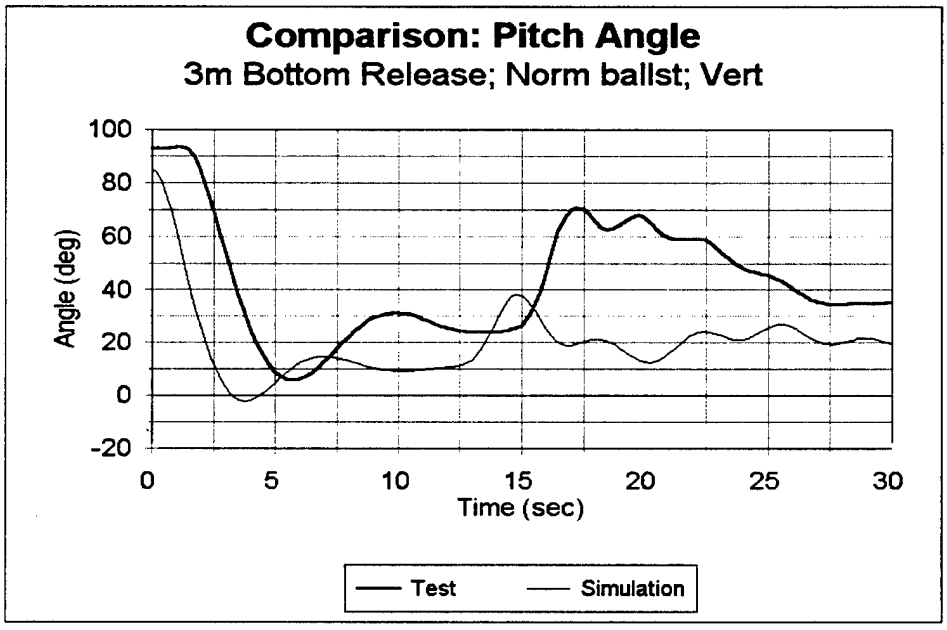

Figure C-16. Comparison of pitch angle from test and simulation: Bottom release at 3 m with normal ballast and horizontal orientation (original coeff).

It is seen that there is discrepancy in the initial rise profile of about two sec., with the simulation reaching maximum height earlier than in the test. The pitch time history has the same shape, and correctly predicts that the dummy will rotate from the horizontal to the vertical configuration. But the change takes place faster in the simulation. The auxiliary pitch sensor on channel 15 was used for this test.

To improve the agreement, the following modifications were made to the drag coefficient and added mass coefficient.

drag coefficient:	$C_D = 1.5$	
added mass:	$A_i = 1.0$	(for all directions)

The new comparisons are shown below in figure C-17 and figure C-18.

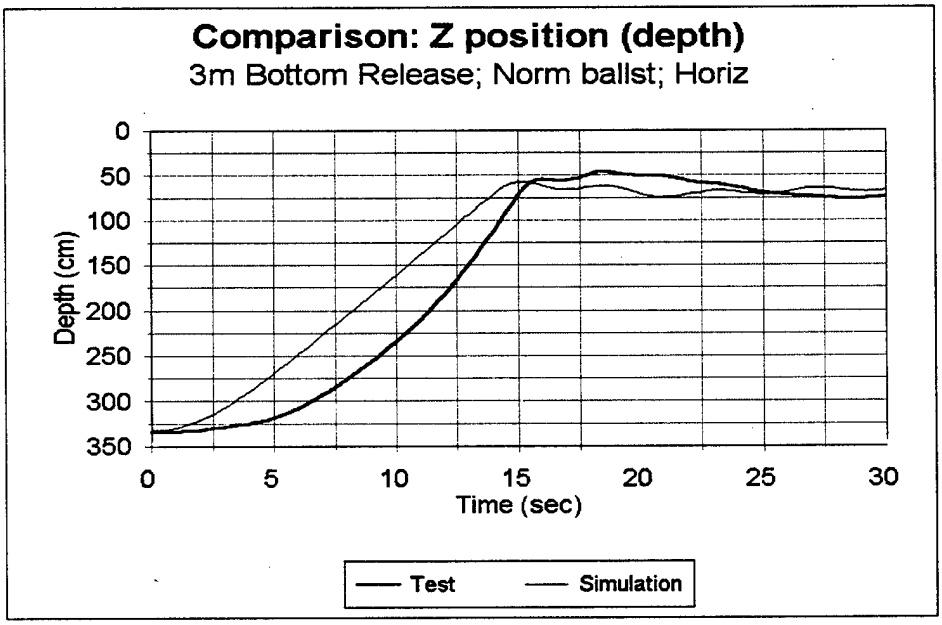

Figure C-17. Comparison of depth from test and simulation: Bottom release at 3 m with normal ballast and horizontal orientation (modified coeff).

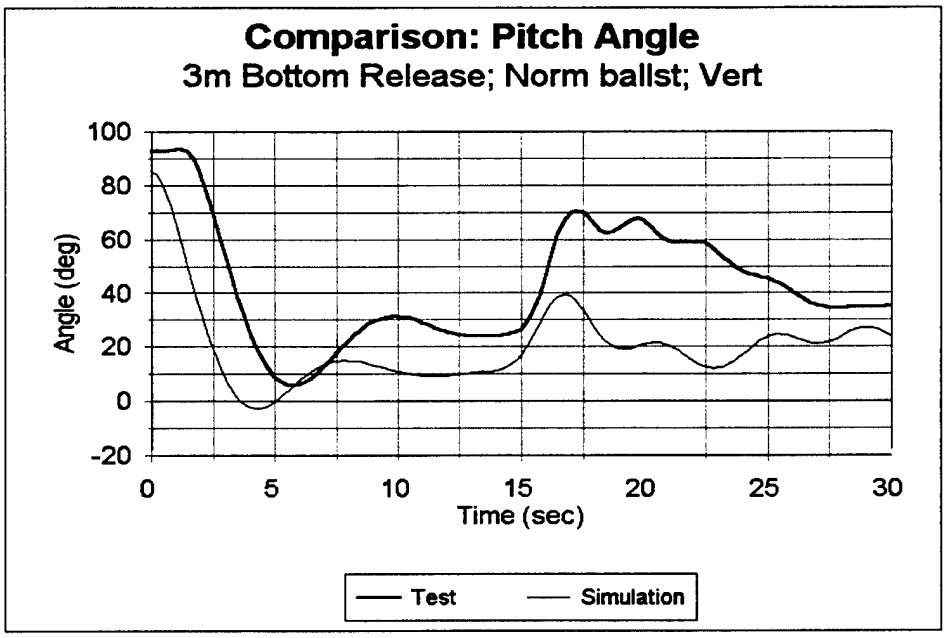

Figure C-18. Comparison of pitch angle from test and simulation: Bottom release at 3 m with normal ballast and horizontal orientation (modified coeff).

It is seen that there is better agreement in rise time, though there still a discrepancy in the rise shape. There was no significant change in the pitch response

iv. Three meter; no ballast; horizontal orientation

The tests from BR3LH2A (runs 1, 2, and 3) were used for evaluating the simulation. The pressure transducer and pitch time-histories were checked to determine the actual depth and pitch angle from which the dummy was released. The variations appeared to be similar to that seen for the previous tests.

Run #2 was used as the specific test run for comparison. The initial conditions from the pressure and pitch sensors from this run provided the following initial conditions:

Depth (from avg. of right and left pressure transducers):	126 inches (3.20 m)
Pitch (from pitch sensor - channel 15):	105 deg.

The position of the lower torso CG based on the preceeding depth was taken to be 131 inches. For the

initial simulation the following values for the coefficients were used:

drag coefficient:	$C_D = 1.2$	(from test)
added mass:	$A_i = 0.5$	
wave damping:	$a_0, a_1 = 0.0, 0.0$	

The time histories for the depths are shown in figure C-19 and for the pitch angles in figure C-20.

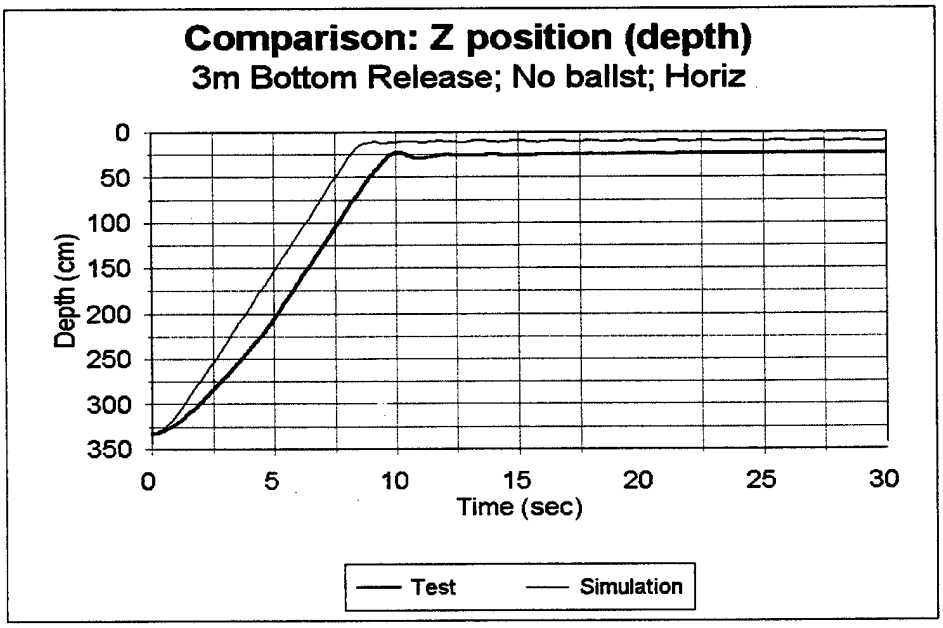

Figure C-19. Comparison of depth from test and simulation: Bottom release at 3 m with no ballast and horizontal orientation (original coeff).

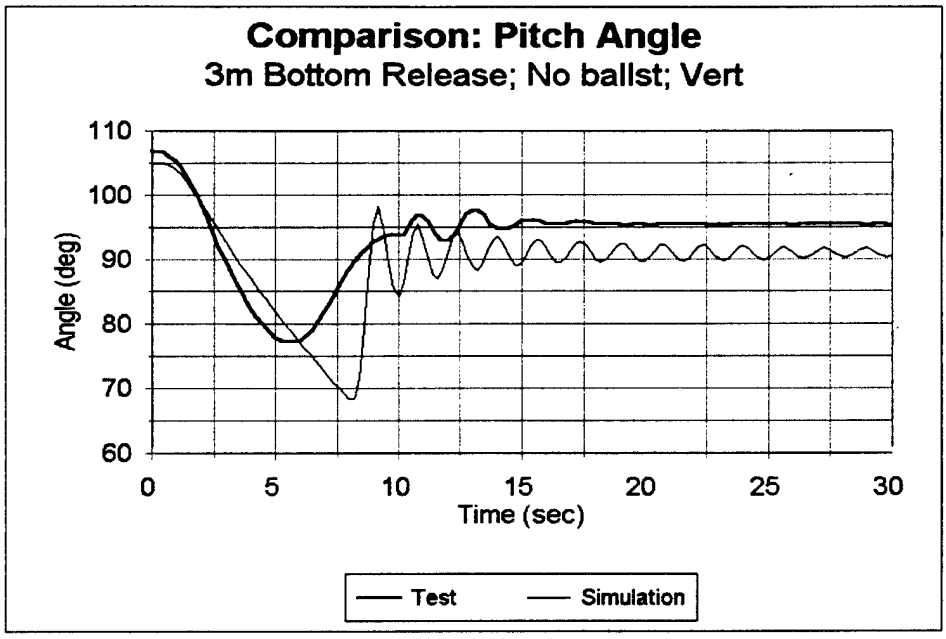

Figure C-20. Comparison of pitch angle from test and simulation: Bottom release at 3 m with no ballast and horizontal orientation (original coeff).

It is seen that there is discrepancy in the initial rise profile, of about two sec., with the simulation reaching maximum height earlier than in the test. The pitch time history shape follows the test, but the simulation predicts a larger maximum angle change (35 deg. for simulation; 27 deg. for test). The pitch oscillations are more pronounced than in the test.

To improve the agreement, the modifications made to the drag coefficient and added mass coefficient for the normal ballast case were used:

drag coefficient:	$C_D = 1.5$	
added mass:	$A_i = 1.0$	(for all directions)

The new comparisons are shown in figure C-21 and figure C-22.

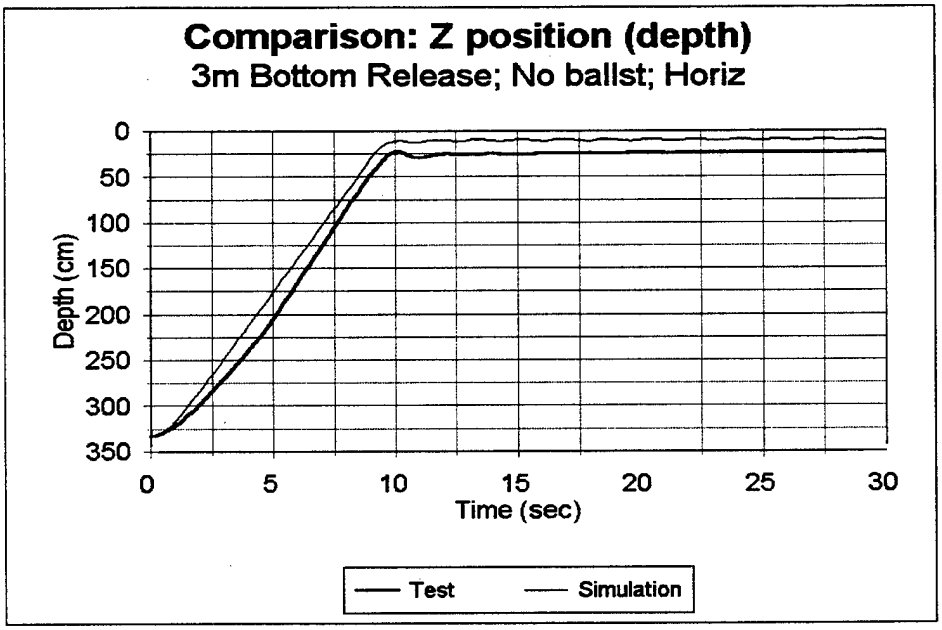

Figure C-21. Comparison of depth from test and simulation: Bottom release at 3 m with no ballast and horizontal orientation (modified coeff).

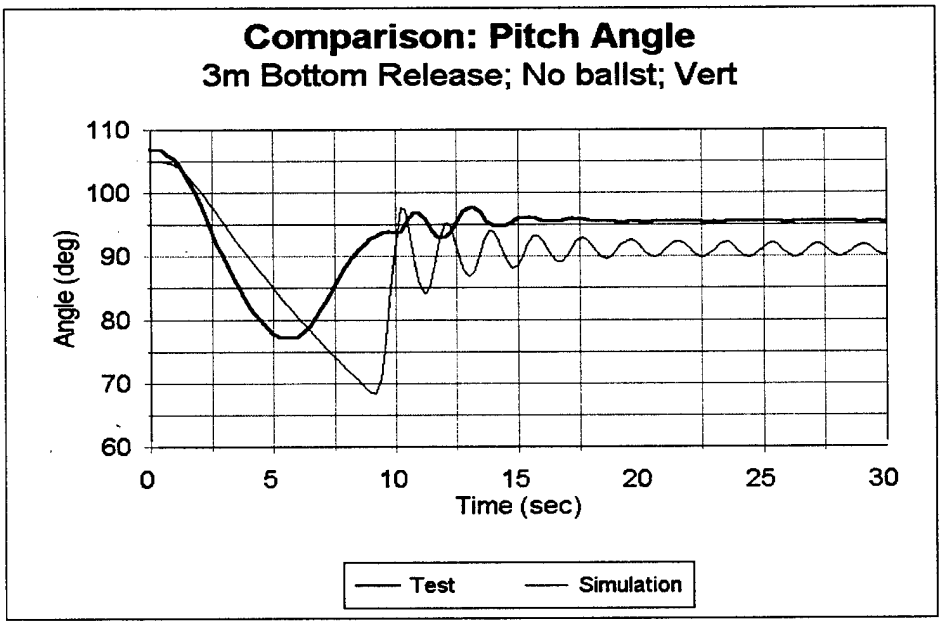

Figure C-22. Comparison of pitch angle from test and simulation: Bottom release at 3 m with no ballast and horizontal orientation (modified coeff).

It is seen that there is now a better agreement in rise profile, though the simulation predicts that the dummy will rise a little higher than in the test. There was no significant change in the pitch response.

v. Three meter; normal ballast; right-angled orientation

The tests from BR3MNR32 (runs 2, 3, and 5) were used for evaluating the simulation. The pressure transducer and pitch time-histories were checked to determine the actual depth and pitch angle from which the dummy was released. The variations appeared to be similar to that seen for the previous tests.

Run #3 was used as the specific test run for comparison. The initial conditions from the pressure and pitch sensors from this run provided the following initial conditions:

Depth (from avg. of right and left pressure transducers):	125 inches (3.17 m)
Pitch (from pitch sensor - channel 15):	10 deg.

The position of the lower torso CG based on the preceeding depth was taken to be 131 inches. For the initial simulation the following values for the coefficients were used:

drag coefficient:	$C_D = 0.85$	(from test)
added mass:	$A_i = 0.5$	
wave damping:	$a_0, a_1 = 0.0, 0.0$	

The time histories for the depths are shown in figure C-23 and for the pitch angles in figure C-24.

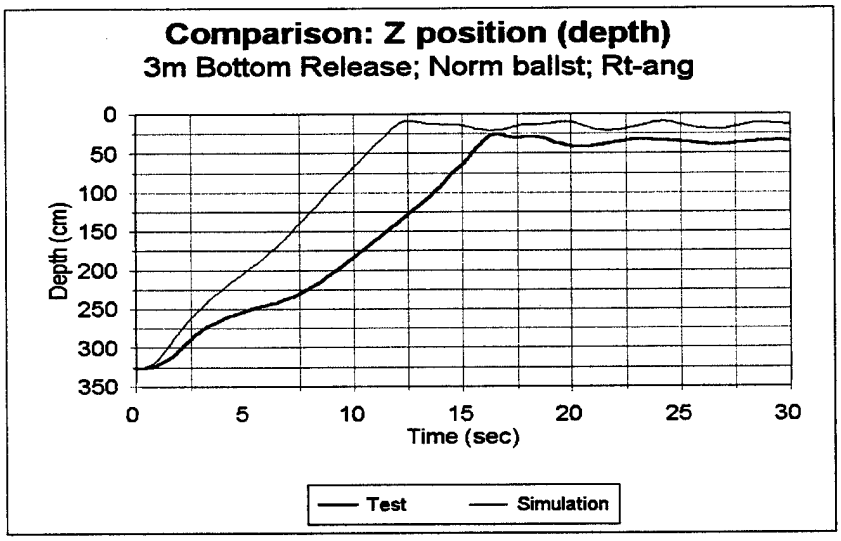

Figure C-23. Comparison of depth from test and simulation: Bottom release at 3 m with normal ballast and right-angled orientation (original coeff).

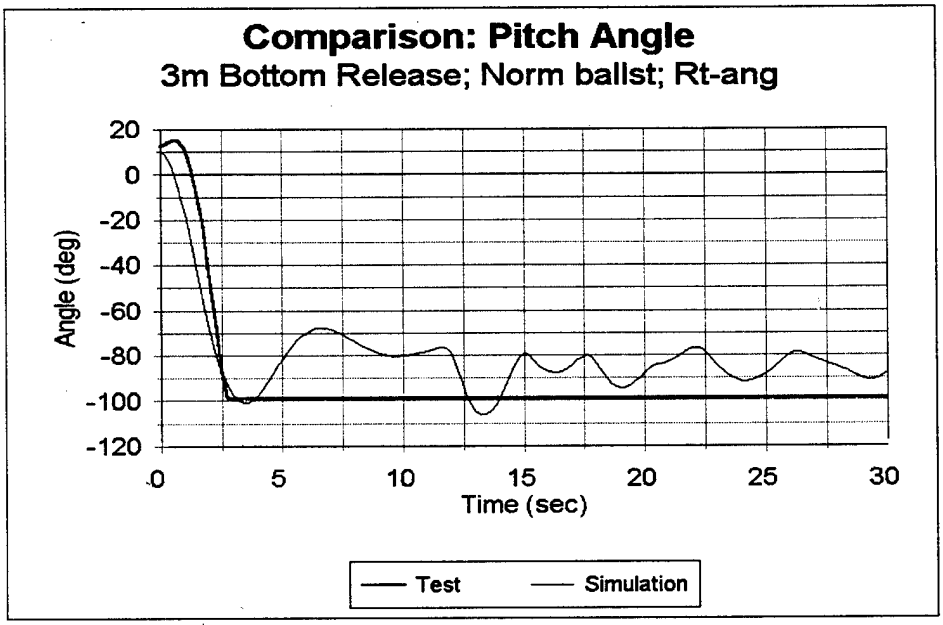

Figure C-24. Comparison of pitch angle from test and simulation: Bottom release at 3 m with normal ballast and right-angled orientation (original coeff).

It is seen that there is significant discrepancy in the rise time of about five sec., with the simulation reaching maximum height earlier than in the test. The low amplitude heave oscillations are reproduced, though the simulation shows higher frequency. The pitch time history shape follows the test up to the point when the pitch sensor locks up (the auxiliary pitch sensor data were not available for this test), so it is not possible to compare this response beyond the maximum pitch.

To improve the agreement, the modifications made to the drag coefficient and added mass coefficient for the normal ballast case were used:

drag coefficient:	$C_D = 1.5$	
added mass:	$A_i = 1.0$	(for all directions)

These are the same values used for the horizontal tests. The new comparisons are shown below in figure C-25 and figure C-26.

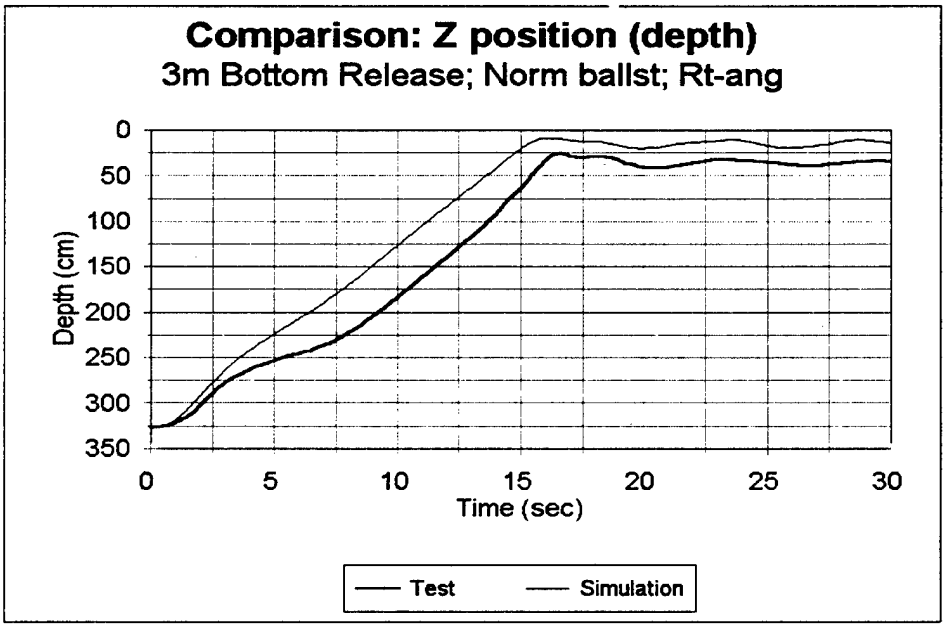

Figure C-25. Comparison of depth from test and simulation: Bottom release at 3 m with normal ballast and right-angled orientation (modified coeff).

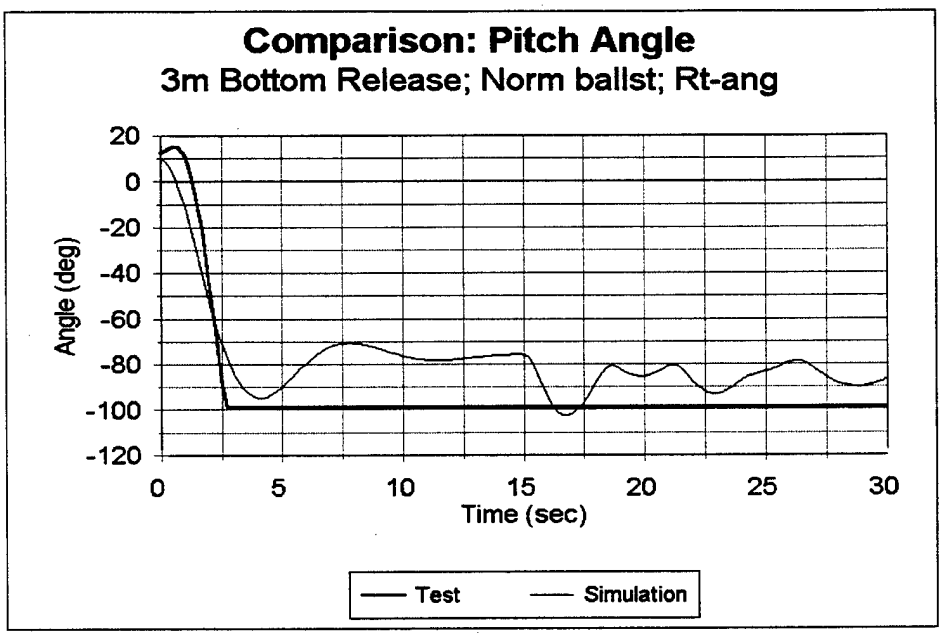

Figure C-26. Comparison of pitch angle from test and simulation: Bottom release at 3 m with normal ballast and right-angled orientation (modified coeff).

There is now a better agreement in rise profile, with good agreement in the rise time, though the simulation predicts that the dummy will rise a little higher than in the test. There was no significant change in the pitch response.

vi. Three meter; no ballast; right-angled orientation

The tests from BR3MLR32 (run 1) and BR3MLR2A (run 2) were used for evaluating the simulation. The pressure transducer and pitch time-histories were checked to determine the actual depth and pitch angle from which the dummy was released.

Two runs for this configuration were compared to examine the degree of variation expected from the tests. The plots from two tests of the output of the pressure transducers (converted to depth) are shown in figure C-27. The plots from the same two tests of the output of the pitch sensor are shown in figure C-28.

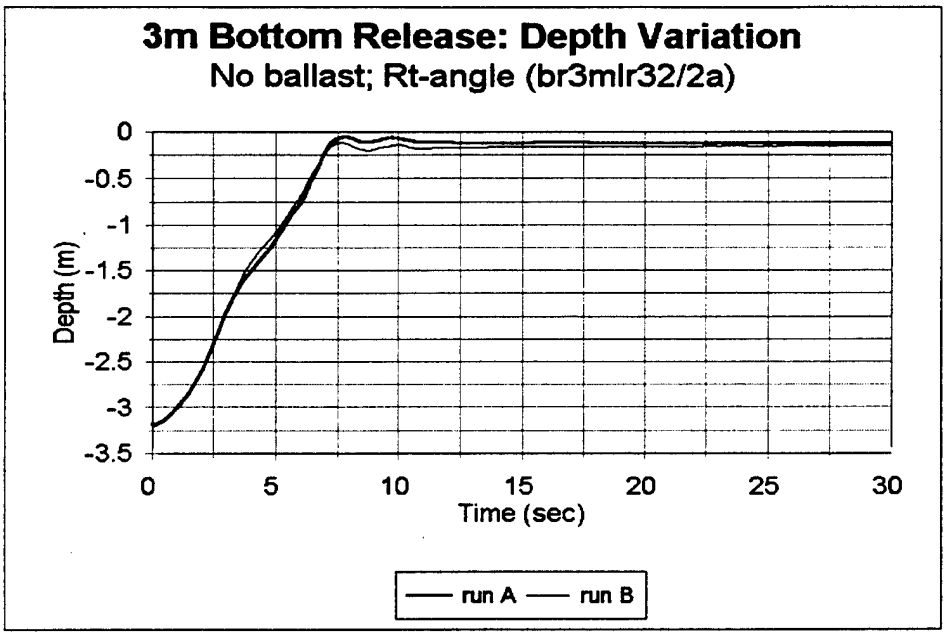

Figure C-27. Variation in depth time history for two repeat runs (3 m bottom release with no ballast and right-angled orientation).

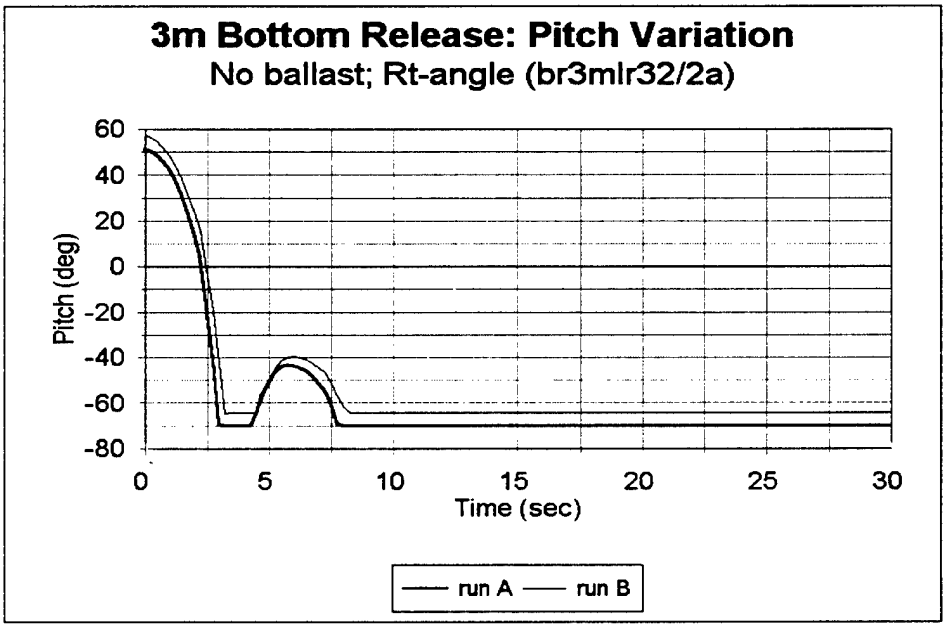

Figure C-28. Variation in pitch for two repeat runs (3 m bottom release with no ballast and right-angled orientation).

It is seen that there is good repeatability in the rise profiles, with maximum differences around 10 cm. The pitch cannot be compared well, since the sensor cut off around 60 deg. (and the auxiliary pitch sensor data were not available), but does show a difference of about 5 deg. in the range where the sensor was working.

Run #1 from Test BR3MLR32 was used as the specific test run for comparison. The initial conditions from the pressure and pitch sensors from this run provided the following initial conditions:

Depth (from avg. of right and left pressure transducers):	124 inches (3.15 m)
Pitch (from pitch sensor - channel 4):	50 deg.

The position of the lower torso CG based on the preceeding depth was taken to be 128 inches. For the initial simulation the following values for the coefficients were used:

drag coefficient:	$C_D = 0.85$	(from test)
added mass:	$A_i = 0.5$	
wave damping:	$a_0, a_1 = 0.0, 0.0$	

The time histories for the depths are shown in figure C-29 and for the pitch angles in figure C-30.

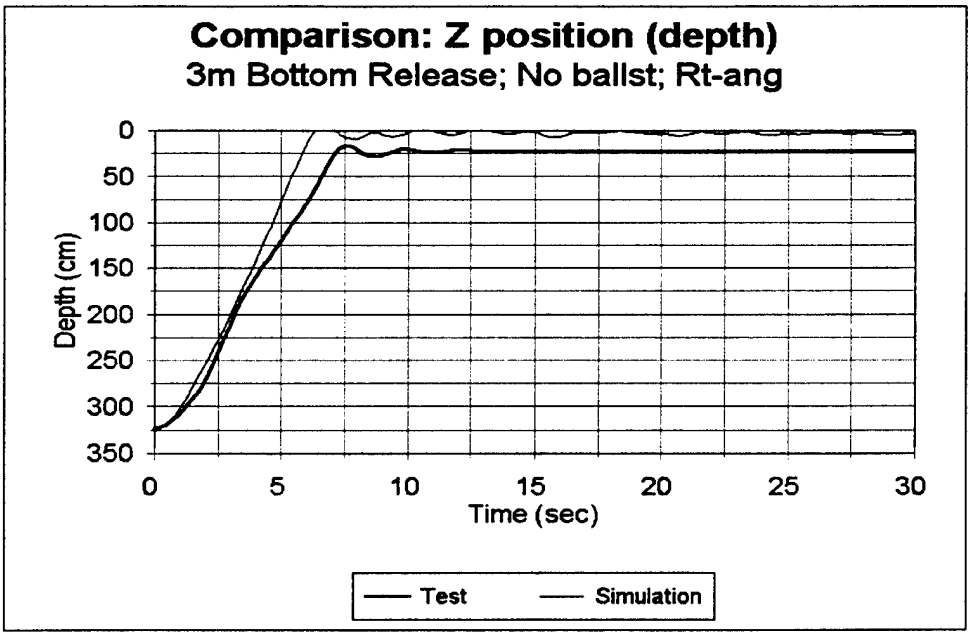

Figure C-29. Comparison of depth from test and simulation: Bottom release at 3 m with no ballast and right-angled orientation (original coeff).

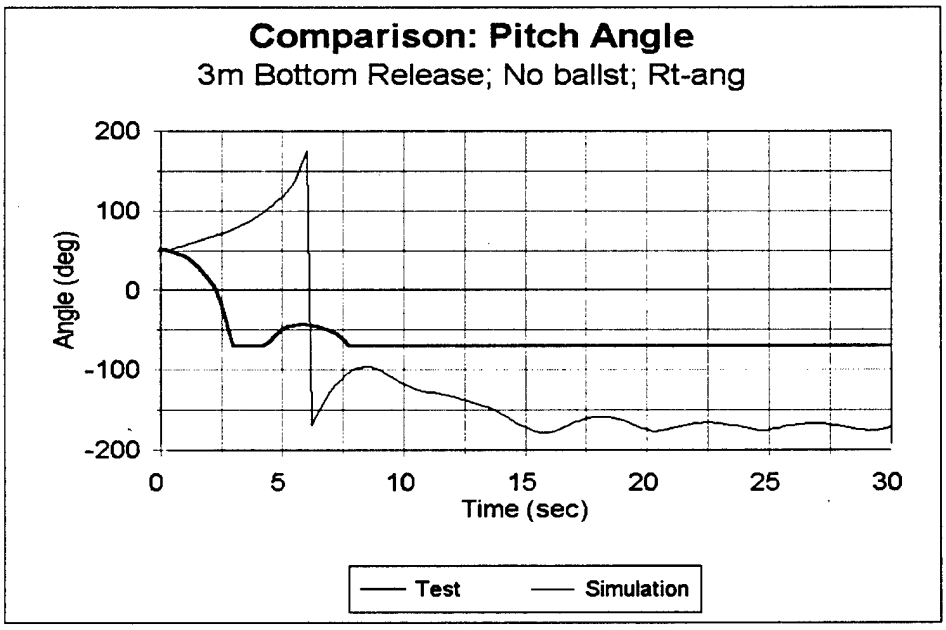

Figure C-30. Comparison of pitch angle from test and simulation: Bottom release at 3 m with no ballast and right-angled orientation (original coeff).

It is seen that there is discrepancy in the initial rise profile of about one sec., with the simulation reaching maximum height earlier than in the test. The simulation indicates the dummy to be a slightly higher level than in the test. The pitch time history shows a significant difference between simulation and test. Prior to the cut-off in the test data, the rotation appears to be in opposite direction. It is not clear what is the reason for this abnormal simulation. Only the final equilibrium angle appears to be similar, though one will have to rely on the video information to confirm. One possibility for the large discrepancy is that a reliable CG and CB for the no ballast case is not available, and the estimate made by the program, based on the available data is in error.

To improve the agreement, the following modifications were made to the drag coefficient and added mass coefficient.

drag coefficient:	$C_D = 1.5$	
added mass:	$A_i = 1.0$	(for all directions)

These values are the same for the other horizontal and right-angled cases. The new comparisons are shown below in figure C-31 and figure C-32.

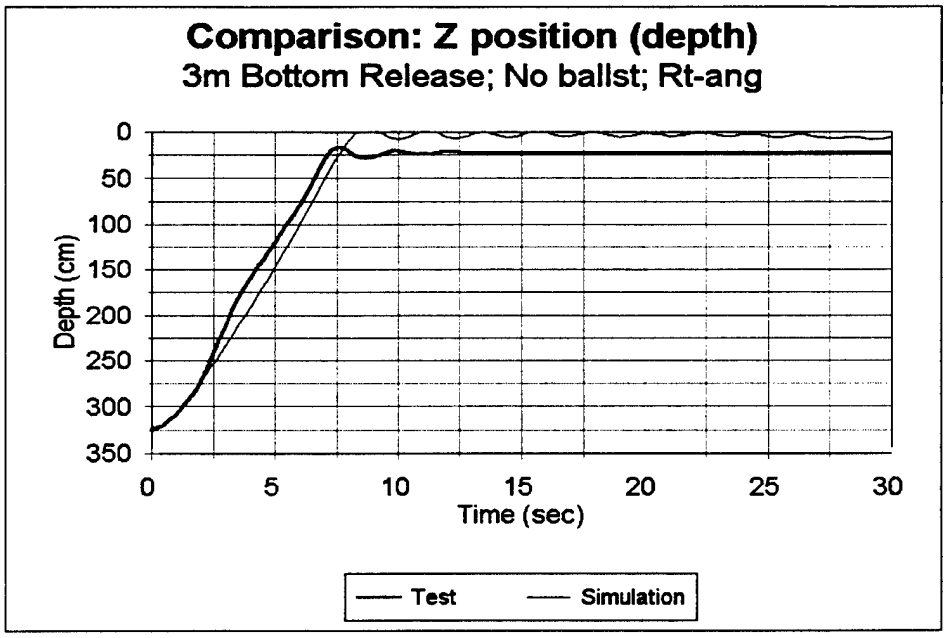

Figure C-31. Comparison of depth from test and simulation: Bottom release at 3 m with no ballast and right-angled orientation (modified coeff).

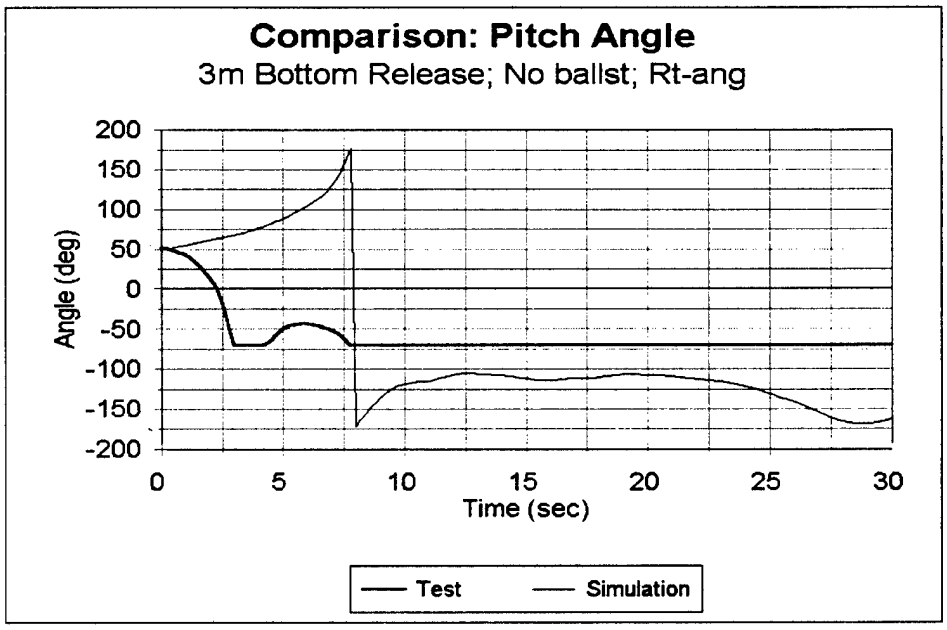

Figure C-32. Comparison of pitch angle from test and simulation: Bottom release at 3 m with no ballast and right-angled orientation (modified coeff).

It is seen that there is better agreement in rise time, and this time the simulation shows that the dummy reaches maximum height slightly later than the test. There was no significant change in the pitch response and the anomalous response seen with the previous coefficients is still seen.

vii. Four meter; no ballast; vertical orientation

The tests from BR4M31LS (runs 2, 3, and 4) were used for evaluating the simulation. The pressure transducer and pitch time-histories were checked to determine the actual depth and pitch angle from which the dummy was released. The variations appeared to be similar to that seen for the previous tests.

Run #3 was used as the specific test run for comparison. The initial conditions from the pressure and pitch sensors from this run provided the following initial conditions:

Depth (from avg. of right and left pressure transducers):	131 inches (3.32 m)
Pitch (from pitch sensor - channel 4):	25 deg.

The position of the lower torso CG based on the preceeding depth was taken to be 135 inches. For this tests, the modified coefficients used for the corresponding 3 m bottom release were used without any further modification. The objective was to determine how well the model predicted for a different release depth. The coefficients used were:

drag coefficient:	$C_D = 0.8$	
added mass:	$A_i = 0.3$	(for all directions)

The results are shown below in figure C-33 and figure C-34:

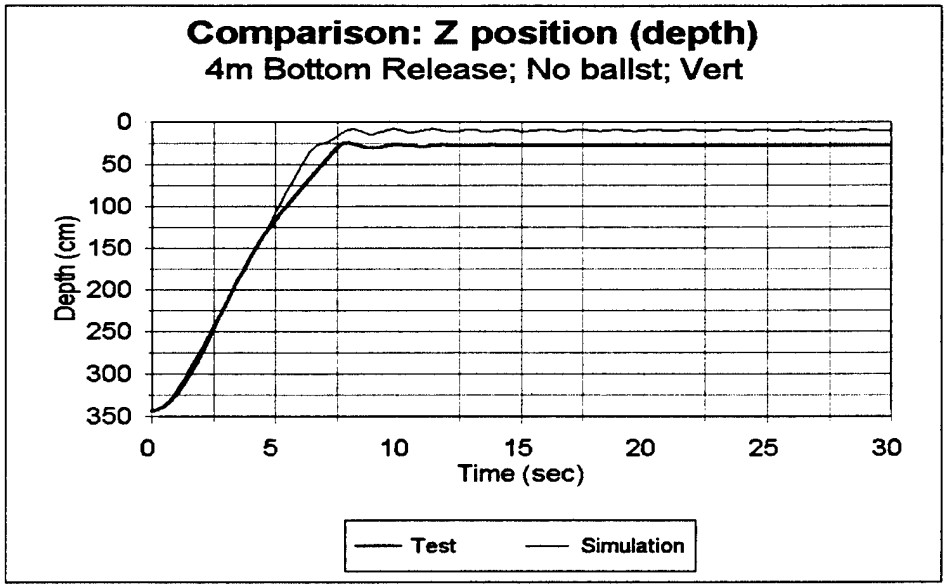

Figure C-33. Comparison of depth from test and simulation: Bottom release at 4 m with no ballast and vertical orientation (3 m coeff).

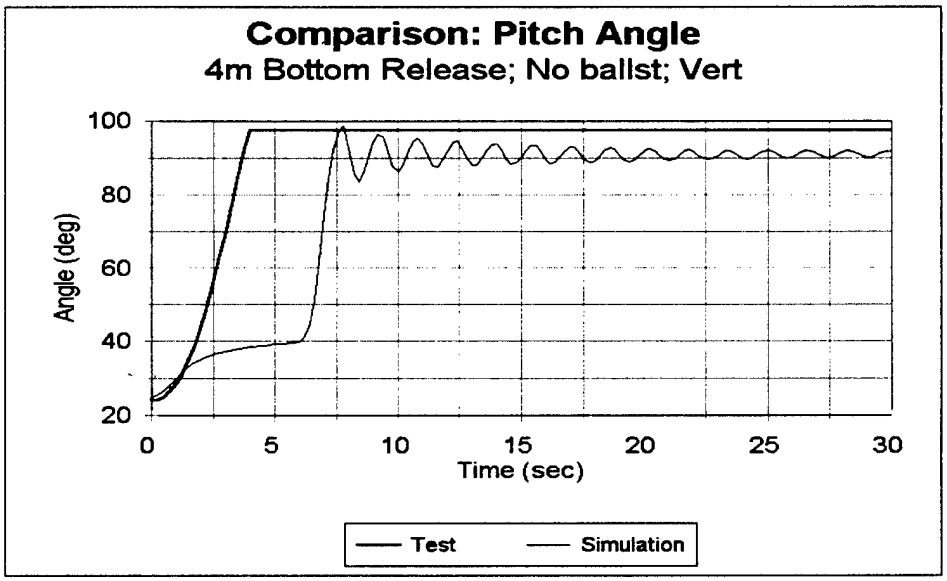

Figure C-34. Comparison of pitch angle from test and simulation: Bottom release at 4 m with no ballast and vertical orientation (3 m coeff).

There is a reasonable agreement in the rise time, though once again, the simulation shows the dummy to be at a higher level than the test. The pitch time history does not match well, with the simulation predicting that it would take much longer to reach the peak pitch angle. It appears that the maximum pitch angle achieved is close. Complete data were not available for the pitch sensor since it cut off around 90 deg.

[This page intentionally left blank.]

APPENDIX D

WHOLE BODY IN WAVE TESTS

The tests in waves were of great interest with regard to the WAFAC model, since this was the first time the software was tested against this condition. The previous ellipsoid tests were all done in calm water. The WAFAC model actually inputs the wave condition using the wavelength, and the standard correspondence between frequency and wavelength for gravity waves was used to calculate the wavelength. This relation was:

$$\lambda = \frac{g}{2\pi f^2}$$

where: λ = wavelength
g = acceleration due to gravity (9.8 m/s^2 or 386 I
f = frequency

Thus the corresponding wavelengths were: 17.3 m (682 in), 6.2 m (246 in), and 3.2 m (126 in).

One problem in the wave tests was to determine an appropriate initial condition. For a wave test, a 30-second slice was taken as the interval for comparison, during which the motion was periodic, i.e. all initial instabilities were removed well before the wave train was stopped. In the WAFAC model, there will also be an initial period in which the motion is initiated which is ignored during the comparison, though it is presented in the plots.

An additional initial condition that had to be dealt with was the correspondence of the phase of the periodic motion seen in the simulation and the test. The simple procedure was to shift the time of the test or the simulation such that the first maximum of the test matched the maximum from the simulation. Any departure in frequency after this point would be seen as a difference in the times at which subsequent peaks are reached.

In comparing the data from the simulation and the test, we were still relying on the information from the pressure transducers. The problem with this technique, in the case of wave motion, is that it gives the depth relative to the surface of the water which is always changing in time. The simulation, in its current form, outputs the motion relative to the average water surface. It should be possible to modify the program to output it relative to the actual depth below the actual wave shape.

The accelerometer data would normally be the data that would be used for retrieving displacement

information relative to an inertial coordinate system. But in these tests, as indicated in a previous section, the accelerometer response did not have enough resolution to be used accurately. The data tended to overestimate the velocity and displacement changes. Thus only a qualitative comparison can be given between the simulation and the test results. The pitch angle response, where available could be compared, though it was found that for some tests, where the angles exceeded the range of the sensor, the data would be cut off.

The basic information we ended up comparing was the frequency and shape of the periodic depth and pitch response. The amplitude of the pitch response could also be compared since direct measurement was available from the test (except for a few tests where the data was not available).

The following provides a summary of the results from the wave simulations.

i. 0.3 Hz Waves; Normal ballast; Straight Configuration

The tests from WANSL4 (runs 3 and 4) were used for evaluating the simulation. The pressure transducer and pitch time-histories were checked to determine the depth and pitch angle to be used for the initial condition in the simulation.

Run #4 was used as the specific test run for comparison. The initial conditions from the pressure and pitch sensors from this run provided the following initial conditions:

Depth (mean depth from avg. of right and left pressure transducers): 30 inches (0.76 m)
Pitch (mean pitch from sensor - channel 4): 40 deg.

The position of the lower torso CG based on the preceeding depth was taken to be 32 inches. The wavelength was 682 inches. (17.3 m) and the wave amplitude was 10 inches (0.25 m).
For this test, a number of values for the hydrodynamic coefficients were used, since there was no prior experience in handling simulations of objects in waves with the WAFAC model. The objective during this phase was not to arrive at the best match of simulation with test, but to achieve a reasonable level of

agreement. The values of the coefficients that were finally used were:

drag coefficient:	$C_D = 2.0$	
added mass:	$A_i = 0.5$	(for all directions)
wave damping:	$a_0, a_1 = 0.1, 0.25$	

These values were in the range used during the single ellipsoid simulations earlier. The results are shown below in figure D-1 and figure D-2:

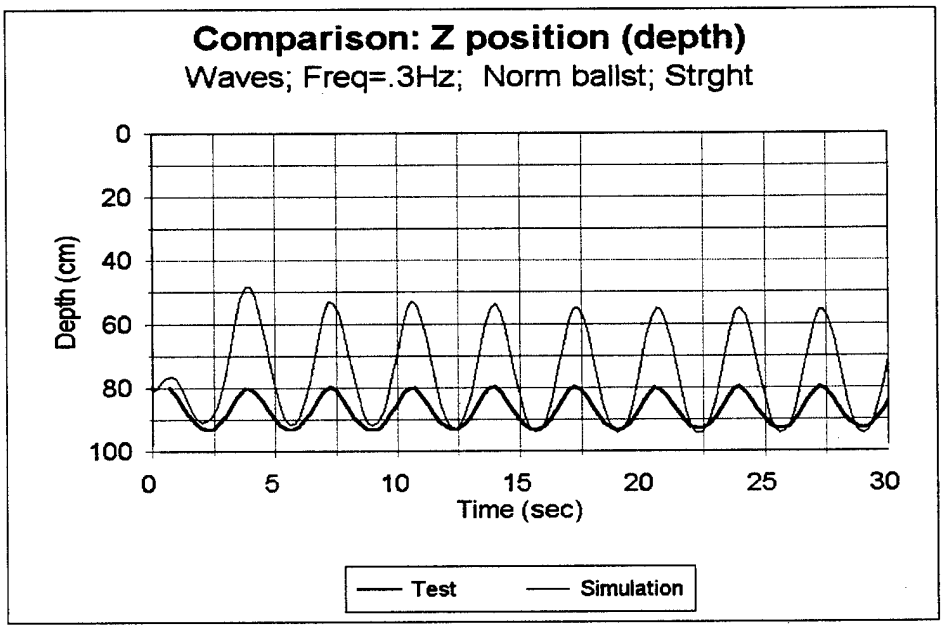

Figure D-1. Comparison of depth from test and simulation: In waves; freq. = 0.3 Hz; normal ballast and straight configuration.

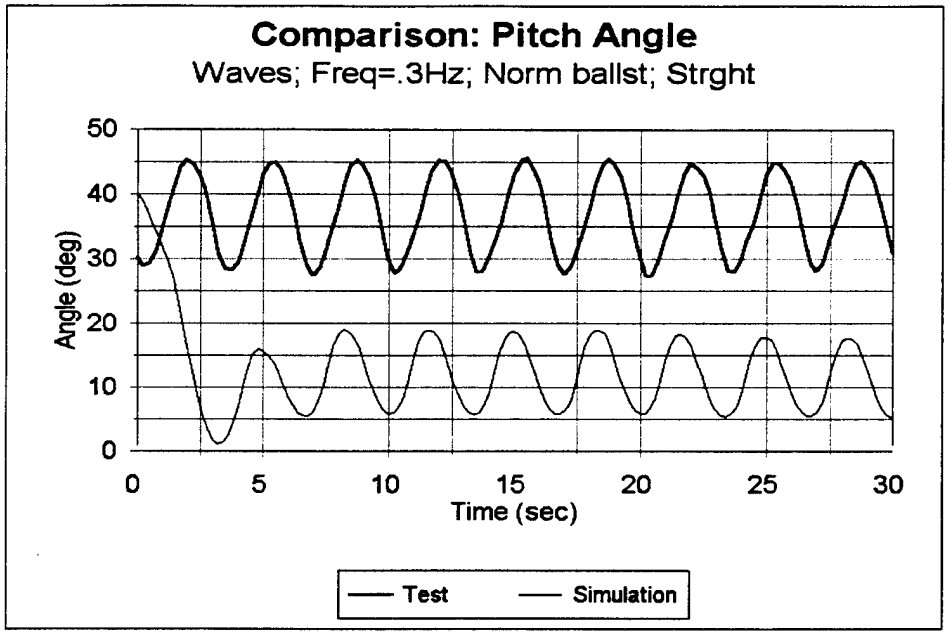

Figure D-2. Comparison of pitch angle from test and simulation: In waves; freq. = 0.3 Hz; normal ballast and straight configuration.

There are a couple of characteristics that are evident in the plot for the depth time histories. The periods generated in both the depth and pitch time histories match those from the tests, indicating that the forces from the external waves are being modeled correctly and combine properly from the reaction forces generated by the drag and wave damping components. On the other hand, the amplitude of the oscillations for depth are significantly higher than in the test. In the discussion earlier in this section, it was pointed out that the pressure transducer was providing depth information relative to the wave surface while the DYNAMAN simulation was providing it relative to a fixed coordinate system. Thus there would be periods in which the discrepancy between the test and simulation would be expected to be on the order of a wave amplitude or 25 cm. Since the body will usually ride the crest as the wave passes by, the actual motion relative to a constant surface would be greater than recorded by the pressure transducers. This should make the agreement between simulation and test closer.

The pitch data also agree with regard to period. The average pitch seen in the simulation is about 20 deg. lower than in the test. As pointed out previously, this characteristic is probably related to the exact location of the CB relative to the CG. As shown in table 11, there was some discrepancy in the CB location found in the simulation when compared to that found from testing.

ii. 0.5 Hz Waves; Normal ballast; Straight Configuration

The tests from WANSL4 (runs 8 and 9) were used for evaluating the simulation. The pressure transducer and pitch time-histories were checked to determine the depth and pitch angle to be used for the initial condition in the simulation.

Run #9 was used as the specific test run for comparison. The initial conditions from the pressure and pitch sensors from this run provided the following initial conditions:

Depth (mean depth from avg. of right and left pressure transducers):	30 inches (0.76 m)
Pitch (mean pitch from sensor - channel 4)	40 deg.

(These were identical to the initial conditions for the 0.3 Hz waves.)

The position of the lower torso CG based on the preceeding depth was taken to be 32 inches. During the tests, it was seen that the head went under the water at every other wave. That is, there was higher amplitude motion at half the wave frequency. An attempt was made to find a set of hydrodynamic coefficients which would generate this kind of dual period. The values that were used were:

drag coefficient:	$C_D = 0.5$	
added mass:	$A_i = 0.4$	(for all directions)
wave damping:	$a_0, a_1 = 0.2, 0.4$	

The results are shown below in figure D-3 and figure D-4.

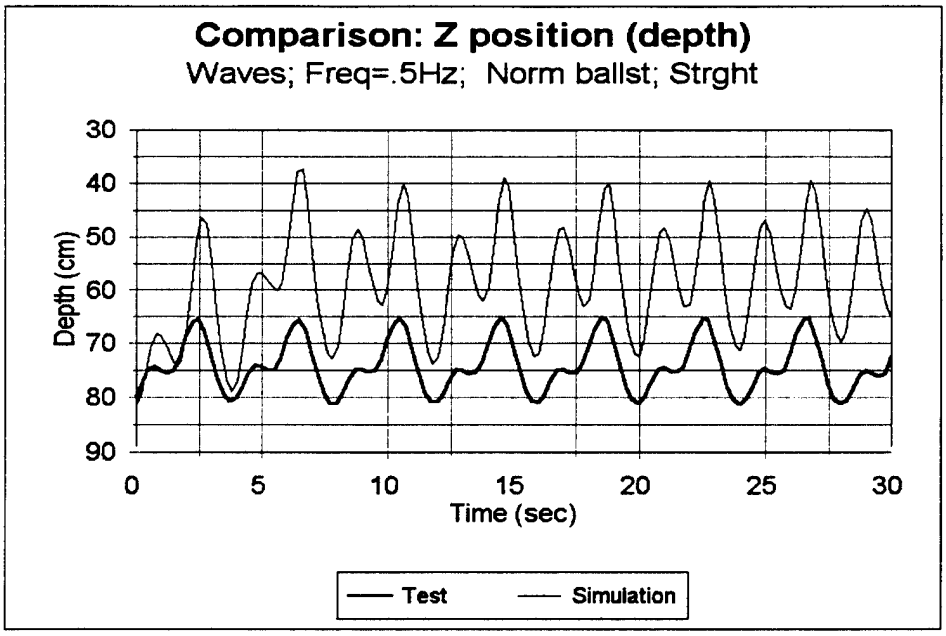

Figure D-3. Comparison of depth from test and simulation: In waves; freq. = 0.5 Hz; normal ballast and straight configuration.

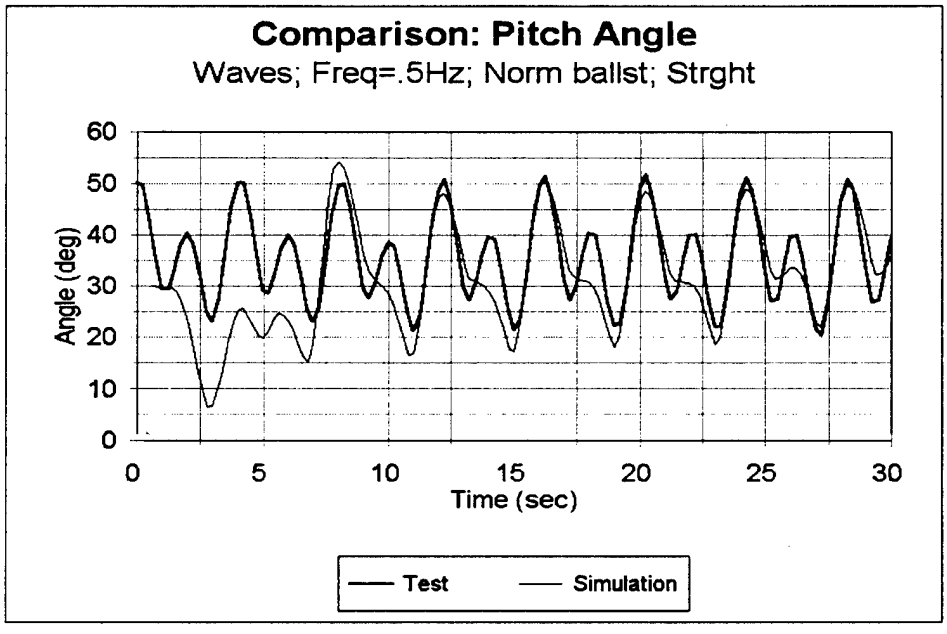

Figure D-4. Comparison of pitch angle from test and simulation: In waves; freq. = 0.5 Hz; normal ballast and straight configuration.

For this initial setup, the dual period character could be reproduced. Once again, the discrepancy in the amplitude of the Z- motion is probably due to the difference in how the depth is calculated in the simulation and in the test and should be smaller when referred to the same system. For this frequency, there appeared to be good reproduction of the behavior of the pitch response, though in the test the dual frequency was not as pronounced. It was encouraging to note that by suitable definition of the hydrodynamic coefficients, a fairly complex response could be simulated.

iii. 0.7 Hz Waves; Normal ballast; Straight Configuration

The tests from WANSL4 (runs 11 and 12) were used for evaluating the simulation. The pressure transducer and pitch time-histories were checked to determine the depth and pitch angle to be used for the initial condition in the simulation.

Run #11 was used as the specific test run for comparison. The initial conditions from the pressure and pitch sensors from this run provided the following initial conditions:

Depth (mean depth from avg. of right and left pressure transducers):	30 inches (0.76 m)
Pitch (mean pitch from sensor - channel 4)	40 deg.

(These were identical to the initial conditions for the 0.3 Hz waves.)

The position of the lower torso CG based on the preceeding depth was taken to be 32 inches. The coefficient values used in this simulation were:

drag coefficient:	$C_D = 0.5$	
added mass:	$A_i = 0.5$	(for all directions)
wave damping:	$a_0, a_1 = 0.3, 0.5$	

These values were a small modification from the 0.5 Hz case.

The results are shown below in figure D-5 and figure D-6.

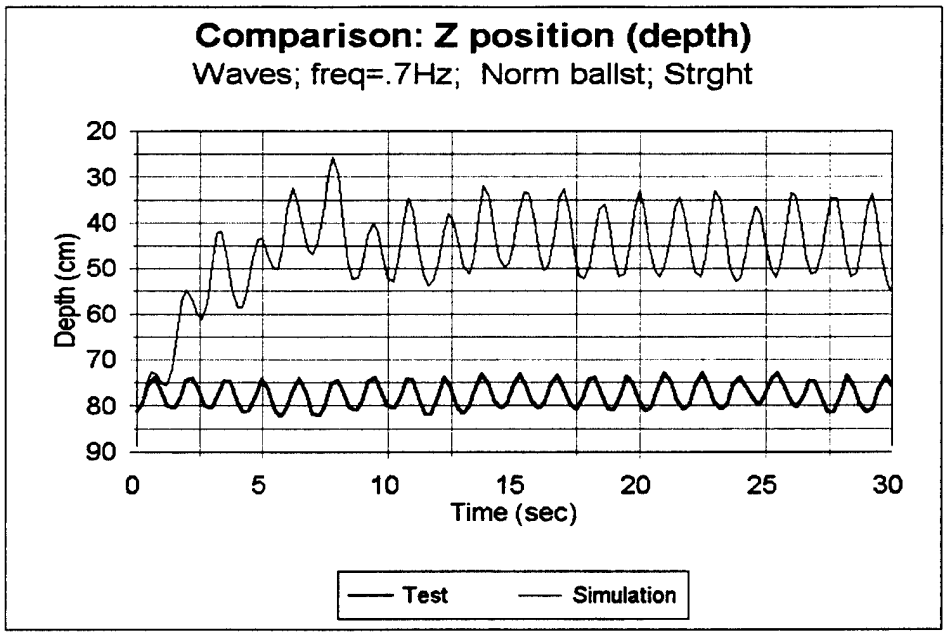

Figure D-5. Comparison of depth from test and simulation: In waves; freq. = 0.7 Hz; normal ballast and straight configuration.

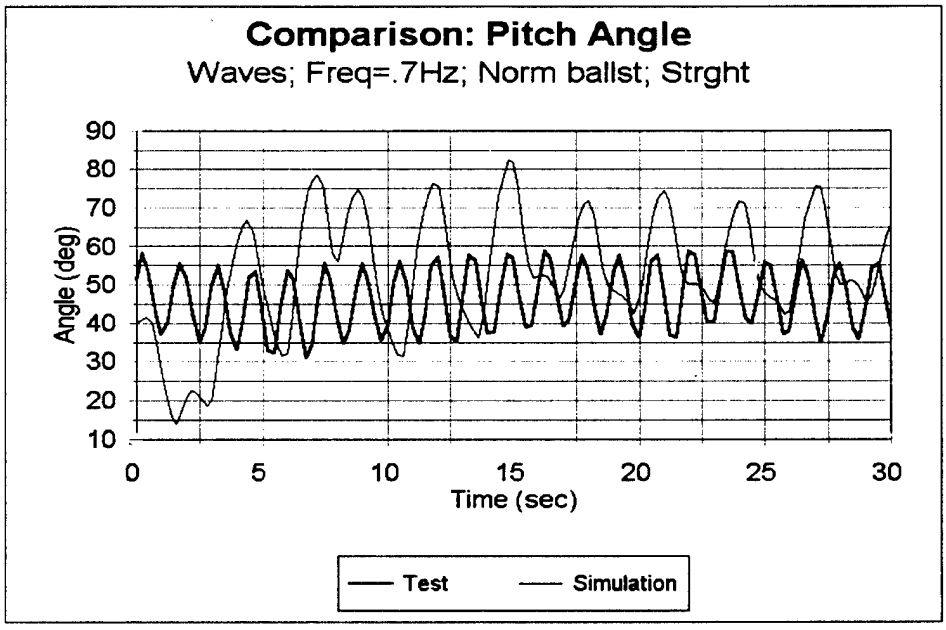

Figure D-6. Comparison of pitch angle from test and simulation: In waves; freq. = 0.7 Hz; normal ballast and straight configuration.

The agreement in this case was not as good as the previous test. The imposed frequency was reproduced well, but there were discrepancies in both the mean depth and the change in depth seen in the simulation as compared to the test. Part of this is again attributable to the difference in measurement schemes as described previously. But the overall discrepancy is large enough to suggest that the coefficients may be to some extent frequency dependent. The pitch response showed better agreement, though the amplitude was significantly higher in the simulation.

iv. 0.5 Hz Waves; No ballast; Straight Configuration

The tests from WBLJLS3 (runs 1, 2, and 3) were used for evaluating the simulation. The pressure transducer and pitch time-histories were checked to determine the depth and pitch angle to be used for the initial condition in the simulation.

Run #2 was used as the specific test run for comparison. The initial conditions from the pressure and pitch sensors from this run provided the following initial conditions:

Depth (mean depth from avg. of right and left pressure transducers):	10 inches (0.25 m)
Pitch (estimated)	90 deg

None of the pitch sensors were operational for this test. The initial angle was estimated based on the approximate equilibrium position seen previously with the unballasted dummy.

The position of the lower torso CG based on the preceeding depth was taken to be 10 inches. The coefficient values used in this simulation were:

drag coefficient:	$C_D = 2.0$	
added mass:	$A_i = 0.5$	(for all directions)
wave damping:	$a_0, a_1 = 0.25, 0.5$	

These values were similar to those used for the 0.3 Hz case.

The results are shown in figure D-7 and figure D-8.

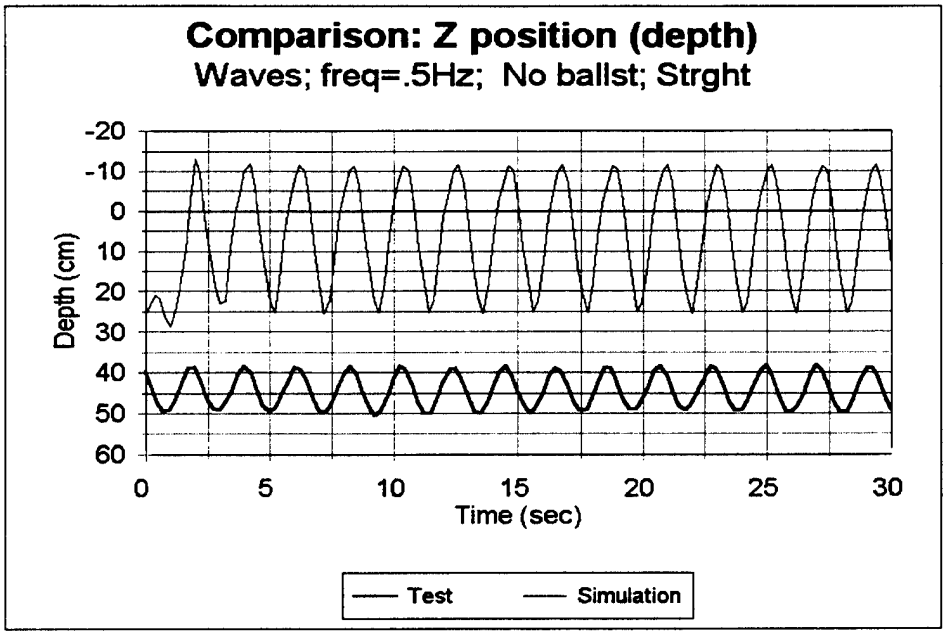

Figure D-7. Comparison of depth from test and simulation: In waves; freq. = 0.5 Hz; no ballast and straight configuration.

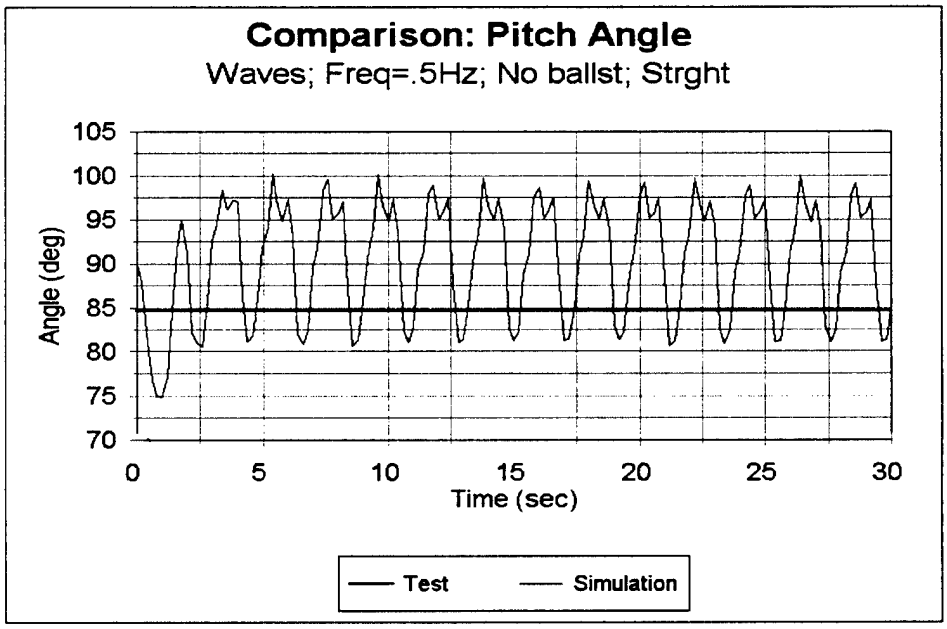

Figure D-8. Comparison of pitch angle from test and simulation: In waves; freq. = 0.5 Hz; no ballast and straight configuration.

Once again the frequency characteristics were reproduced and the mean depth and amplitude differed significantly. It is probable that with appropriate modification of the coefficients and with a consistent reference system, the agreement for the depth measurement would be closer. The response for the pitch cannot be compared in the absence of pitch data from the test. The simulation shows a peculiar structure to the pitch response, probably due to insufficient damping, which would tend to smooth out the bumps.

v. 0.5 Hz Waves; Normal ballast; Right-angle Configuration

The tests from WBNLR4 (runs 1 and 2) were used for evaluating the simulation. The pressure transducer and pitch time-histories were checked to determine the depth and pitch angle to be used for the initial condition in the simulation.

Run #2 was used as the specific test run for comparison. The initial conditions from the pressure and pitch sensors from this run provided the following initial conditions:

Depth (mean depth from avg. of right and left pressure transducers):	12 inches (0.30 m)
Pitch (estimated)	-95 deg.

None of the pitch sensors were operational for this test. The initial angle was estimated based on the approximate equilibrium position seen previously with the ballasted dummy in this configuration.

The position of the lower torso CG based on the preceeding depth was taken to be 12 inches. The coefficient values used in this simulation were:

drag coefficient:	$C_D = 1.5$	
added mass:	$A_i = 0.5$	(for all directions)
wave damping:	$a_0, a_1 = 0.25, 0.5$	

These values were similar to those used for the previous case with the unballasted dummy. The results are shown below in figure D-9 and figure D-10.

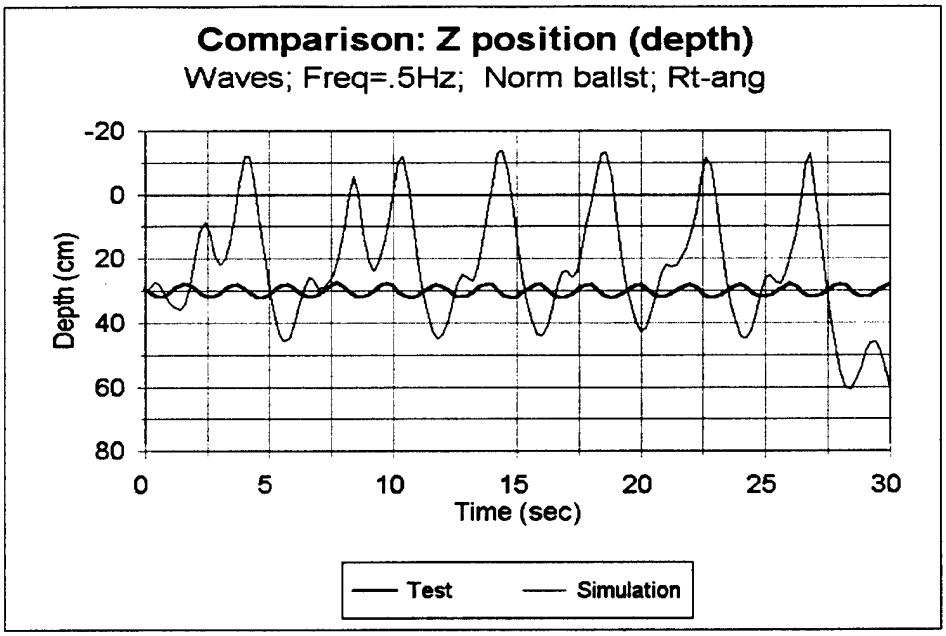

Figure D-9. Comparison of depth from test and simulation: In waves; freq = 0.5 Hz; normal ballast and right-angle configuration.

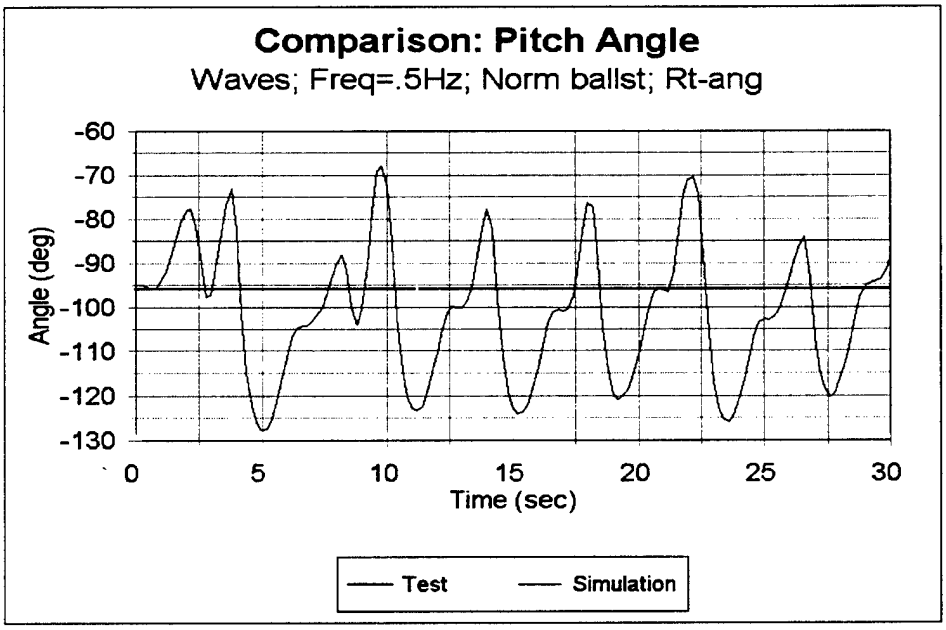

Figure D-10. Comparison of pitch angle from test and simulation: In waves; freq = 0.5 Hz; normal ballast and right-angle configuration.

The frequency characteristics are generally reproduced, but the simulation does take a while to settle down. A slightly deformed wave shape, similar to that described in section ii, is seen for the simulation. The test data do not seem to indicate such a response. Since the right-angle configuration appeared to have the largest error in the determination of the CB and CG, the imprecision in their location may have contributed to the response seen. The pitch response could not compared because of lack of available test data.

vi. 0.5 Hz Waves; Normal ballast; Straight Configuration; Unlocked Joints

One series of tests were done with some of the principal joints unlocked. The right and left hip and the right and left shoulder joints were unlocked to allow movement in both forward/backward and side/side directions.

From the visual inspection and sensor readings, there were significant motions generated, even when the wave amplitude was increased to 30 cm. It is not certain if the skin/skin interactions when the dummy is in water made the joints stiffer than normal. In air, it appeared to be relatively easy to move the segments about the joints. One test from WBNJU (run 3) was used for evaluating the simulation. The pressure transducer and pitch time-histories were checked to determine the depth and pitch angle to be used for the initial condition in the simulation. The initial conditions from the pressure and pitch sensors from this run provided the following initial conditions:

Depth (mean depth from avg. of right and left pressure transducers):	30 inches (0.76 m)
Pitch (estimated)	30 deg.

None of the pitch sensors appeared to be operational for this test. The sensor connect to channel 4 did have variable output but the magnitude was very high for this configuration. The initial angle was estimated based on the approximate equilibrium position seen previously with the ballasted dummy at this frequency.

The position of the lower torso CG based on the above depth was taken to be 32 inches. The coefficient values used in this simulation were:

drag coefficient:	$C_D = 1.0$	
added mass:	$A_i = 0.5$	(for all directions)
wave damping:	$a_0, a_1 = 0.3, 0.5$	

In this case, the output of the hip and shoulder rotary potentiometers were also compared with the corresponding data from the simulations. The results are shown below in figure D-11 and figure D-12.

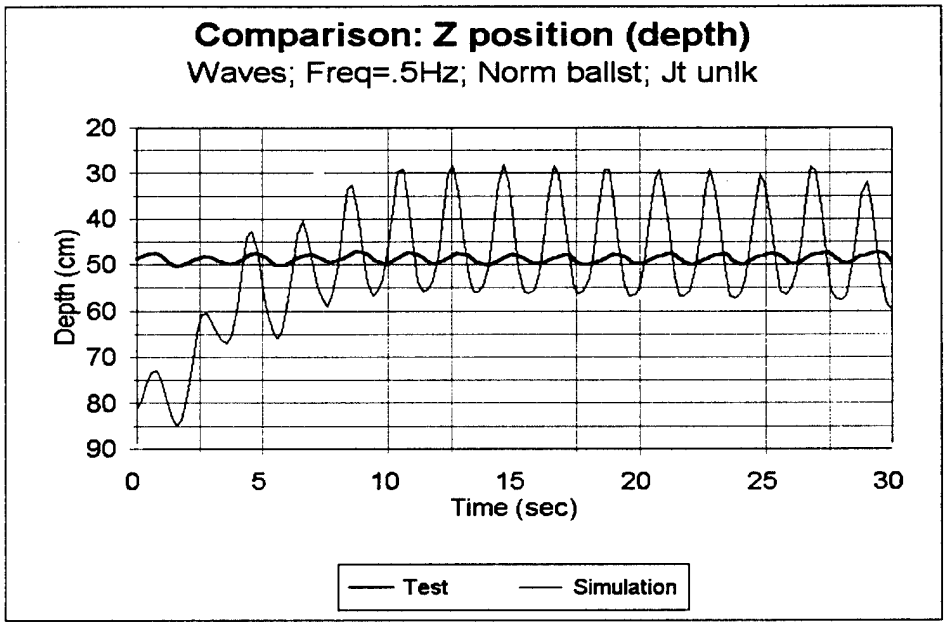

Figure D-11. Comparison of depth from test and simulation: In waves; freq. = 0.5 Hz; normal ballast; straight configuration; unlocked joints at hip and shoulder.

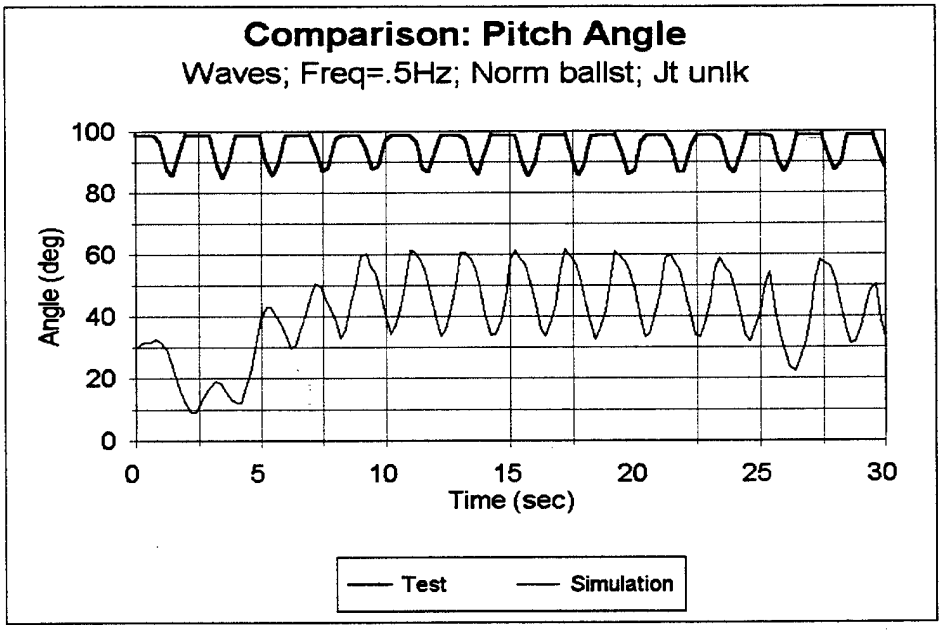

Figure D-12. Comparison of pitch angle from test and simulation: In waves; freq. = 0.5 Hz; normal ballast; straight configuration; unlocked joints at hip and shoulder.

The depth time histories are similar to has been observed for the other wave tests: namely that the frequency is well duplicated but the amplitude is much higher in the simulation. The pitch sensor appears to run with an offset and shows a cut off at angles above 100 deg. The mean pitch angle seen in the simulation appears to agree with previous experimental data for a similar wave form.

In order to compare the motion of the joints, the output of the right hip and right shoulder were compared in the forward/back directions. These are shown in figure D-13 and figure D-14.

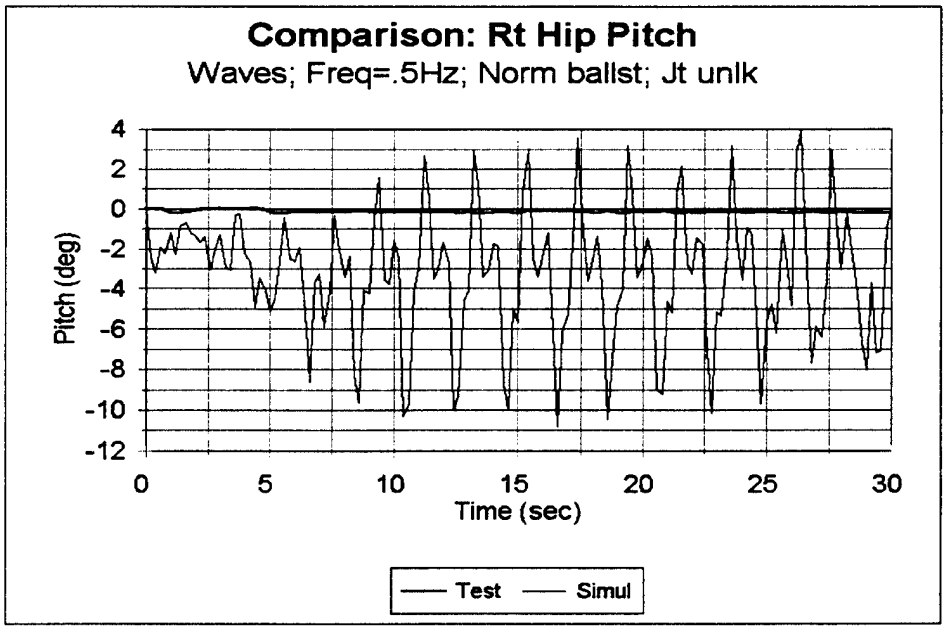

Figure D-13. Comparison of right hip rotation from test and simulation: In waves; freq. = 0.5 Hz; normal ballast; straight configuration; unlocked joints at hip and shoulder.

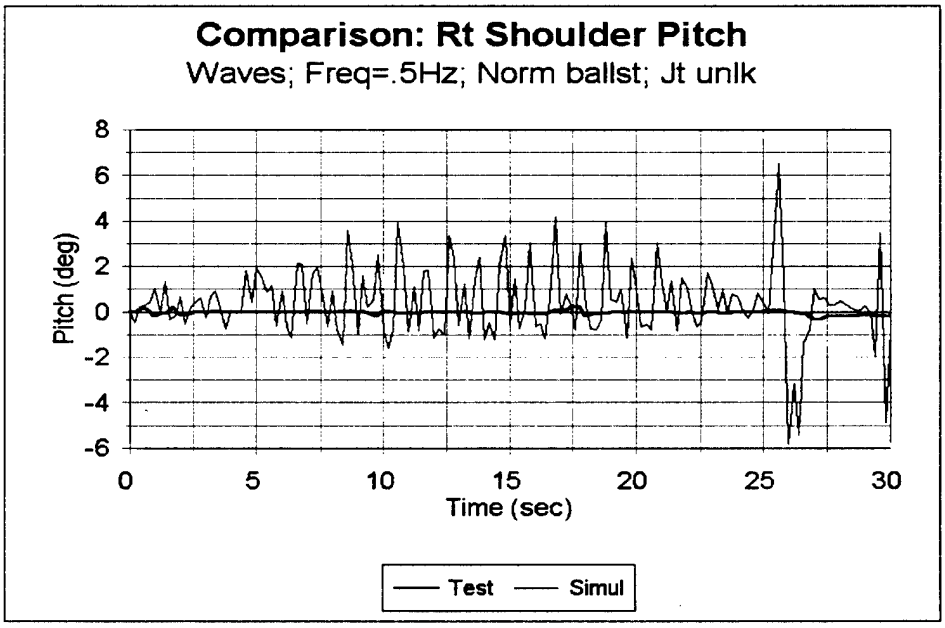

Figure D-14. Comparison of right shoulder rotation from test and simulation: In waves; freq. = 0.5 Hz; normal ballast; straight configuration; unlocked joints at hip and shoulder.

It is seen that there is very little motion observed in the test data. The simulation shows somewhat higher motions and are still limited to relative rotation in the range of ± 5 deg for the hip and ± 3 deg for the shoulder. The hip and shoulder motions are controlled by the rotational stiffness at these joints, and their values were in the original data set supplied by Coast Guard. During initial testing, the program showed some unusual numerical variations. In order to control them, the original values were modified and changed to a lower value. Despite softening the joints, there still did not appear to be any significant relative motion at the joints.